TALLINN UNIVERSITY OF TECHNOLOGY
DOCTORAL THESIS
26/2018

Molecularly Imprinted Polymers Designed to Detect Antibiotic Pollutants in Water

AKINRINADE GEORGE AYANKOJO

TTÜ PRESS

TALLINN UNIVERSITY OF TECHNOLOGY
School of Engineering
Department of Materials and Environmental Technology

This dissertation was accepted for the defense of the degree of Doctor of Philosophy in Natural and Exact Sciences on 14.05.2018

Supervisor: Dr. Vitali Syritski
Department of Materials and Environmental Technology
Tallinn University of Technology
Tallinn, Estonia

Co-supervisor: Prof. Andres Öpik
Department of Materials and Environmental Technology
Tallinn University of Technology
Tallinn, Estonia

Opponents: Krzysztof Noworyta, Assistant Professor
Department of Physical Chemistry of Supramolecular Complexes, Institute of Physical Chemistry Polish Academy of Sciences, Warsaw, Poland

Toonika Rinken, PhD, Senior Research Fellow
Faculty of Science and Technology
Institute of Chemistry
University of Tartu, Estonia

Defense of the thesis: 14.06.2018 at 12:00, Tallinn

Declaration:
Hereby I declare that this doctoral thesis, my original investigation and achievement, submitted for the doctoral degree at Tallinn University of Technology has not been previously submitted for any academic degree.

Akinrinade George Ayankojo

---
signature

European Union
European Regional Development Fund

Investing in your future

ISSN 2585-6898 (publication)
ISBN 978-9949-83-267-5 (publication)
ISSN 2585-6901 (PDF)
ISBN 978-9949-83-268-2 (PDF)

TALLINNA TEHNIKAÜLIKOOL
DOKTORITÖÖ
26/2018

Molekulaarselt jäljendatud polümeerid antibiootikumide määramiseks vesikeskkonnas

AKINRINADE GEORGE AYANKOJO

Contents

List of publications

The thesis is based on the following publications, which are referred to in the text by the Roman numerals I-III:

I **Akinrinade George Ayankojo**, Aleksei Tretjakov, Jekaterina Reut, Roman Boroznjak, Andres Öpik, Jörg Rappich, Andreas Furchner, Karsten Hinrichs, and Vitali Syritski. Molecularly imprinted polymer integrated with a surface acoustic wave technique for detection of sulfamethizole, *Analytical chemistry* 88(2) (2016) 1476-1484.

II **Akinrinade George Ayankojo**, Jekaterina Reut, Roman Boroznjak, Andres Öpik, and Vitali Syritski. Molecularly imprinted poly(meta-phenylenediamine) based QCM sensor for detecting Amoxicillin, *Sensors and Actuators B: Chemical 258 (2018) 766-774.*

III **Akinrinade George Ayankojo**, Jekaterina Reut, Andres Öpik, Aleksei Tretjakov and Vitali Syritski. Enhancing Binding Properties of Imprinted Polymers for Small Molecules Detection, *Proceedings of the Estonian Academy of Sciences*, 67 (2) (2018).

Copies of these articles are included in Appendix.

Author's contribution to the publications

The contribution by the author to the papers included in the thesis is as follows:

I Experimental work, participation in data processing, major role in the manuscript writing.

II Experimental work, major role in data processing and in the manuscript writing.

III Experimental work, major role in data processing and in the manuscript writing.

List of abbreviations

AFM	Atomic Force Microscopy
AMO	Amoxicillin
CV	Cyclic Voltammetry
DEAE-Dex	Diethylaminoethyl Dextran
DFT	Density Functional Theory
EDOT	3,4-ethylenedioxythiophene
EQCM	Electrochemical Quartz Crystal Microbalance
FIA	Flow Injection Analysis
HPLC	High Performance Liquid Chromatography
IF	Imprinting Factor
LoD	Limit of Detection
MAAM	Methacrylamide
MIP	Molecularly Imprinted Polymer
MIT	Molecular Imprinting Technique
MIM	Molecularly Imprinted Membrane
mPD	meta-phenylenediamine
NIP	Non-Imprinted Polymer
NMR	Nuclear Magnetic Resonance
PBS	Phosphate Buffered Saline
P(mPD)	Poly(meta-phenylenediamine)
Py	Pyrrole
QCM	Quartz Crystal Microbalance
SAW	Surface Acoustic Wave
STP	Sewage Treatment Plant
SMZ	Sulfamethizole
SPE	Solid Phase Extraction
SPR	Surface Plasmon Resonance
TEOS	Tetraethoxysilane
UV-Vis	Ultraviolet Visible spectroscopy
VTMOS	Vinyltrimethoxysilane

Introduction

Environmental pollution has continued to be a global concern due to the large categories of organic and inorganic pollutants escaping into the environment, heightened by increasing urbanization and industrialization. A larger share of these environmental pollutants end up in water bodies through treated and untreated wastewater disposals. Pesticides and pharmaceuticals make up one of the largest group of water pollutants because of their increasing usage in agriculture and medicines [1]. Of the groups of pharmaceutical pollutants being constantly released into water body, antibiotics constitute a major class owing to their increasing utilization in human and veterinary medicines, escape from sewage treatment plants (STPs) as well as waste disposal from various industrial processes [2]. Consequently, antibiotics have been detected in water bodies and wastewater treatment plants (WWTPs) effluents in many part of the world [3-7]. Antibiotic water pollution constitutes a global threat to public health and aquatic ecosystem. For instance, the persistence of antibiotics in the environment has been linked to the developments of virulent strains of pathogens that are resistant to antibiotics (antibiotics resistance) [8]. Antibiotic resistance jeopardizes the effectiveness in the treatment and prevention of infections caused by pathogenic microorganisms. This may be seen in the ruin of surgery, HIV or malaria therapy and cancer chemotherapy achievements. It could also lead to prolonged illness duration, increased cost of healthcare and permanent disability and death[1].

Therefore, monitoring and detection of antibiotic molecules in environmental water is highly significant to the protection of aquatic life while ensuring water safety for human consumption and thus, deserves an unrelenting research attention. Most traditional analytical techniques targeted towards environmental pollutants monitoring consisted primarily of chromatography and/or mass spectrometry or their couple. However, these methods demand huge immobile instrumentation, complex sample preparation, and specialized training before operation. More critical is the lack of specific compound selectivity that limits single analyte analysis in real samples, due to the complexity of the sample matrix in which the target pollutant is present with other numerous non-target molecules [9]. Thus, sensing of these substances in their matrices of occurrence is a challenge for contemporary analytical chemists, but urgently demanded because of its potentially broad impacts on human and animal health. As a result, there still exists a current trend and demand for sensitive, selective, simple, portable, but cost effective analytical devices for detection of pollutants in aquatic environments.

To meet up with these demands, recent research has focused on the design and application of selective sorbents for monitoring environmental pollutants. Molecular imprinting techniques (MITs) present synthetically tailor-made receptors called molecularly imprinted polymers (MIPs) for various analytical applications. Molecular imprinting is one of the state-of-the-art techniques to generate robust materials with antibody-like ability to bind and discriminate between molecules [10]. MIT can be defined as the process of template-induced formation of specific molecular recognition

[1] WHO media centre, Antimicrobial resistance, fact sheet. Retrieved from: http://www.who.int/mediacentre/factsheets/fs194/en/. Accessed 12th of April, 2018.

sites in a polymer matrix. Specific interests in MIP research stem from the outweighing advantages of MIP over natural receptors. Such advantages include high stability, improved shelf life, ease of preparation, low preparation cost, and target directed detection for analytes for which no natural receptor is available. Hence, MIPs have been shown to be promising alternatives to natural receptors in biosensors [11, 12]. Inevitably, applications of MIP have been extended to the selective detection of environmental water pollutants including pesticides and antibiotics [9, 13-18].

However, in the design of a MIP-based sensor, a robust interfacing or integration of MIP with a sensor transducer constitutes an important step. The transducers permit an accurate analysis of MIP performance by converting the molecular recognition events occurring on the MIP surface to a processable signal in the form of either optical, electrochemical, piezoelectric, magnetic, thermometric signals. Label-free sensor transducers such as quartz crystal microbalance (QCM), surface plasmon resonance (SPR), and surface acoustic wave (SAW) are significant to MIP performance analysis because they support a quick signal generation and real-time analysis. More importantly, the label-free environment provided by such sensing platforms permits accuracy of measurement results by preventing potential alteration to the intrinsic properties of biomolecules by compounds used as labels. Howbeit, these sensor platforms bear similarities in their non-utilization of labels and real-time analysis, they differ in their basic principles of transduction of the molecular recognition activities. While QCM utilizes bulk acoustic wave and quartz piezoelectric properties to monitor the change in mass of an adsorbed material through a corresponding change in frequency, SPR uses an evanescent wave to monitor changes in the refractive index (R.I) occurring on the sensor surface due to adsorption events and/or a change in medium properties, which are then observed as signal changes. SAW on the other hand, though similar to QCM in its intrinsic composition of piezoelectric substrate, differs in its operation at higher frequency (50 MHz to a few GHz as compared to 5 to 20 MHz in QCM) [19] and utilization of a surface acoustic wave (either Rayleigh or Love waves) propagating between two sets of interdigitated transducers (IDTs). This wave is sensitive to changes in the properties of medium occurring on the sensor surface, thus modulating both the velocity and amplitude of the wave, which are read as phase and amplitude shifts respectively.

To ensure a robust interface of MIP with various transducers, varying approaches can be employed depending on the intended usage and final configuration of the recognition layer. Thus, MIP exists in several formats, including thin film, particles, membranes, monoliths, and nanowires [20]. Thin film constitutes the best configuration for sensing, especially with label-free detection platforms. This is because of the short diffusion path length through which the analyte must travel to the binding sites existing in the MIP layer interfaced with the transducer, thereby leading to a faster recognition (higher sensitivity) [21]. As a result, several techniques were developed for fabricating thin MIP film and integrating the same on sensor electrodes to ensure a close contact between the MIP and the transducer surface. These techniques can be categorized into two main approaches involving either in-situ polymer synthesis on the surface of transducer (e.g., electropolymerization, photopolymerization), or interfacing a preformed polymer with the transducer by the sol-gel technique, followed by coating or screen printing. Of these, electropolymerization and sol-gel processing provide a very simple and direct methodology for the synthesis of a robust polymer on the surface of a conducting

transducer. This is because they allow a good control of polymer growth rate (by selecting appropriate synthesis conditions) and film thickness (by using an appropriate electrical charge dosage in electrosynthesis or by adjusting coating speed in sol-gel processing). Also, the inner morphology of the final polymer could be easily controlled by these techniques [22-25]. Furthermore, in meeting the demand of a simple and portable sensing device for low molecular weight environmental pollutants such as antibiotics, an electrochemically synthesized or sol-gel derived MIP film on a sensor transducer provides a considerable option for obtaining a lab-on-chip analytical device. Nevertheless, electrosynthesis technique is limited by the requirement of a conducting surface and electropolymerizable monomers, which are not as numerous as acrylic monomers and may therefore limit the choice of functional monomers. The overall effects of these may be observed as a constraint in the fabrication of certain improved MIP films such as organic-inorganic hybrid MIPs. However, to overcome this challenge, the sol-gel technique provides an easy means of combining organic and inorganic polymer in a hybrid form. When coupled with coating techniques, it provides an alternative way of obtaining thin MIP films on sensor surfaces. Consequently, several reports are also available for the integration of MIP films with the sensor transducers by spin coating, dip coating and/or casting techniques [26, 27].

Although MIPs have witnessed a wide utilization in diverse applications; however, in the field of environmental analysis, application of MIPs for sensing system is far from being fully explored. Likewise, the current status in the development of low-cost MIP-based sensors for accurate and fast detection of environmental contaminants, especially antibiotic water pollutants, is still in their developing stages. This is mostly due to some of the challenges of MIP when operated in natural media. Such challenges have their limitations as regards ruggedness, long term stability and sensitivity [28]. Notwithstanding, antibiotics detection using MIP techniques deserves increasingly critical research focus owing to the tremendous growth in the usage of antibiotics and their continuous identification as potential danger due to the spread of antibiotic resistant genes.

The research described in this thesis aims at developing antibiotic-imprinted polymer (antibiotic-MIP) films for the selective detection of antibiotic water pollutants utilizing specific molecules from two large antibacterial families as modelled targets. Preparation of such films should permit their integration with different label-free sensor transducers such as QCM, SPR and SAW to ensure the design of a sturdy and reproducible analytical sensor applicable for use in environmental water. A combined use of computational and experimental studies was employed for the optimal selection of functional monomers for antibiotics-MIP synthesis. Thin MIP films having selective cavities for specific antibiotic(s) recognition were interfaced with the sensor surfaces. The QCM, SPR and SAW sensors provided platforms for a direct and real-time monitoring of the molecular recognition interactions occurring on the antibiotic-MIPs as well as the assessment of their sensitivity and selectivity towards the target analytes. The prepared antibiotic-MIP sensors were also characterized in terms of their suitability and repeatability of usage in the prospective aqueous media, and the limit of detection. Lastly, an experimental protocol was exemplified as a window of opportunity to further improve the sensor performance.

1. Theory and literature review

1.1 Environmental pollution

Environmental pollution has been reported to be the most critical of all environmental challenges, posing vital threats to human health as well as to the global ecosystem [29]. Pollutants can be described as any substance which when released into the environment accumulate at the rate exceeding the ecosystem neutralizing capacity; hence, it alters the physical, chemical or biological characteristics of the environment such that human, animal and plant lives are affected [30]. Environmental pollution has varying classification systems but a more general classification may be based on the environment of occurrence, e.g., air, water, soil and/or the nature or type of pollutants, e.g., organic/inorganic, biological, radiological pollutants. Environmental pollutants continue to contribute to the list of human health hazards with many studies demonstrating the link between these pollutants and the development and/or influence of several sicknesses or diseases. Specifically, the disorders of immune system, energy metabolism and nutrient adsorption have been linked to the effects of pollutants on gut microbiota [31]. Also, pollutants effects have been identified in breast cancer, due to pollutants acting either as mammary gland carcinogens or activating carcinogenesis within mammary gland [32]; hypertension and cardiovascular diseases in which pollutants increase sensitivity to certain hormones and altering the expression of molecules involved in blood pressure regulation [33], and adverse influence of lung function in asthmatic patients [34].

From the foregoing, environmental pollution is increasingly becoming a global concern; hence, soliciting for a constant review of environmental monitoring and protection regulations [35]. Although numerous pollutants exist in the air and soil, the water bodies could contain a larger share of pollutants. The reason is that the majority of air and soil pollutants would eventually end up in the water by dissolution, runoff or erosion until they ultimately arrive at the water body [36]. Owing to the direct and indirect utilization of environmental water by humans, animals, plants or other microorganisms, monitoring of environmental water body is significant to human, animal and ecological well-being. However, a routine monitoring of environmental water is yet to be attained [36].

1.2 Antibiotics as environmental water pollutants

Pesticides and pharmaceuticals are major contributors to the list of environmental pollutants, undoubtedly because of their landmark influence in agriculture and medicines. Unfortunately, these can enter into surface and groundwater through both treated and untreated waste disposals [1]. However, the elevated number of such compounds, their persistence in the environment as well as the potentially dangerous effects of their transformation products have made them a matter of increasing concern. Antibiotics comprise one of the most popular pharmaceutical agents because of their wide prescription in the treatments of various diseases caused by many pathogenic microorganisms. Antibiotics inhibit the growth of pathogens by hindering either protein synthesis or cell wall formation [37, 38]. Ever since penicillin was

discovered in the 1940s, the utilization of antibiotics in medical treatments and prevention of bacterial diseases has greatly advanced antibiotic market. Apart from the use in human and veterinary medicines, they are also used regularly as growth promoters in agriculture, specifically, livestock, apiculture (beekeeping) and aquaculture [39, 40]. As a result, the development of a huge number of these pharmaceutical products has taken place globally over many decades [41]. Thus, numerous antibiotics exist, some bearing broad spectrum over both gram-positive and gram-negative bacterial.

Howbeit, because most antibiotics are relatively water soluble, they show partial absorption in the guts; hence, up to about 80% of ingested antibiotics may be released through urine or feces in their original form or as a metabolite, which may also be further transformed to the original drug or other active substances [42-44]. In addition, some antibiotics are unknowingly passed together as effluents directly to the river due to their escape from sewage treatment plants (STPs), as reported in [4, 39, 45-47]. Furthermore, antibiotics used in veterinary medicines may be directly passed to surface or groundwater, e.g., in aquaculture or indirectly by drainage or runoff of contaminated sewage sludge and manure used on farms [48, 49]. Consequently, varying concentrations of antibiotics have been detected in lakes, rivers, surface water and wastewater in many countries [31, 50, 51]. Water quality is a major concern in many countries because of the challenges encountered in providing safe drinking water owing to the contamination of tap water by antibiotics in some of these countries [52-54]. Sulfonamides and beta-lactams probably constitute two of the major antibiotics classes commonly found in water. These drugs are used as herbicides, as potent treatment and prevention of respiratory and urinary infections in human and veterinary medicines, as well as in aquaculture [55].

The concern about antibiotic pollution is not exclusively due to the high production volume but more importantly about the environmental persistence and chemical activity of such pollutants that may affect vital biological functions. Consequently, exposure to antibiotic pollutants has potential toxic effects in humans, animals, plants as well as microorganisms [56]. Thus, there is an ongoing indication of the link between antibiotics pollutants and organisms DNA damage, change in enzyme activities, alteration of plant cellular protein synthesis, plastid division, photosynthesis and growth [57-63]. Also, its effects on gut microbiota and human susceptibility to diseases and infections have been reported. For example, very low concentration of certain antibiotics could alter the composition of microbiomes within the gut of an animal leading to microbial imbalance (dysbiosis) and health challenges [31].

Notwithstanding, the clearest and most widely known effect of antibiotic pollution is the selection and development of resistant strains of microorganisms (antibiotic resistance) [64]. Antibiotic resistance has accentuated the study of the impact of antibiotics in the environment, resulting in an increasing volume of scientific publications. With pathogenic and environmental antibiotic resistant bacterial strains in the ecosystem, an increasing number of infections would no longer be curable with the currently prescribed antidote. This will compromise the treatments of infections and diseases caused by these pathogenic microorganisms, thus, prolonging illness and increasing the cost of healthcare. As a result, individual resistance and multiple resistances have been observed for certain bacteria causing epidemic diseases, as reported by Fent K. et al. [48]. The need for urgency in the current study is evident in a very recent report released by the British Food Standard Agency on antimicrobial

resistance, indicating record levels of antimicrobial resistant campylobacter in fresh whole chickens at retail supermarkets in UK[2]. According to the report, up to 55% of the test samples demonstrated antibiotic resistance to some of the strongest antibiotics tested. Besides the resistance of bacteria to known antidotes, more noteworthy is the fact that an increasing population of antibiotic resistance genes in the environment by itself have intrinsic potential to serve as environmental pollutants [65]. A good illustration of this is the recent determination of antibiotics resistant genes in treated tap water in China and US [66, 67]. Therefore, although antibiotics such as beta-lactams represent the commonest antidote for bacterial infections, they are also the pronounced causative agents of resistance among gram-negative and gram-positive bacteria and as a result, their utilization must be cautiously met with an appropriate standard to detect their presence and monitor their interaction with the ecosystem.

1.3 Antibiotic detection methods

From the foregoing, the environment deserves a critical and unrelenting monitoring to guarantee safety of humans, animals, plants as well as the sustainability of the natural ecosystem. To that effect, there exist continuously reviewed laws and regulations in many countries enforced to ensure cleanliness and safety of drinking water, prevention of pollution as well as protecting water bodies and drinking water sources. Also, on the European and global scale, monitoring of the environment is prioritized owing to the identified relationship existing between human health, socioeconomic growth and pollution [68]. A major aspect in environmental water monitoring is the detection and/or separation of pollutants and substantial research efforts are being put into designing fast, cost effective, sensitive, and selective analytical techniques for routine assay of environmental water pollutants. Currently, several techniques are employed, including solid phase extraction, chromatography and mass spectrometry to determine such pollutants [69-72]. However, these traditional techniques show some disadvantages either in relation to the expensive instrumentation involved or the requirement of complex sample preparation procedures and well trained operation personnel. Other more critical limitations include the immobility of the analytical equipment that prevents on-site analysis, hence, delay and time wastage.

Therefore, the use of such traditional techniques for the analysis of these pollutants constitutes a significant limitation to the desired routine assay. In response to this, other technologies, mainly biosensors and enzyme-linked immunosorbent assay, were developed as alternative methods that appear more suitable as analytical methodology to meet these needs [73]. Although there is no doubt that biosensors hold potentially beneficial properties in terms of sensitivity and selectivity, nevertheless, biosensors usage in environmental monitoring still suffers certain setback. This is because of the inherent limitations of the biological recognition elements used in biosensors. Such limitations include short term stability, short shelf life, loss of sensitivity of immobilized biological elements as compared to the free analogue, as well as the time wastage in recovery of the active biomolecule [74, 75]. Thus, the design of robust analytical devices that combine high sensitivity and

[2] FSA Project FS241044 Antibiotic Resistance Report for FS241044 - Sept 2016 (Final). Retrieved from: https://www.food.gov.uk/sites/default/files/phe-report-amr.pdf

selectivity with high stability, cost effectiveness, ease of operation, and portability potentials are still very urgently required.

1.4 Molecularly imprinted polymers

Nature, by its intrinsic characteristics, consists of biological systems that have a remarkable ability to recognize certain molecules while discriminating against others. This term called molecular recognition is important to life because they play vital roles in biological processes of humans and other living organisms. However, some molecules, which are of interest to humans, do not have these natural receptors for their recognition. Hence, research community has been fascinated by the possibility of fabricating artificial biomimetic recognition materials for such molecules. More so, natural biological recognition elements suffer from a low stability or short shelf life when used outside their natural environment. Molecularly imprinted polymers (MIPs) are tailor-made receptors prepared through the widely expanded technology called molecular imprinting. Molecular imprinting is said to be part of the most prominent technology for achieving a definite molecular recognition [76].

1.4.1 Principles of molecularly imprinted polymers

Molecularly imprinted polymers (MIPs) are functional materials consisting of synthetic polymeric matrix with pre-formed selectivity for detecting any given analyte. MIPs could mimic natural receptors including antibodies and biological receptors in discriminating between molecules; thus, they could be potentially suitable for fabricating state-of-the-art analytical devices [10, 77]. MIPs are prepared by the molecular imprinting technology in which molecular cavities of specific recognition are created within synthetic polymers. This is achieved by polymerizing suitable functional monomers in the presence of relevant target analyte(s) or similar molecules (surrogate) acting as template molecules [78]. Removing the template molecules after polymerization reveals binding sites which are complementary to the target molecules in shape, size and coordination of functional groups. The scheme for the molecular imprinting development is shown in Fig. 1.1.

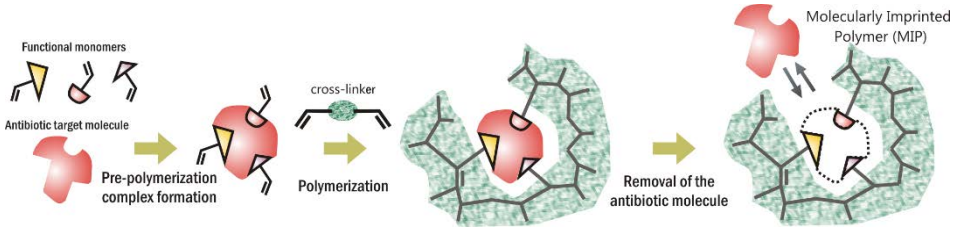

Figure 1.1. Schematic protocol of molecular imprinting.

Prior to the polymer synthesis, the template molecules and the carefully selected functional monomers (based on the consideration of their capacity to interact with functional groups existing on the template molecules) are brought together in a porogenic solvent that permits chemical interactions between them to form a pre-polymerization complex. Polymerization of the solution complex in the presence of a cross-linking agent and an appropriate polymerization initiator generates the

reticulated network of the polymer with an embedded template molecules, which, when removed or washed out with a suitable washing solution yield a robust polymer matrix with specific cavities for the target molecules. In summary, creating an MIP for specific recognition of a target molecule involves the generation of physicochemical interactions between the target molecule and the selected polymer matrix. This is achieved by memorizing, cementing and activating these interactions during the pre-polymerization stage, polymerization and/or cross-linking, and after template extraction, respectively [79]. Generally, the key factors to be considered in MIP preparation entail the nature of the target, accurate selection of monomers, porogenic solvent as well as the polymerization conditions.

1.4.2 Imprinting strategies

From the foregoing, it is apparent that pre-polymerization chemical interactions between the template and functional monomers are essential to the performance of MIP; hence, several interaction approaches called imprinting strategies are employed in MIP preparation. Five major imprinting strategies exist, including non-covalent, covalent, semi-covalent, ionic, and metal center coordination [78]. Of these strategies, about three are very commonly reported. These include either covalent imprinting in which the complex formation entails reversible covalent bond formation between the template and functional monomers, or noncovalent imprinting where the bonds formed are either based on hydrogen or van der Waal interactions or their combination. A third intermediate strategy, semi-covalent imprinting, uses a combination of both covalent and noncovalent bonds to ensure a good interaction between the template and monomers. Notably, of these three methods, the noncovalent imprinting is the most commonly used [9]. This is both due to the greater choice of functional monomers and the simple chemistry involved, thus, aiding flexibility of preparation [80, 81]. However, in the noncovalent approach, a greater number of functional groups must be present on the template molecules to ensure an optimum interaction between the template and monomers [82]. These preformed imprinted binding sites of MIP could demonstrate affinities and selectivities similar to natural recognition molecules such as antibodies; hence, MIPs were earlier referred to as antibody mimics [77, 83].

1.4.3 MIP applications

The highly cross-linked MIP polymer matrix attributes to the final material its robustness, stability and the possibilities to use under very harsh environmental conditions, including acidic and basic solutions [11]. Also, the ease in preparing the synthetic recognition materials by adopting several already well-established polymerization techniques, the low cost involved as well as the high miniaturization possibilities, makes MIPs potentially suitable for generating state-of-the-art recognition devices. Therefore, as a result of the many interesting features of MIPs, an increasingly wide number of research laboratories are adopting the molecular imprinting technology to design novel functional materials for different analytical applications, including catalysis, separation, drug delivery, and chemical sensors [84-87].

Furthermore, interest in MIP research has seen a drastic shift from the solely laboratory research into future commercialized materials for industrial applications. This is in response to the persistent growth of research in molecular imprinting development, which has allowed for the acquisition of established knowledge suitable for scaling up to its industrial demands in various applications [88]. Consequently, advanced progress has been recorded in the use of MIP for applications, including chromatographic separation, solid phase extraction for sample preconcentration and selective extraction. Also, MIPs for chiral separation of drugs, plastic antibodies in pseudo-immunoassays, enzyme mimics, therapeutics, and chemical/biological sensors for many relevant analytes of diverse industrial applications have been developed. To demonstrate the innovativeness of the MIP technology, its applications are already becoming the core processes and procedures of several companies, including Semorex Inc., Sphere Medical Ltd., Biotage, and Toximet Ltd. These companies, the heart of which are experienced MIP researchers, provide notable services in solid phase extraction, food security, cancer targeted drug release, or point of care diagnostics [88].

1.4.4 Configuration of MIP matrices

As indicated above, the influential importance of MIPs in many research fields has generated rapid interest in academic community and even in industries for several targeted applications. However, to ensure an effective utilization of MIPs for these purposes and for a successful commercial implementation, different configurations (formats) of MIPs are required. As a result, increasing efforts are put into the generation of protocols for preparing different MIP polymer matrices. Such efforts would, as a matter of importance, consider improvement in the creation of receptor sites and polymer optimization for imprinting and subsequent rebinding. Previously, early imprinting researchers most commonly utilized bulk polymerization to generate polymeric materials in the form of monoliths that are subsequently ground into smaller particles. Although this approach is interesting, more rational MIP designs are needed to meet up with the industrial scale. Concerted efforts of many researchers have resulted in several MIP formats suitable for different applications. These formats are generally classified based on their appearance or preparation into: nanoparticles, membranes and thin films [89].

Nanoparticles

Generally speaking, nanomaterials display interesting properties much better than the material at macroscale; therefore, it was believed that MIP at the nanoscale would yield better imprinting results. This is observed in nanoparticles in which their large surface area enables their surface functionality to be exploited. The growth of knowledge in polymer chemistry has permitted various nanoparticles with improved properties that are suitable for MIP nanoparticle synthesis to be achieved. Therefore, uniform MIP nanoparticles or beads in the form of core-shell, nanosphere and hollow spheres are now achievable using established polymerization methods such as precipitation, solution and mini-emulsion polymerizations. Precipitation polymerization appears to be the simplest of the three methods and helps to easily achieve uniform and narrow size particle distribution after careful control of

polymerization parameters. Also, it is well suited for polymerization in aqueous media to yield water soluble MIP nanoparticle which can be adopted as enzyme inhibitor [90]; however, it is deficient in the use of excessive amount of solvent. With a continued progress in imprinted nanoparticles, some of the challenges encountered in the practical applications of MIPs can be easily overcome. While monoliths are mainly used in SPE, chromatography and SPE are two of the most common applications of MIP nanoparticles. However, MIP nanoparticles are also widely employed in bioseparation, controlled delivery, catalysis, as well as sensing [81].

Membranes

Molecularly imprinted membrane (MIM) is another format suitable for MIP application. Generally, membrane can be described as a barrier or interphase existing between adjacent phases that allows or regulates the selective transport and permeation of some materials between the different phases while holding on to certain others [91]. Transport of a molecule through a membrane is influenced by the nature of the barrier, either microporous or nanoporous; its potential gradient driven passive diffusion, as well as the shape, size and electronic charge of the molecule [79]. Hence, membranes are adapted for applications involving separation of materials because of their unique mass transport processes involving both adsorption of molecules and diffusion into the membrane core. Nevertheless, to introduce molecular recognition ability into and facilitate the selectivity of a membrane, specific binding sites must be created within the material [79, 92]. MIMs can be classified, as a function of their structural barrier (porosity), in the form of dense (pore sizes are < 1 nm) and porous adsorbents (pore sizes are > 1 nm) for separating large or small molecules or as films deposited on previously formed membrane substrates. They are formulated using 3D or 2D imprinting methods by techniques including in situ polymerization, membrane deposition, grafting etc. [92].

MIMs have been quite well reported in literature with common examples including antibody (IgG) imprinted membrane via grafting [93], polypropylene hydrogel and electrospun fiber membranes for bovine serum albumin and hemoglobin [94], chitosan imprinted membrane [95], polysulfone imprinted polymer membrane for polycyclic aromatic hydrocarbons.

Thin films

MIPs configurations also exist in the form of thin films (< 100 nm) immobilized on the surface of sensor transducers that allow the monitoring of binding interactions using different transduction techniques. Such transduction techniques include piezogravimetric, e.g., quartz crystal microbalance (QCM) and surface acoustic wave (SAW); optical, e.g., surface plasmon resonance (SPR); electrochemical (voltammetry, amperometry, capacitive impedimetry etc.) transducers. Thin film is of particular significance in environmental monitoring because of its suitability for producing portable pollutant detection devices. As a result, in sensing applications, selective thin film of MIP based sorbents is used in the analysis and detection of various targets, ranging from small, (e.g., environmental pollutants), to large (e.g., proteins), molecular weight analytes [9, 96-101].

Although thick MIP films can also be prepared and integrated with a transducer, binding events occurring on imprinted sites at certain distances beyond the region of

transduction of the particular sensor, may not be detected by the transduction system, hence, leading to low signal and improper analysis of sensor performance. Also, such films may reduce the ease of diffusion of analyte through the polymer matrix unto the active sites that are located deep within the matrix. Thus, loss of signal and the long diffusion path through which an analyte may have to travel constitute the limitation in the use of a thick MIP film for recognition. Therefore, in designing MIPs for sensor application, thin film format offers the best compatibility with the available sensor transducers. This is also in part because of the possibility to control and obtain a high value for the surface-area-to-volume ratio, which helps to improve the sensor sensitivity by introducing porosity into the film [92, 102]. Thin MIP film also facilitates a better control of binding kinetics by simply altering the film thickness. Thin MIP films can be prepared and integrated on the transducer surface using two general approaches including immobilization of previously prepared MIP by physical or chemical means [103, 104] and in situ polymerization of MIP directly on the transducer surface [9, 105]. A number of well-established methods are available for in situ polymerization of thin MIP film on different transducers. They include photopolymerization, electropolymerization, lithography, sol-gel technology etc.. The potential application of a thin MIP film for environmental pollutant detection is evident in the increasing number of publications existing on the subject.

1.5 MIP preparation methods

A MIP preparation method is one of the factors that determine the properties of any fabricated MIP. Polymerization methods used for MIP synthesis could be generally classified into free-radical polymerization and sol-gel processing techniques [78]. A more broad classification may be based on the expected configuration (format) and/or the intended application. Thus, bulk polymerization exists for monolithic MIP preparation while for MIP particles, suspension, emulsion, multi-step swelling and precipitation polymerizations are generally used. However, in preparing MIP films to be used in sensor applications, electrochemically induced free-radical polymerization and sol-gel processing techniques offer easy MIP fabrication at room temperature and the possibility of its integration on various sensor transducers. These, coupled with other advantages of both methods, constitute the basis for their utilization in this work.

1.5.1 Electrosynthesis of thin MIP films

Electropolymerization is a facile technique for generating thin polymer films with controlled thickness and morphology [106]. It involves the anodic oxidation of an electropolymerizable monomer employing different modes of potential stimulus to form radical cation. These unstable radicals quickly react with other monomers thereby forming oligomers and subsequently the final polymer chain. Such polymerization requires an electrolyte in the form of a solvent containing a doping salt or an ionically conducting medium. With electropolymerization, polymer films can be directly obtained on the surface of any flat conducting electrode, such as gold, platinum, glassy carbon, tin, with a robust adherence [107].

Electropolymerization is beneficial to MIP synthesis because of the ease involved in the experimental set-up, fast operation and minimal technical intervention and the

possibilities to control MIP thickness by simply adjusting charge dosage [23, 108]. The room temperature operation of the technique also makes it very attractive to MIP researchers. However, to obtain a good imprinting efficiency, it is essential to ensure the preservation of the structural integrity of the template molecules during the electrosynthesis by excluding the possibility of template oxidation during the electropolymerization [98]. Though electrosynthesis presents an interesting technology for a robust MIP fabrication, its polymerization parameters require careful control for an optimal performance of the electrosynthesized MIP. Furthermore, to ensure its excellent performance, the choice of monomer(s) is very essential; thankfully, a variety of electropolymerizable monomers are available. Of these, pyrrole (Py) [23, 109], aniline [110], thiophene [111], 3,4-ethylenedioxythiophene (EDOT) [112] and their derivatives, are among the most commonly used in MIP research.

1.5.2 Sol-gel synthesis of MIP films

Sol-gel is a common synthesis method that utilizes hydrolysis and polycondensation of alkoxide precursors to form a polymer. Sol-gel technique is very attractive and widely used for diverse applications due to its room temperature preparation and ease of fabrication on various substrates [113]. In MIP research, the application of sol-gel derived polymer is due to its low preparation cost, long shelf-life and good optical and mechanical properties. Moreover, the flexibility in the design of sol-gel MIP promotes host-guest interaction, hence, an improved recognition [114]. More importantly, sol-gel processing permits the synthesis of hybrid MIP materials possessing improved properties as compared to a solely organic acrylic polymer. For example, a hybrid MIP could possess an improved porosity, thus, a higher specific surface area as well as a localized concentration of functional groups with an overall effect of sensor sensitivity and selectivity [115].

Consequently, a sol-gel fabricated hybrid MIP is reported to be more favorable than the solely organic acrylic polymer due to the ease of preparation and faster diffusion times through which analytes have to travel to the polymer active sites and reduction of nonspecific binding [116]. In an environmental monitoring system, silica hybrid MIP is reasonable because of the relatively inert nature of the silica as compared to a totally acrylic based sensor. Furthermore, since sensor development requires the integration of a recognition layer with the sensor transducer and the conversion of chemical interaction into a processable signal, the optical transparency of sol-gel derived silica hybrid MIP film could permit its suitability for use with optical sensors such as SPR to monitor molecular detection [117]. Luckily, there exists a window of possibility to design portable SPR sensor; thus, interfacing a sol-gel derived MIP with a portable SPR sensor will further enhance on-site environmental monitoring [118, 119].

1.6 MIPs for antibiotics detection. A brief overview

Using the molecular imprinting technology, MIP can be prepared for detecting a wide range of molecules or families of molecules possessing a very definite arrangement of functional groups. Since antibiotics are usually identified and classified by their unique possession of distinctly arranged functional groups, their detection using molecular imprinting could be easily achievable. Consequently, the detection of antibiotics using

MIPs has been a subject of several research laboratories and increasing publications are available on the subject for different applications. High performance liquid chromatography (HPLC) and solid phase extraction (SPE) represent the techniques where MIP separation applications have been mostly employed. This is probably due to the ease involved in preparing bulk polymer matrix that is easily ground into smaller monoliths suitable for easy parking into chromatography columns. It could also be due to the identifiable magnified recognition properties of MIP in these techniques because of the high number of theoretical plates existing in the column [120]. As a result, almost all of the early reports of antibiotics detection by MIP have been based on their utilization in either HPLC or SPE.

The first recorded antibiotic MIP report was made in 1997 by the Klaus Mosbach group [121] where selective erythromycin, tylosin and oleandomycin imprinted polymers were prepared for use as stationary phases in high performance liquid chromatography (HPLC). These imprinted polymers were prepared as bulk materials subsequently ground into smaller particles suitable for parking in HPLC column. By employing the noncovalent imprinting approach, interaction complex was formed between methacrylic acid-ethylene glycodimethacrylate functional monomer and the antibiotic template molecules in an organic solvent. Shortly afterwards, a chloramphenicol MIP combined with HPLC was reported by another group [122] for successful detection of chloramphenicol in patient's serum. Similar to the previous, the MIP was built as bulk polymers, grounded and parked into HPLC column for analysis. Although functional monomers consisting of methacrylate unit and noncovalent imprinting strategy were used, the target molecule was detected in the chromatography column by a competitive displacement of a chloramphenicol-dye

Table 1: Reports of antibiotic-imprinted polymer from 1997 to 2005

Template	Functional Monomer	Imprinting Strategy	Format	Application	Ref
Erythromycin, tylosin, oleandomycin	Methacrylic acid-ethylene glycoldimethacrylate	Noncovalent	Bulk	HPLC stationary phase	[121]
Chloramphenicol	MAA, DEAEM, 4-VP	Noncovalent	Bulk	HPLC stationary phase, HPLC + fluorescent assay	[122, 123]
Penicillin V, oxacillin, penicillin G	MAAM, 4-VP, EDMA, MAA-co-TRIM	Noncovalent	Bulk	HPLC stationary phase, Radioligand binding assay	[124, 125]
Sulfamethazine, sulfamethoxazole	MAA, 4-Vpy, MAAM,	Noncovalent	Bulk	HPLC stationary phase	[126-128]
Vancomycin, phenethicillin	Cyclodextrins		Bulk	HPLC	[129]
Ampicillin		Noncovalent	Bulk	HPLC + UV detector	[130]
Cefaclor	Silica gel	Noncovalent	Bulk	HPLC stationary phase	[131]
Cephalexin	2-trifluorom-ethyl acrylic acid (TFMAA)	Noncovalent	Bulk	solid phase extraction (MISPE)	[132]
Labelled penicillin G	MAAM, 4-VP	Noncovalent	Bulk	bifurcated quartz bundle (optical fibers)	[133]
Tetracycline, oxytetracycline	MAA	Noncovalent	Bulk	HPLC stationary phase	[134]
Cefathiamidine	4-VP	Noncovalent	Bulk	MISPE	[135]

conjugate from the imprinted polymer. Following these pioneer reports, many other interesting articles on the HPLC analysis of antibiotics using MIP in the bulk polymer particle formats (Table 1) were increasingly reported. About a decade after the first report, the in situ synthesis method of MIP monolithic stationary phase was developed by Liu et al. [136] for detecting sulfamethoxazole. The MIP showed high surface area and demonstrated selectivity for the target rather than structurally similar analogue.

More recently, Marco Frasconi et al. [137] were probably the first to report about the analysis of antibiotic MIP on a lab-on-chip label-free optical platform such as SPR. In their work, gold nanoparticles (AuNPs) were modified with electropolymerizable monomer and ligands for the association of the target antibiotics (neomycin, kanamycin and streptomycin). The boronic acid-functionalized AuNPs were utilized so as to amplify the surface plasmon resonance after analyte binding, thereby obtaining an enhanced recognition signal. After this, increasing outstanding attempts are being reported on label-free detection platform such as SPR, SAW and QCM.

MIPs are very promising and attractive materials for antibiotics detection due to their relatively low cost of fabrication, robust stability, and selective properties similar to those of natural recognition molecules (e.g., antibody). However, commercializing MIP for general individual usage is still far from being realized. On the one hand, this could be a result of the intrinsic challenges encountered in MIP design including mass transfer limitations, binding sites heterogeneity etc. [138]. Another conceivable obstacle could be the challenge of using these materials within the natural matrix or media where the targets antibiotics are found owing to incompatibility and/or cross reactivity. Therefore, vigorous and continual research efforts are still needed in MIP synthesis to achieve its aim within the shortest space of time.

1.6.1 Sulfamethizole and amoxicillin as antibiotic target molecules

Antibiotics represent a very large family of drugs, which when administered, alter the growth of microorganisms. Various classifications exist for antibiotics and could either be based on their mechanism of action, including inhibitors of cell wall synthesis, protein synthesis, DNA synthesis, RNA synthesis, mycolic acid synthesis, and folic acid synthesis. They could also be classified based on similarities in their chemical structure into beta-lactams (including penicillins and cephalosporins), tetracyclines, sulfonamides, amphenicols, quinolones etc. Because of this wide classes emanating from their varying chemical nature, simultaneous analysis of all these molecules by a single analytical methodology may be almost impossible [120].

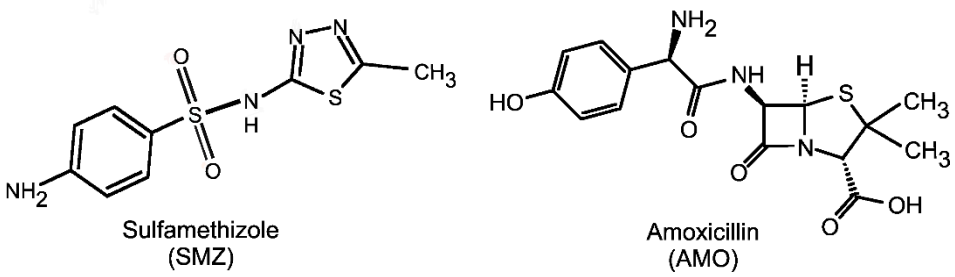

Figure 1.2. Molecular structures of the selected antibiotic target molecules.

Therefore, the antibiotic targets studied in this thesis comprise two widely used antibiotic drugs, sulfamethizole (SMZ) and amoxicillin (AMO), Fig. 1.2. They were selected from two large groups of antibiotics, sulfonamides - SMZ and penicillins - AMO. They possess a broad spectrum of activity; hence, they are used for preventing or treating varying bacterial infections and diseases. Expectedly, their wide usage will, on the contrary, lead to their increasing release or escape into the environment; thus, it is required to monitor their environmental occurrence. Therefore, their selection as modelled antibiotic environmental pollutants for this thesis is anticipated to be a beneficial contribution to the most sought-after detection of such pollutants in the aquatic environment.

Sulfamethizole (SMZ)

Sulfamethizole is extensively prescribed for the prevention and cure of infections caused by both gram positive and gram negative bacteria in humans and animals [139]. It is a short-lived sulfonamides (serum half-lives of 5 - 10 hrs) and poorly soluble antibiotic drug commonly used to treat urinary tract infections in humans, especially those caused by Escherichia coli [140, 141]. It is also a major antibiotic prescribed to pregnant women for the treatment of urinary tract infection within the first two trimesters, although an increased risk of miscarriage has been suggested to exist with sulfamethizole administration in such pregnant women [142]. In veterinary medicines, SMZ is used for aquatic and terrestrial animals to protect or cure them of infectious diseases [143]. Its mechanism of action is by competing with p-aminobenzoic acid, a metabolite that is needed for synthesizing folic acid in the pathogen [144]. SMZ has low absorption in the body, thus about 80% of the original medication can be excreted via urine and faeces [42]. This fact, coupled with its wide administration in human and veterinary medicines, leads to the increase in their environmental presence. SMZ pollutants were previously detected in wastewater, surface and groundwater and sometimes in bottled mineral water [145-147]. Detection or monitoring of SMZ is important to prevent possible danger of its constant exposure. For example, the report of sulfamethizole induced liver injury exists in literature [148].

Amoxicillin (AMO)

Amoxicillin is a semi synthetic broad spectrum antibiotic characterized by the presence of a beta-lactam ring, a carboxyl, an amino and a hydroxyl group. It is a similar analogue of ampicillin, differing only in the inclusion of a p-hydroxyl group in its side chain. Amoxicillin is widely prescribed for the treatment of infections, mainly sinusitis, otitis media (inner ear infection), tonsillitis, respiratory tract infections, typhoid fever and other Salmonella infections. It is also commonly used either alone or in combination with other antibiotics for the treatment of infections of skin, lungs etc. [149]. Due to the low metabolism rate of amoxicillin in the body, its continuous excretion is expected to reach levels that could be of environmental concern [150]. As a consequence, amoxicillin contaminated water has been reported for surface and ground water at concentrations higher than some other pharmaceutical pollutants [151]. Amoxicillin, as well as other aminopenicillins, are not frequently detected in environmental water or wastewater but its increasing usage suggests large chances of escape into the environment. Therefore, non-frequent detection of amoxicillin in

environmental water could be a result of analytical methods incompatibility, or its ring opening degradation process by beta lactamase [152].

Analytical methods mostly used in amoxicillin detection include high performance liquid chromatography (HPLC), capillary electrophoresis and diffuse reflectance infrared Fourier transform spectroscopy. However, these methods may not show high efficiency and the use of toxic agents in the form of solvents, makes these techniques a disadvantage; hence, it is necessary to develop efficient but environmental-friendly approaches [149].

1.7 Evaluation of MIP analytical performance

MIPs by their nature are capable of selective recognition of the target molecules in a matrix mixture with non-target molecules. But in order to evaluate the performance of MIP, characterizing the chemical interactions occurring on the imprinted sites is paramount. Since MIPs are solid materials, characterization methods that may require polymer solutions, such as gel permeation chromatography or solution NMR techniques, may not be adaptable to probing MIP binding sites. Likewise, MIPs' amorphous nature prevents employing crystallographic or efficient usage of microscopic methods. Therefore, physical characterization of MIP is limited to IR spectroscopy, surface area and porosity and/or solid state NMR measurements [153]. Notwithstanding, limited information on the binding sites is obtainable from these techniques.

MIPs are generally heterogeneous in nature. This implies that the binding sites occurring on a MIP material may not all be identical. Heterogeneity in MIP may arise from incomplete utilization of all monomers in pre-polymerization complex formation, thus presenting in the final polymer diverse areas differing in monomer-template complexation units. Also, post-polymerization processes of MIP may contribute to MIP sites heterogeneity, e.g., by binding site damage during template removal, or incomplete template removal at certain sites as compared to others. Nevertheless, characterization of these sites to generate average properties of all existing sites is essential to the investigation of MIP performance [154]. To confront the heterogeneity nature of MIPs while analyzing their binding properties, affinity distribution (plot of number of binding sites versus the association constant) calculation was proposed [155] but the complexity of the method and its sensitivity to experimental errors limit its continuous utilization [156].

To accurately analyze the recognition performance of MIP and optimize its synthesis for improving their overall utility, binding assays that generate binding isotherms that can be modelled by established mathematical equations of binding interactions are essential. Fitting experimental data of binding interactions to appropriate models enables the determination of the properties of the imprinted binding sites, including affinity, kinetic, equilibrium parameters as well as the selectivity of the imprinted material. Moreover, a critical interpretation of such binding parameters requires its comparison with those obtained from a reference material in the form of a non-imprinted polymer (NIP) that is prepared similar to the MIP but excluding the template molecule in the preparation protocol. The NIP, by the virtue of the polymer surface random functionality, is expected to display some weak interaction (binding) with the analyte. Thus, while the MIP response consists of a combination of both specific and nonspecific analyte interactions, the NIP would be

more indicative of nonspecific binding and their differences would therefore portray only specific binding due to the imprinted sites on the MIP. Thus, in sensing applications, a major goal is to maximize the specific interactions by ensuring a higher binding response on the MIP with reference to the NIP. Below, common parameters and interesting properties obtainable from a MIP binding sites are described in brief.

1.7.1 Kinetics

Determination of the binding kinetics is often vital to the evaluation of the strength or affinity of interaction in a molecular binding process. Many sensor developments generally require a short analysis time, hence, fast recognition, and a slow rate of dissociation when exposed to the trace concentration of an analyte. Binding kinetics can provide useful information about the rate constants of reaction, thermodynamics, as well as equilibrium parameters, thereby giving details about the speed and generating data for further analysis. A molecular recognition can be modeled as a reversible interaction between an analyte *A*, and a receptor surface *S*, and can be summarized as follows:

$$A + S \underset{k_d}{\overset{k_a}{\rightleftharpoons}} AS \tag{1}$$

where *AS* is the complex formed between *A* and *S*, k_a ($mol^{-1}s^{-1}$) is the rate of complex formation per unit concentration of *A* and *S*, and k_d (s^{-1}) is the rate of *AS* dissociation back into the reactants *A* and *S*.

At the beginning of the reaction and before complex formation, association and dissociation rates are at the highest and lowest values, respectively. As the reaction progresses and more *AS* is formed, the association rate slows down while the dissociation rate gradually increases. At a particular point in the reaction sequence, a dynamic equilibrium would be reached in which the rate of complex formation will be equal to that of dissociation. Experimentally, to obtain rate constants from a MIP sensor, the rebinding process is monitored and recorded as a plot of binding signal versus reaction time, which can be further analyzed by fitting to an appropriate mathematical model. A typical binding signal generally consists of two phases: an association and a dissociation phase. Since the association phase consists of simultaneous complex formation and dissociation, fitting this part of the signal to a non-equilibrium rate model will generate the rate constants and extrapolate equilibrium concentration of the analyte. To simulate MIP adsorption behavior in this non-equilibrium condition, the first and second-order kinetics (Table 2) [157, 158] are commonly used because of their capacity to model both the rapid initiation and the slow tendency towards a plateau [159].

1.7.2 Adsorption isotherms

Binding or adsorption isotherm refers to the measurement of a polymer binding efficiency over a range of concentration at a fixed temperature. It is usually expressed as a plot of bound analyte concentration against the concentration of free analyte in solution at equilibrium over the range of tested concentration [160]. With an adsorption isotherm, the relationship existing between equilibrium concentrations of

bound and free analytes can be easily estimated by conducting a batch rebinding experimental study within a range of analyte concentration [156]. Fitting of the experimental data points on the binding isotherm to an appropriate theoretical model allows further understanding of the molecular recognition process. This permits the determination of more interesting parameters, including maximum saturation signal (Q_{max}) and equilibrium dissociation constant (K_D). These parameters have been proposed as a common measure of affinity of molecularly imprinted polymers [161]. Several theoretical models are available for fitting binding isotherm data and the choice of an ideal model could be either empirical based or by theoretical knowledge of the properties of binding sites created within the polymer matrix. Generally speaking, MIP binding sites are characterized by heterogeneity, in which case the binding sites may differ in the geometry of functional groups, accessibility or polarity of its local environment [154], which in turn leads to variation in the binding capacity across the matrix.

The Langmuir and Freundlich isotherm models (Table 2) are two mathematical models commonly employed in evaluating molecular recognition. While Langmuir isotherm is strictly based on the assumption of homogeneity of adsorption sites, Freundlich isotherm fits heterogeneous binding surfaces much better. Thus, since MIPs generally have a certain degree of heterogeneity, the Langmuir model may not give a good fit to the experimental data. Although the Freundlich isotherm model provides a much better fit to lots of MIPs' experimental data, it is limited to a certain range of concentrations. Likewise, its inadequacy to accurately model the saturation region of the adsorption isotherm and inability to describe the behavior of MIPs with increased homogeneity constitute its restrictions [156]. Notwithstanding, a composite model of these two namely Langmuir-Freundlich (LF) isotherm (Table 2) was shown to define more accurately both homogeneous and heterogeneous MIP surfaces even at extremes of concentrations [101]. This is because the LF isotherm model may reduce to either the Langmuir or the Freundlich model at certain conditions and thus could be successfully used in modeling the adsorption behavior of MIPs.

The equilibrium dissociation constant K_D, (the analyte concentration which gives 50% of maximum adsorption response) is an important parameter that reveals the affinity of the MIP receptor sites for the analytes. A lower K_D value indicates a lower dissociation tendency, hence, a higher affinity. Thus, a fit of an adsorption isotherm can give information relating to the affinity of the imprinted cavities created within the polymer matrix during MIP preparation.

Table 2: Mathematical equations of kinetic and equilibrium adsorption models commonly employed in characterizing MIP recognition properties

	Equation
Kinetic Model	
First-order	$Q = Q_{eq}[1-e^{-kobs*t}]$
First-order with bulk shift	$Q = Q_{eq}[1-e^{-kobs*t}] + BS$
Second-order	$Q = [Q_{eq}^2 k_2 t]/[1+Q_{eq}k_2 t]$
Isotherm Model	
Langmuir	$Q = Q_{max}C/(C+K_D)$
Freundlich	$Q = Q_{max}C^m$
Langmuir-Freundlich	$Q = Q_{max}C^m/(C^m+K_D)$

1.7.3 Imprinting factor

A common parameter for estimating the performance of an imprinted recognition material is the imprinting factor (IF). It describes the adsorption capacity of a MIP towards a target relative to the NIP; thus, it is mathematically calculated as the ratio of an analyte binding capacity on the imprinted polymer to that on the non-imprinted reference under identical conditions (Eq. (2)). In this equation, Q_{MIP} and Q_{NIP} may either be the maximum or equilibrium adsorption capacities on both MIP and NIP surfaces.

$$IF = Q_{MIP}/Q_{NIP} \quad (2)$$

It is expected that an MIP should display IF greater than 1. This is because the NIP is envisaged to have a greater monomer self-association during the pre-polymerization stage than the MIP, thereby reducing the number of free functional groups, hence, exhibiting lower analyte recognition. More significantly, the preformed imprinted sites existing on the MIP should further provide a stronger affinity to the target molecules, thus increasing analyte binding on the MIP. Therefore, IF could be a rough validation of the presence of imprinted sites in a MIP.

Although the IF allows a quick estimation of the relative adsorption capacity of the imprinted polymer, it may not be sufficient for indicating the overall performance of MIP. It has been suggested that the polymer matrix resulting in a high efficient MIP for a particular target analyte may also display a correspondingly increased interaction on the NIP [162]; therefore, further estimation of MIP binding characteristics combined with the IF is essential in MIP evaluation.

1.7.4 Selectivity

Another very important parameter for evaluating MIP performance is the selectivity. Selectivity of a sensor determines its ability to identify and bind the target analyte in a solution mixture with other molecules (interferents), while discriminating against others. To obtain information about the MIP sensor selectivity, the selectivity coefficient/factor, k or α is usually calculated. This is computed by the ratio of response resulting from the rebinding of interferent molecules on the MIP to that of a target analyte under identical experimental conditions Eq. (3):

$$k = (Q_i)/(Q_t) \quad (3)$$

where Q_i and Q_t are adsorption responses of MIP towards the interferent and target molecules, respectively.

The selectivity factor could also be calculated from the ratio of IF values of an interfering substance to that of the target molecules. The IF values for both interferent and target molecules could be calculated from their binding responses on the MIP and NIP using Eq. (2) as described previously.

1.8 Label-free sensor platforms

Analytical chemists are continually faced with the challenge of developing accurate, reliable, cost effective and quick detection methods for analysis of substances for several aims, such as environmental monitoring, among others. However, as stated

earlier, the disadvantages inherent in the traditional analytical techniques limit their potential utilization. More so, some developed techniques including enzyme-linked immunosorbent assays (ELISA) and radioimmunoassay could still present easily automated analytical methods; they require the use of labels as indicators, thus demanding more time and increased cost of analysis, an undesirable effect in sensor development. More limiting is the fact that these methods may not differentiate between association and dissociation stages of binding interactions [163]. Label-free detection provides an alternative approach without requiring the use of chemical labels, hence, saving time and cost. Label-free detection ensures a simple protocol for sensing by eliminating the complexity that may be encountered in the use of labelling, such as the interaction of label with binding sites, inhomogeneous distribution of label around the target molecule (e.g., in large protein molecules) and disruption of labels by the analysis condition (e.g., fluorescence label quenching). Also, labels were found to modify the chemical structure of the analyte (e.g., native proteins) and influence their hydrophilic-lipophilic balance in aqueous media, thereby altering the interfacial activity of such labelled protein [164]. Essentially, label-free detection techniques unlike the labelled ones do not simply establish the presence of detector molecules. Rather, they allow a direct and real time monitoring of binding interaction occurring on the sensor surface [165]. This is realized by converting the chemical interaction between the analyte and the receptor to measurable signals, including changes in the optical, piezoelectric or electrochemical properties of the sensor. Furthermore, such label-free sensor platforms as quartz crystal microbalance (QCM), surface plasmon resonance (SPR) and surface acoustic wave (SAW) have demonstrated high efficiency in the analysis of both association and dissociation stages of molecular interaction. As a result, kinetic and equilibrium data can be quickly obtained within a short period of time with an acceptable level of accuracy. Therefore, combining such label-free sensors with thin MIP films certainly holds a great beneficial potential for environmental monitoring and detection.

1.8.1 Acoustic wave sensors

Acoustic wave sensors including QCM and SAW, enable to modulate acoustic waves propagating through or on the surface of the sensor tansducer. These waves interact with the surrounding in a way to supply measurable information regarding the properties of the medium. The medium around the vicinity of the wave propagation can affect the travelling wave either by perturbing its velocity or damping its amplitude [166]. Information obtainable from such interactions may include density, viscosity, surface mass, and temperature of the medium. Likewise, information about biological interactions can be obtained following sensor surface functionalization by appropriate receptors for the target analytes [167]. Varying categories of these sensors exist, differing in the nature of wave propagation but similar in decreasing frequency (frequency shift) in relation to an adsorbed mass [168]. However, based on the utilization of the piezoelectric effect, two major categories can be observed, bulk acoustic wave (BAW) and the surface acoustic wave (SAW). While BAW propagates through the entire interior of the substrate, the propagation of the SAW waves is confined to the surface.

Quartz crystal microbalance (QCM)

Quartz crystal has unique properties discovered by Jacques and Pierre Curie, in which the application of a mechanical stress unto a quartz generates an electrical potential across the material whereas a mechanical strain is produced after an electrical potential is applied to it [169]. This effect called the piezoelectric effect is the basic principle for the operation of the quartz crystal microbalance (QCM). QCM generates bulk acoustic wave (BAW) oscillating in a mechanically resonant shear mode by the application of an alternating high frequency electric field unto electrode metallic layers (e.g., gold), which are usually deposited onto both sides of the disk (Fig. 1.3). This piezoelectric property of quartz is used to measure the mass of a material deposited on its surface by a corresponding change in frequency. The resultant resonant frequency of QCM after mass deposition would be a combined influence of the thickness of the quartz, the underlying electrode and the deposited mass. Therefore, a difference (frequency shift) between the unloaded fundamental frequency of QCM and the resultant frequency after mass deposition would only be due to the influence of the deposited mass. Interestingly, the Sauerbrey's equation (Eq. (4)) established the relationship between the frequency and mass changes taking place on QCM:

$$\Delta f = -(f_0^2 \Delta m)/N\rho = -C_f \Delta m \quad (4)$$

where Δf is the resonant frequency change (Hz), f_o, fundamental frequency of the crystal (Hz), Δm, mass change (g/cm^2), N, frequency constant for quartz (167 kHz·cm), ρ, density of quartz (2.65 g/cm3), C_f, sensitivity factor (for 5 MHz quartz crystal, 56.6 Hz·µg-1·cm^2).

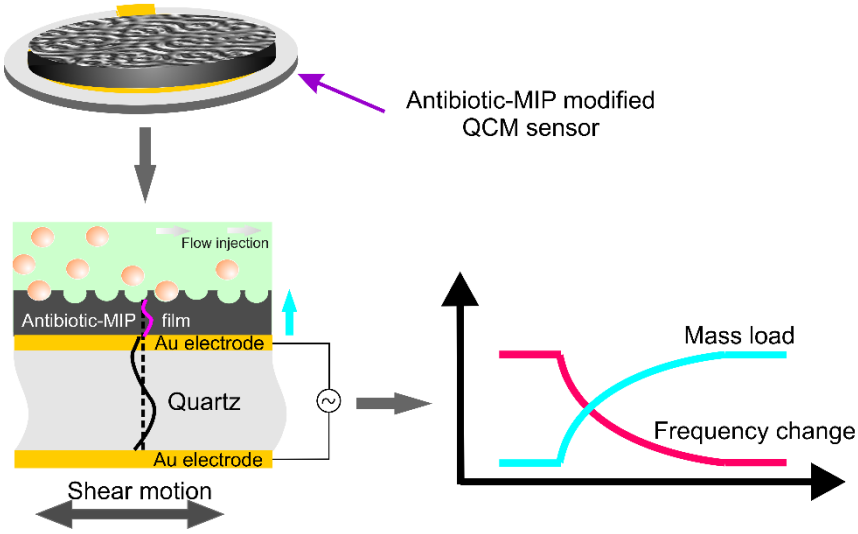

Figure 1.3. Schematic of QCM operating principle.

QCM sensor has been used for measurements in vacuum and gas. Similarly, because the thickness-shear mode is predominant in QCM, its operation in liquid is made possible, in which case the frequency shift is a function of the viscosity and density of the liquid [170]. Furthermore, the possibility of combining the QCM

technique with electrochemistry to obtain an electrochemical QCM system (EQCM) facilitates a simultaneous evaluation of mass and electrochemical data in one experiment.

However, QCM measurements are mostly carried out at room temperature with few reports to indicate their potential utilization for high and very low temperature environment [171, 172]. This is because at low temperature, quartz displays excellent properties, such as high mechanical quality factor (i.e., high sensing precision), high electrical resistivity and low temperature coefficient [173] which disappear at very high or low temperature. Due to the distinctly sharp nature of the resonance frequency; hence, a high precision in the sample analysis, detection and/or resolution of trace amounts of deposited material per unit area of the surface is made possible. Thus, QCM in combination with a flow injection analysis (QCM-FIA) is known as a simple but powerful technique for the in situ monitoring of binding interaction between an analyte and a recognition layer on the quartz crystal [174]. Owing to the adaptability of QCM in sensor analysis and the ease of interfacing with the MIP recognition layer, the use of QCM interfaced with MIP in the detection of numerous analytes including antibiotics has been broadly reported and reviewed [98, 99, 165, 175, 176]. Moreover, the possibility to design and use portable, energy efficient piezoelectric sensors in environmental monitoring makes QCM combined with MIP attractive for antibiotics detection in this research [165].

Surface acoustic wave (SAW)

In a SAW sensor device, the acoustic wave is generated by the application of an AC voltage to the interdigitated transducer (IDT) that is composed of two interlocking comb-shaped metallic electrodes patterned on the piezoelectric substrate (Fig. 1.4) [177]. Similar to QCM, an adsorbed or accumulated mass will influence a frequency shift. Notably, a higher sensitivity may be obtained in a SAW sensor as compared to QCM because the former operates at a higher frequency (100 MHz to a few GHz) and its surface bound acoustic wave should be more easily perturbed by surface interactions as compared to the bulk wave.

The Rayleigh acoustic wave appears to be the most commonly used in SAW sensor devices; however, due to losses from radiation, they are unsuitable for liquid operation [168]. Love waves, on the other hand, are adaptable for utilization in liquid operation because they consist of shear-mode vibrations, and hence are found in many SAW devices adapted for liquid measurements [178, 179]. For sensing purposes, SAW devices are usually coated with a thin film of molecular receptor (e.g., MIP) and connected to a frequency counter. Interaction between the acoustic wave and a medium leads to a corresponding change in wave velocity and amplitude. The phase is shifted in response to velocity change and amplitude shift respond to the attenuation of the wave; thus, both changes are monitored in a measurement experiment [177]. SAW sensors have been shown to be extremely useful for the analysis of any kind of target molecules, including organic vapors [180], inorganic gases [181] and bioanalytes [100].

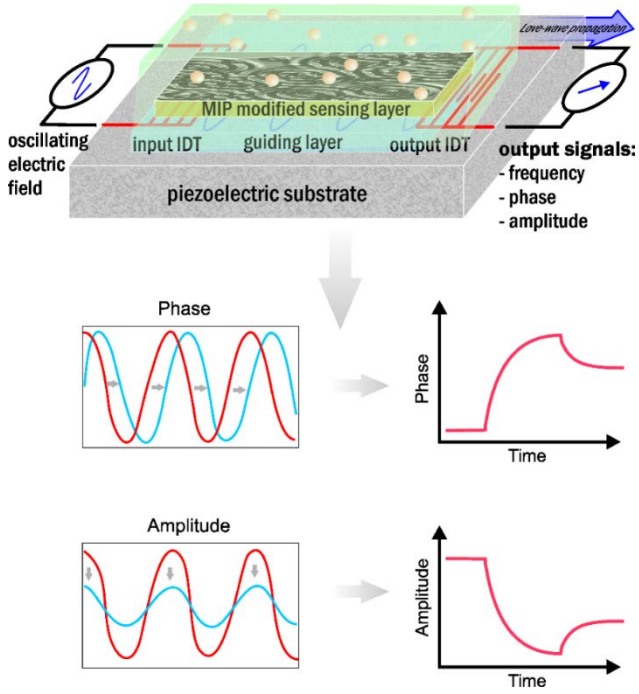

Figure 1.4. Schematic of the basic operating principle of SAW sensor.

1.8.2 Surface plasmon resonance (SPR)

Surface plasmon resonance (SPR) belongs to the group of sensors generally referred to as optical sensor transducers. Optical transducers operate based on the principle that molecular recognition reactions cause alteration in the structural properties of certain substances, leading to a corresponding change in their optical properties [182]. SPR spectroscopy monitors biomolecular interactions taking place at a close vicinity on the surface of a transducer by following the change in the refractive index corresponding to the binding interaction [183]. The SPR set-up has a basic configuration shown in Fig. 1.5 where a monochromatic plane polarized light is shone through a prism unto a sensor containing a thin metal film, sandwiched between the sensor and an external medium of different refractive indices. Because part of the incident light is reflected by the metal at angles dependent on the incident angle, the plane polarized light can be incident at an angle in which the reflected light is a minimum, i.e., when total internal reflection occurs.

At this angle, called the resonance or SPR angle, the electrons from the metal are excited (surface plasmon) and oscillate in a wave-like manner (evanescent wave), propagating perpendicular to and with energy concentrated at the close vicinity of the metal surface [184]. The energy transfer between the incident beam and excited surface plasmons reduces the reflected light intensity, which is measured as the SPR signal or sensorgram, a plot of response unit (RU or RIU) against real time, in seconds by a photodetector.

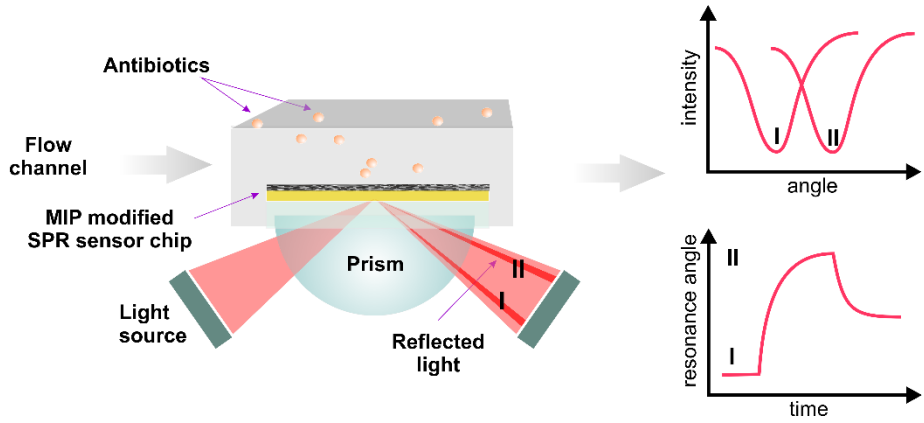

Figure 1.5. Schematic of SPR configuration and working principle.

Because the SPR angle is closely related to the refractive index on the immediate environment of the sensor, the angle and the SPR signal changes could be related to the binding adsorption or change in medium properties [185]. With SPR sensor, information regarding the amount of bound analyte, binding affinity and kinetics of interactions can be easily obtained [186]. However, like other sensing platforms, SPR requires surface modification to allow its selective recognition. For this purpose, MIP is a well suitable recognition layer that can be easily immobilized on the SPR sensor. This accounts for the plethora of publications for SPR detection using MIP as the selective elements [187]. Furthermore, the possibility to produce SPR in miniaturized or portable formats may have contributed to the wide utilization of SPR by numerous research groups [188] and their suitability for antibiotics environmental monitoring.

1.9 Summary of the literature review and objectives of the study

Environmental pollution is a well-established global challenge. The water body may contain a larger share of pollutants due to the eventual end up of most pollutants in environmental water. Thus, exposure of humans, animals and other organisms to contaminated water may constitute a potential threat to human health and ecosystem sustainability. Antibiotics have been identified as a group of pharmaceuticals with environmental water pollution potential. This is an effect of their wide utilization in human and veterinary medicines as well as agriculture. Antibiotics-contaminated water is hazardous to humans and the ecosystem in general, due to their known inhibition of biological functions. Hence, a prolonged exposure to antibiotics even at low concentration could result in acute or chronic toxicity, thus, leading to the onset or deterioration of various disease conditions. Other than this menace, the most commonly known effect of antibiotics environmental pollution is the inducement and/or exacerbation of resistant strains of microorganisms that will eventually lead to the vicious cycle of constant vulnerability to infections and continuous production of more potent antibiotic medications. The overall effect of these may be observed in a prolonged duration of illness, increased cost of healthcare, disability, and death.

From the foregoing, sensitive, selective and cost-effective analytical methods to monitor and detect antibiotics in aqueous environment are essential. Traditional

methods, such as solid phase extraction, chromatography, mass spectrometry, enzyme-linked immunosorbent assay, are currently employed in the determination of such pollutants. However, inherent disadvantages of such methods, including the requirement of large, immobile instrumentation, complex sample preparation, lack of target specific selectivity as well as low shelf-life, constitute their limitations. Molecularly imprinting technique presents a cost effective method to design very sensitive and selective robust recognition layer called molecularly imprinted polymers (MIPs). MIPs have been reported to demonstrate recognition potential similar to natural recognition elements with much better stability. Therefore, tailoring MIP design towards antibiotics detection in water could offer a prospective analytical tool for a reliable determination of such molecules in water. MIPs exist in several configuration formats yet, for sensing purposes, thin MIP film represents the best format mainly due to the low diffusion path through which an analyte has to pass into the binding sites existing in the MIP.

To characterize thin films of MIP for analyte recognition capability, their integration with sensor transducers that convert the molecular recognition event to analyzable signals is very essential. Label-free sensing platforms provide a direct possibility to monitor molecular interaction occurring on the surface of a recognition layer interfaced with a sensor transducer. Thus, such label-free platforms allow the real-time monitoring and recording of analyte binding events on a MIP film deposited on its sensing surface with satisfactory precision. Piezoelectric (QCM, SAW) and optical (SPR) transducers are especially suitable for investigating MIP recognition since they present the ease of kinetic and equilibrium analysis and the feasibility to study the selective properties of a prepared MIP layer. Fortunately, several techniques exist for synthesizing and incorporating a thin film of MIPs on sensor transducers that will ensure a sturdy stability. Examples of such techniques include electrochemical synthesis and sol-gel synthesis coupled with spin/deep coating methodologies. The advantages of such methods, including fast synthesis, room temperature processability and the ease in controlling the deposition process, make these techniques quite outstanding.

Since SMZ and AMO belong to two large antibiotic groups with wide utilization in medicines and agriculture, their escape into the environmental water body, hence, contamination of drinking water is highly probable. Thus, achieving MIP chemosensors with label-free sensor transducers such as QCM, SAW and SPR that are targeted towards detecting these antibiotic molecules in water may be a great feat that could constitute or contribute to the needed breakthrough in the fabrication of selective antibiotic pollutants detection.

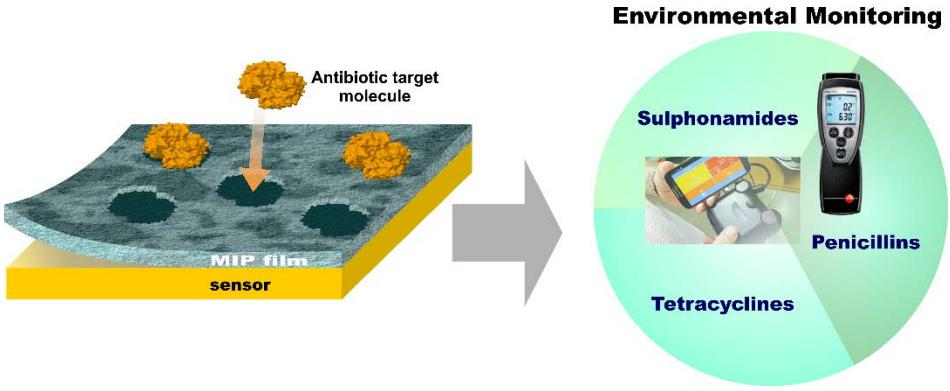

Figure 1.6. MIP-sensors as a tool to monitor antibiotic entry into the natural environment.

The overall aim of this thesis research is to fabricate thin polymeric films as a recognition layer on QCM, SPR and SAW sensor transducers for a robust and selective antibiotic detection in aqueous media using molecular imprinting technology (Fig. 1.6). Thus, to achieve this aim, the following objectives are specified:

a. To develop electrosynthesis and/or sol-gel methodologies that allow a direct fabrication of SMZ-MIP and AMO-MIP films on the surface of QCM, SAW and SPR.
b. To probe and validate the recognition capabilities of the SMZ-MIP and AMO-MIP by analyzing their responses upon interactions with both SMZ and AMO.
c. To analyze the performance of SMZ-MIP and AMO-MIP in low analyte concentrations to determine their limits of detection.
d. To analyze the selective properties of the SMZ-MIP and AMO-MIP in the representative or prototypical aqueous media so as to validate their suitability for use in the target environment.

2. Experimental

2.1 Strategy for the preparation of the antibiotic MIP films

The approach for fabricating the antibiotic MIP films is based on the principle of the molecular imprinting technology. The imprinting process can be categorized into the following consecutive methodological steps:

a. Functional monomer selection
b. Polymer matrix formation
c. Interfacing of antibiotic containing films with sensor transducers
d. Formation of antibiotic molecular imprints in the polymer matrix
e. Evaluation of the antibiotic-MIP

2.2 Functional monomer selection

The functional monomers used for optimal preparation of the antibiotic MIP films was chosen from randomly selected monomers including electropolymerizable monomers such as pyrrole (Py), 3,4-ethylenedioxythiophene (EDOT), and m-phenylenediamine (mPD). Adequate information guiding the rational selection of the optimal monomer for fabricating MIPs with specific antibiotic recognition properties were obtained by employing a combination of computational modeling and spectroscopic studies. For the computational study, monomer-antibiotic complexes were generated by GaussView 5.0.9 software followed by optimizing their geometries using the semi-empirical PM3 method with Gaussian'09 software so as to predict hydrogen bonds formation. Density functional theory (DFT) method at B3LYP/6-31+G level was utilized in calculating the conformational optimizations and binding energies for the complexes with the help of Gaussian'09 software. Spectroscopic study of the monomer-antibiotics interaction complex was achieved with nuclear magnetic resonance (NMR) employing the Bruker SMART X2S benchtop diffractometer model. Sample solutions of individual monomer and antibiotic target as well as their mixture (1:1 molar ratio) were prepared in deuterium oxide (D_20) solvent.

2.3 Polymer matrix formation

Polymer matrices used for MIP preparation in this work were formed either by in-situ electrochemical polymerization or sol-gel technology. Electrochemical polymerization of m-PD was conducted in a custom-designed three electrode cell, in which the gold electrode of QCM or the gold sensing surface of SAW served as the working electrodes. A spiral shaped wire or rectangular shaped plate of platinum was used as counter electrode and $Ag/AgCl/KCl_{sat}$ as the reference electrode. All three were connected to an electrochemical workstation (Reference 600, Gamry Instruments, Inc., USA). The synthesis of a hybrid sol that will form the hybrid polymer involves free-radical co-polymerization of methacrylamide (MAAM), an organic monomer and vinyltrimethoxysilane (VTMOS), an inorganic coupling agent in the presence of the template molecules (AMO). The free alkoxy group of VTMOS located at the surface of the polymer was used for the subsequent sol-gel hydrolysis and co-condensation with

a functional alkoxide precursor, tetraethoxysilane (TEOS) to form a highly cross-linked hybrid sol.

2.4 Interfacing of antibiotic containing films with sensor transducers

Thin films of P(mPD) and P(mPD)/SMZ were electrodeposited on the sensing surfaces of SAW chip while P(mPD) and P(mPD)/AMO were electrodeposited on the gold electrodes of QCM sensor. Both QCM and SAW chips were placed into either 25 mL or 2 mL electrochemical cell designed to expose only the gold electrode of either 5 MHz QCM (Max-tek, Inc.) or sensory elements of SAW chips (NanoTemper Technologies GmbH, München, Germany), respectively, to the synthesis solution. The electrodeposition on the electrodes was achieved by the application of a constant potential (0.6 V vs Ag/AgCl/KCl_{sat}) to the electrodes previously exposed to PBS buffer solutions containing either 5 mM mPD or mixture of 5 mM mPD and 5 mM AMO for the QCM or 5 mM mPD and 3.5 mM SMZ for the SAW.

To monitor the electrodeposition on the QCM to ensure the same thickness of films for P(mPD) and P(mPD)/AMO, an electrochemical quartz crystal microbalance (EQCM) was utilized. This was performed by using the QCM100 system (Stanford Research Systems, Inc., Sunnyvale, CA, USA) that is connected to the reference 600TM potentiostat (Gamry Instruments, Inc.) and the PM 6680B counter (Fluke Corporation). The instrumental setup was previously described by Syritski, et al. 2008 [23]. Following this arrangement, the film deposition was continued until the required frequency shift was achieved, the thickness of which was estimated by the Sauerbrey equation (Eq. 4 Section 1.8.1).

To control the P(mPD) and P(mPD)/SMZ electrodeposition process at 0.6 V on the SAW surfaces, an electrical charge, previously obtained from spectroscopic ellipsometric calibrations of thickness vs applied charge, was passed through the electrode of the sensor. Measurement of film thickness was determined by a spectroscopic ellipsometer (SE 850, Sentech Instruments GmbH, Berlin, Germany). Ellipsometric Psi and Delta spectra (350 - 850 nm) at an incidence angle of 70° were measured in ambient air on three different spots of each film. SpectraRay 3 permitted spectra evaluation by a simultaneous fit on the film properties (thicknesses and dielectric function) utilizing air/film/gold optical layer model. The dielectric function of the film (Epsilon) was modeled using a constant part and a Gaussian oscillator to describe the electronic transitions in the benzene ring of the polymer. After electrodepositions, the electrodes of the sensors were rinsed with distilled water before drying under nitrogen stream.

To interface a sol-gel derived hybrid film with the gold sensor of SPR chip, the prepared hybrid sol was spin coated and dried on the SPR sensor surface. The coating was performed in a nitrogen atmosphere by a dynamic dispense of the sol on the gold surface of SPR held by vacuum down the chuck of a Laurell spin coater (LAURELL WS-650MZ-23NPPB spin coater). Following spin coating, the film was allowed to polymerize and dry in vacuum. To ensure a reproducible thickness of films, film thickness was controlled by varying the rotational speed (in RPM) of the spin coater and correlating the speed of deposition with spectroscopic ellipsometry measurements to obtain a calibration plot of thickness vs speed (in RPM) of spin coating.

2.5 Formation of antibiotic molecular imprints in the polymer matrix

To reveal the imprinted binding sites, it is required to remove the entrapped template molecules. This is attained through the washing out procedure by selecting an appropriate washing solution. To remove SMZ or AMO from the P(mPD)/SMZ or P(mPD)/AMO films, respectively, their modified SAW or QCM electrodes were immersed in acetic acid-methanol (1:3) or (1:1) solution mixture under constant stirring for 24 hrs. By this procedure, SMZ-MIP or AMO-MIP films were generated. In the case of the hybrid film on the SPR sensor, removing the AMO molecules entails more harsh treatments, including the use of acetic acid-methanol (1:9) solution mixture under constant stirring and heating at 60 ^{o}C, to form a hybrid AMO-MIP film. After rinsing thoroughly by distilled water, the antibiotic-MIP films modified sensors were subjected to rebinding studies.

2.6 Evaluation of the antibiotic-MIP

2.6.1 Rebinding study by SAW

The ability of the prepared SMZ-MIP to recognize SMZ was studied by a SAW sensor system (SamX, NanoTemper Technologies GmbH, München, Germany) at 25 ^{o}C. The system is able to handle two SAW chips, each with four sensing elements and its microfluidics (consisting of autosampler, syringe pump, internal valves, bottle holder with fluidic interconnects, as well as two fluidic cells) provide the possibility of delivering analyte solutions to the SMZ-MIP modified sensor elements either individually or in serial fashion. The modified SAW sensors, after loading into the SAW system, were equilibrated with running buffer (PBS, pH 7.4) at a flow rate of 25 µL/min until a stable baseline was established. Subsequent injections of PBS solutions containing SMZ concentrations of 10.2, 25.6, 64, 160, 400, and 1000 µM were realized and the response signals were monitored.

The data of the recorded sensorgrams were analyzed using Origin 9.1 (Northampton, MA) after data export. The analysis involves the fit of the data to the first order binding model to determine the equilibrium responses for SMZ-MIP and NIP films, which were later used to plot the adsorption isotherms. Maximum binding responses and the K_D values were then obtained from the fitting parameters. After rebinding, surface regeneration was made possible by repeating the washing out process in the acetic acid-methanol (1:3) solution mixture.

2.6.2 Rebinding study by QCM

To study the rebinding of AMO target molecules on the QCM fabricated AMO-MIP film, QCM coupled with a flow injection analysis (QCM-FIA technique) was utilized. The QCM-FIA system comprises programmable precision syringe pumps (Cavro XLP 6000®XLP 6000, Tecan Nordic AB, Mölndal, Sweden), a motorized six-way port injection valve (C22-3186EH, VICI®Valco Instruments Company Inc., USA) that is controlled by a microelectric actuator and a small volume (150 µL) axial flow cell attached to the QCM sensor holder (Stanford Research Systems, Inc.). Injection of analyte sample solution was achieved by a 5 mL disposable plastic syringe. The system has all its elements connected to a PC and is controllable using software written in

Labview. With this setup, real-time monitoring of molecular interactions occurring on the QCM sensor surface was achievable, studied at a constant temperature of 25 ^{o}C. To achieve a stable baseline before analyte injections, a degassed PBS buffer solution (pH = 7.4) was allowed to flow over the sensor at a rate of 25 µL/min until a consistent baseline of the resonance frequency was reached. After this, subsequent injection of AMO sample concentrations at 1.6, 8, 40, 200, and 1000 µM in PBS buffer was accomplished through an injection loop (500 µL). As described previously, the rebinding experiment follows after removing the template molecules in a washing out process in acetic acid-methanol (1:1). Data analysis is the same as described for the SAW rebinding study.

Similar rebinding study was conducted for an SMZ-MIP-modified QCM sensor that was previously modified with a dextran layer (SMZ–MIP(Dex)). For this rebinding study, the QCM sensor modified with SMZ–MIP(Dex) film was loaded unto the QCM-FIA system. After equilibration and baseline stability with PBS (pH 7.4) buffer at a flow rate of 40 µL/min, injections of 0.04, 0.2 and 1 mM SMZ concentrations in PBS were performed and the changes in frequency (frequency shift) were monitored and analyzed.

2.6.3 Rebinding study by SPR

To evaluate the performance of the prepared hybrid AMO-MIP towards AMO target detection, the prepared film interfaced with the SPR sensor was characterized at a constant temperature of 25 ^{o}C for its AMO recognition properties. This was achieved by monitoring the binding events using a two channel SPR system (SR7500DC, Reichert Technologies Inc., Depew, NY, USA). PBS (pH 7.0) was used as the running buffer and to prepare the analyte solutions. After baseline stability, response signals induced by the refractive index changes were obtained and recorded, following the autosampler injection of analyte concentrations from 12.8 nM to 8 µM at a constant flow rate of 25 µL/min. To further reduce nonspecific interaction, 0.02% Tween-20 was added to the PBS buffer (pH 7.0). The data were collected, exported to origin and analyzed by fitting to the first order kinetic model and the equilibrium responses obtained were used to plot adsorption isotherms, which were further analyzed by fitting to an adsorption isotherm model, as described previously.

3. Results and discussions

3.1 Functional monomer selection

The recognition performance and/or selectivity of a MIP greatly depend on the choice of a monomer. Thus, selecting monomer(s) possessing complementary chemical functionality to the template molecule, so as to form quite strong noncovalent interactions between them, is very critical. The noncovalent imprinting strategy is chosen instead of the covalent approach because the former does not restrict the choice of analyte and it allows easy removal of the template by the washing out process [189]. Therefore, to prepare antibiotics selective MIPs (SMZ-MIP, AMO-MIP), a study validating the molecular complexes existing between the template and potential functional monomer molecules is very important. This may be realized by combining theoretical computational modeling and experimental spectroscopic analysis [190]. To illustrate this, the choice of selecting the electropolymerizable monomer is briefly described. To select the optimal electropolymerizable functional monomer, a random collection of electropolymerizable monomers was executed. These monomers, including pyrrole (Py), 3,4-ethylenedioxythiophene (EDOT), and meta-phenylenediamine (mPD) (Fig. 3.1), were studied as potential functional monomers for SMZ-MIP and AMO-MIP formation.

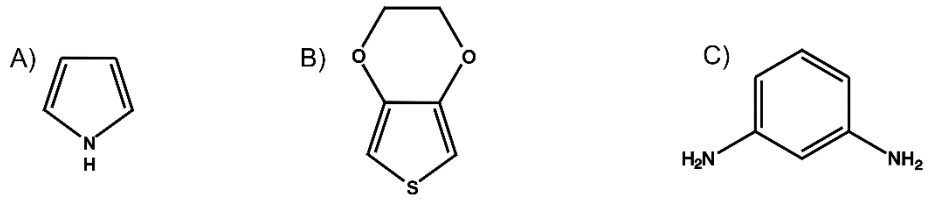

Figure 3.1. Electropolymerizable monomers examined for the preparation of antibiotic MIPs.

3.1.1 Computational modeling

To estimate the strength of interaction between SMZ or AMO template molecules and each monomer, the binding energies and hydrogen bond lengths of their prepolymerization complex were evaluated using the density functional theory (DFT) method. This computational method of estimating strength of interaction is very commonly used among MIP researchers. Using a semi-empirical PM3 method, an optimized geometry of the prepolymerization complexes was generated. An example is shown in Fig. 2, Paper I for SMZ-mPD interaction complex. This geometry permits the estimation of the lengths of hydrogen bonds and the binding energy, calculated using the DFT method. It was found that mPD generates the strongest interaction complex with both SMZ and AMO. This was observable from the higher values of total binding energy and the relatively shorter length of hydrogen bonds (Table 3). Thus, by the computational result, a more selective MIP is expected to be achieved using mPD as the functional monomer for SMZ-MIP and AMO-MIP preparation.

Table 3. Total binding energies and hydrogen bond lengths of monomer-template interaction complex, as obtained from computation calculations

Monomer	Binding Energy of Template-Monomer Complex (kJ/mol)		Lengths of hydrogen bonds of Template-Monomer Complex (Å)	
	SMZ	AMO	SMZ	AMO
mPD	181.203	273.053	1.74	2.54
Py	80.256	63.013	2.62	1.86
EDOT	-	8.401	2.79	4.15

3.1.2 Spectroscopic study

To further confirm the theoretical result, an experimental study of the molecular interactions existing between the template molecules (SMZ and AMO) and mPD was conducted. This included nuclear magnetic resonance (NMR) or Ultraviolet visible (UV-Vis) analysis of the template/monomer complex. The ^{13}C NMR analysis carried out on the solution of individual SMZ or AMO and mPD compounds as well as the template-monomer mixture showed no appearance of new peak(s), hence, the absence of covalent interaction (Fig. 3.2(a) and (b)). This confirms that the SMZ-mPD and AMO-mPD interactions are mainly due to noncovalent rather than the covalent bond formation. In addition, the UV-Vis study of the absorption spectra of AMO or mPD and their mixture (1:1 molar ratio) further confirmed the presence of prepolymerization complex formation, as indicated by the appearance of a new absorption band in their solution mixture (Fig. 3.3).

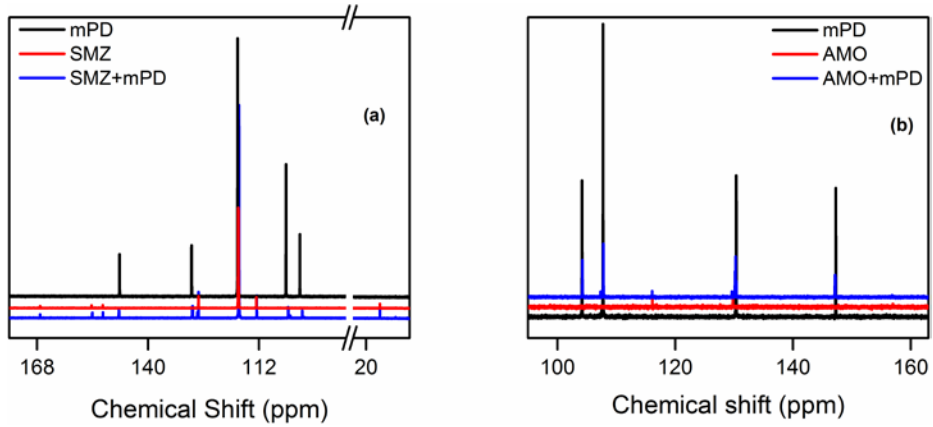

Figure 3.2. (a) ^{13}C spectra of mPD, SMZ and SMZ+mPD mixture (1:1 mass ratio) in D_2O (Paper I) (b) ^{13}C spectra of the mPD, AMO and AMO+mPD mixture (1:1 mass ratio) in D_2O (Paper II).

Thus, by the combined computational and spectroscopic experimental studies, mPD was found to be the more suitable monomer for SMZ-MIP and AMO-MIP formation and was consequently selected as the functional electropolymerizable monomer for this work.

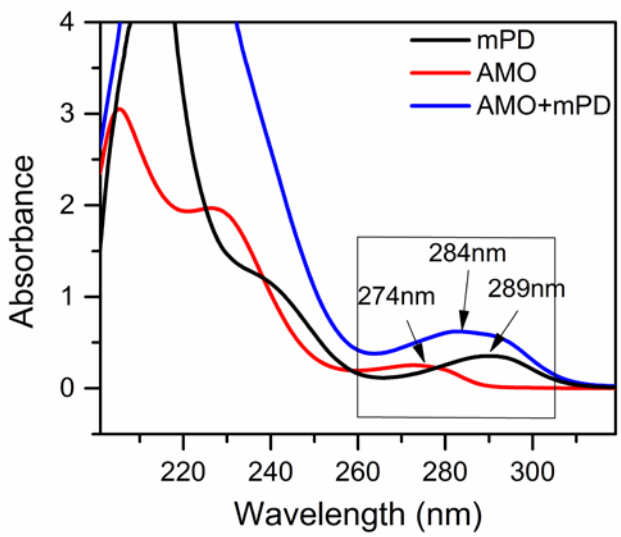

Figure 3.3. UV-Vis spectra of mPD, AMO and their mixture in the concentration ratio 1:1 in PBS buffer solution (pH 7.4) (Paper II).

3.2 Polymer matrix formation and integration with sensor

Thin films of polymer matrices to be used for antibiotic imprinting in this work were prepared either by electropolymerization or sol-gel synthesis techniques. A uniform (homogeneous) thin polymer film synthesis is required in the preparation of MIP chemosensor to be used for sensing purposes. This is essential to achieve a reliable characterization of MIP performance. Thus, during the synthesis of antibiotic-MIPs by electrochemical or sol-gel techniques, focus was on the formation of a homogeneous polymer film.

3.2.1 Film formation by electrosynthesis

Electropolymerization is a well-established method for interfacing a MIP film layer on a sensor transducer with a precise control over the deposited film morphology and thickness. To achieve an optimal condition to synthesize a homogeneous electropolymerized film, P(mPD) polymerization was conducted in both organic, e.g., acetonitrile (ACN) and aqueous (PBS buffer) solutions. The monomer concentrations and electrochemical conditions were also varied to obtain the optimal polymerization conditions. Thus, several modes of potential stimulus were applied, including potential pulse, cyclic voltammetry and potentiostatic modes. It was observed that a homogeneous film could not be achieved in ACN while in PBS buffer (pH 7.4), a very homogeneous film was obtained. Also, electrosynthesis utilizing the potentiostatic mode resulted in a significant increase in film growth rate as compared to potential pulse and cycling (Fig. 3, Paper II).

Thus, for an optimal formation of P(mPD), the electrosynthesis was achieved in PBS solution using the potentiostatic method at 0.6 V. To ensure the preservation of the structural integrity of template (SMZ or AMO) molecules during polymerization, their redox activity within the potential window used for P(mPD) electropolymerization was

elucidated by cyclic voltammetry (CV). It was observed that both SMZ and AMO molecules demonstrate no electrochemical activity at the potential used for P(mPD) formation. Therefore, the electrosynthesis and deposition of P(mPD), P(mPD)/SMZ and P(mPD)/AMO were achieved on the SAW and QCM sensors using the optimal parameters obtained. The synthesis of the polymer film in the presence or absence of the antibiotic molecules results in a non-linear, self-limiting growth (Fig. 3(a), Paper I and Fig. 4(b), Paper II). Moreover, this growth is much slower in the presence of the antibiotics, indicating that the antibiotics molecules affect the conductivity of the growing polymer as compared to the pure P(mPD) film, thus, resulting in a well-pronounced self-limiting synthesis.

In combining a MIP and a label-free sensor transducer, avoidance of nonspecific binding event is paramount. However, since the target molecule is expected to interact with the polymer matrix at random sites on the polymer other than the imprinted sites, a complete elimination of nonspecific binding may be difficult to achieve. To cater for this disadvantage, a similar polymeric material prepared in the absence of the template, a non-imprinted polymer (NIP), is usually prepared as a standard reference material. However, to serve as an appropriate reference, NIP must possess similarities to the MIP in terms of its thickness or surface area, to ensure comparable nonspecific contributions on both surfaces. Thus, to ensure the same film thickness for P(mPD) and P(mPD)/AMO on QCM, the electrodeposition was monitored by EQCM measurements to enable the continuous polymer film synthesis until a desired frequency shift (400 Hz) was reached (Fig. 4(b), Paper II). To control the electrodeposition on the SAW sensor, an ellipsometric thickness measurement vs charge calibration plot was conducted (Fig. 3(b), Paper I). This allows the deposition of a precise film thickness on the electrode by passing an electrical charge that correlates to either P(mPD) or P(mPD)/SMZ through the sensor electrode. The calibration reveals an almost linear variation in their polymer growth with eventual thickness of SMZ-MIP and NIP films ranging from 1 to 24 nm.

It is important to note that a greater surface area of the recognition layer could be more beneficial for the label-free detection of small molecular weight molecules such as antibiotics, e.g., SMZ and AMO. Thus, the thickest possible film thicknesses, 25 nm or 400 Hz, and 24 nm or 10 mC/cm^2, were deposited on QCM and SAW sensors, respectively.

3.2.2 Film formation by sol-gel technique

With the sol-gel technique, a hybrid polymer matrix consisting of a composite mixture of organic and inorganic polymers could be easily prepared at room temperature. Thus, the sol-gel synthesis of hybrid AMO-MIP was carried out by the combination of free-radical polymerization of organic monomer, methacrylamide (MAAM) and hydrolysis/co-condensation of inorganic sol-gel precursor, tetraethoxysilane (TEOS) using an inorganic coupling agent, vinyltrimethoxysilane (VTMOS), in the presence of AMO molecules. This results in a highly cross-linked hybrid sol that is subsequently interfaced on the gold substrate of SPR by a spin coating technique to form the hybrid film (poly(MAAM-VTMOS-TEOS)/AMO). For proper referencing and for easy subsequent evaluation of the yet to be formed hybrid AMO-MIP performance, a reference film (poly(MAAM-VTMOS-TEOS)) to be used as NIP was also prepared following similar protocol but in the absence of AMO template molecules. Ellipsometry

measurements of thickness and its correlation with spin coating speed (in RPM) allows the reproducible generation of similar film thicknesses (ca. 65 nm) for both films.

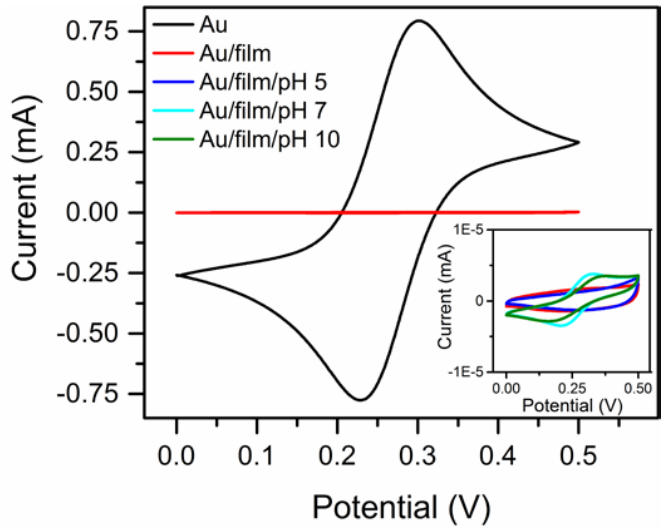

Figure 3.4. Cyclic voltammograms (CVs) of bare gold, Au; gold modified poly(MAAM-VTMOS-TEOS) hybrid film, Au/film; and Au/films after treatments with buffer solutions of different pH. CVs were recorded in 1 M KCl containing 4 mM $Fe(CN)_6^{3-}/Fe(CN)_6^{4-}$ at scan rate 50 mV/s.

To ensure a robust integration of the film on the sensor, a thiolated silicon alkoxide, 3-mercaptopropyl trimethoxysilane (MPTMS) was included to the sol preparation that ensures a strong coordination of its terminal thiol (S-H) groups to the underlying gold surface of SPR. The robust adherence of the film to the gold electrode was confirmed by cyclic voltammetry (CV) measurements, following treatments with different buffer pH. The absence of a significant change in Faradaic current or a facilitated electron transfer that may result from film deterioration, as observed in Fig. 3.4 indicate the film stability. Furthermore, the homogeneous morphology of the films was established by Atomic Force Microscopy (AFM).

3.3 Removal of antibiotic template molecules from polymer matrix

The removal of the antibiotic templates from the polymer matrices is essential to the formation of antibiotic-MIP films (i.e. SMZ-MIP, AMO-MIP, hybrid AMO-MIP). The washing solutions were selected so as to disrupt the noncovalent interactions existing between the templates and the polymer matrices. For this purpose, the PmPD/AMO, PmPD/SMZ and poly(MAAM-VTMOS-TEOS)/AMO were subjected to treatments in acetic-acid/methanol solutions with a volume ratio of 1:1, 1:3 and 1:9, respectively. To ascertain template removal, the polymeric films were characterized using either IR microscopic or cyclic voltammetry (CV) measurements. By these methods, the successful removal of the template molecules was established. This could be seen as either a significant reduction or disappearance of template characteristic vibrational peaks in the IR region or an enhanced permeability of the polymer to ions of redox probe. As an illustration, the spectra of P(mPD), P(mPD)/SMZ and SMZ-MIP are shown in Fig. 4, Paper I, following

IR measurements. As was observed, P(mPD) characteristic peaks were distinct, including aromatic vibration of strong C=N band at 1627 cm^{-1} and a weak C=C band at 1496 cm^{-1}. In the P(mPD)/SMZ spectra, new peaks likely related to the SMZ characteristic vibration of S=O stretching (1134 cm^{-1}) in sulphonamides and N-H bending (1086 cm^{-1}) in amine, aromatic vibration of thiadiazole ring (1442 cm^{-1}) and secondary amine N-H bending (1600 cm^{-1}) were seen. Thus, the decrease or disappearance of these peaks, as observed in the SMZ-MIP spectra, could most probably indicate an effective template removal (Paper I).

3.4 Characterization of the antibiotic-MIP films

To characterize the performance of the prepared antibiotic-MIPs, the films were evaluated for their binding capacity, selectivity as well as their performance in very low concentration of the target analytes. This was made possible by monitoring the analyte-induced signals following the injection of the analyte concentration samples on the respective antibiotic-MIP. For a reliable analysis and to account for the nonspecific contribution, a control experiment with the NIP was also executed. The advantage offered by the label-free platforms, SAW, QCM and SPR, allowed for the ease in monitoring, recording and subsequent analysis of the molecular recognition events.

3.4.1 SMZ-MIP: rebinding study by SAW

SMZ-MIP affinity and selectivity towards SMZ was evaluated by the SAW sensor platform. The SAW system had multichannel measurement possibilities, thereby allowing simultaneous monitoring of binding events on both MIP and NIP surfaces, thus excluding errors due to variation in measurement conditions. Adsorption isotherms (Fig. 3.5(a)) obtained from equilibrium responses on SMZ-MIP and NIP surfaces upon injection of increasing analyte concentrations were fitted to the Langmuir-Freundlich (LF) model (Table 2). From the resulting fitting parameters, the relative binding capacity represented by the imprinting factor (IF) was calculated. The calculated IF shows that SMZ-MIP has more than 8 times the binding capacity of NIP, thus revealing the influence of the preformed imprinted sites in the SMZ-MIP.

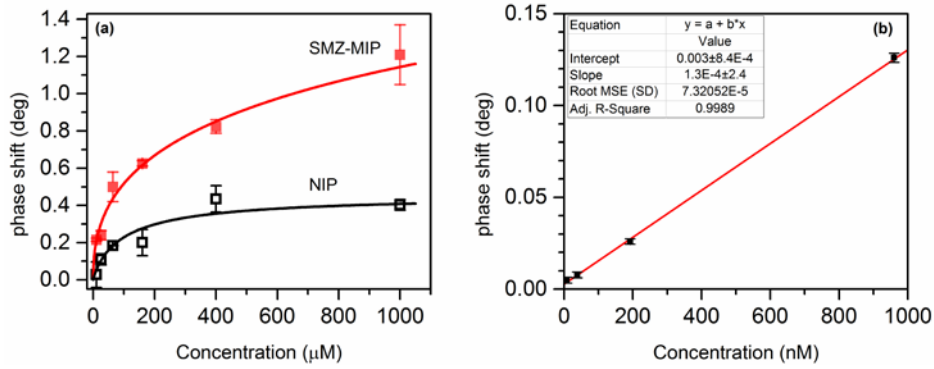

Figure 3.5. (a) Adsorption isotherms of SMZ-MIP and NIP films on SAW sensor following the injection of 1.6 to 1000 µM of SMZ in PBS buffer (pH 7.4). Bold lines represent fits to the LF isotherm model. (b) Linear regression plot of SMZ-induced response on SMZ-MIP after low concentration (8 - 960 nM) injection (Paper I).

$$LoD = 3S_{y/s}/b \quad (5)$$

Moreover, the lower K_D of SMZ-MIP as compared to the NIP reflects a higher affinity for the target molecule. When exposed to low analyte concentrations, SMZ-MIP demonstrates a limit of detection (LoD) down to 1.7 nM, as calculated from the plot of the linear regression (Fig. 3.5(b)) using Eq. (5), where $S_{y/s}$ is the standard deviation of the regression residuals and b is the slope of the regression line.

In the aquatic environment, SMZ exists at the concentration ranging from 0.5 to 7 nM, hence, the fabricated SAW modified SMZ-MIP chemosensor possessing an LoD of 1.7 nM shows a potential for its immediate utilization for detecting SMZ.

3.4.2 AMO-MIP: rebinding study by QCM

AMO rebinding capability of AMO-MIP and NIP was studied by the QCM-FIA system. Signal fluctuations due to changes in temperature were minimized by conducting the rebinding experiments in a custom-designed insulating chamber. The adsorption isotherms obtained for AMO-induced response on both AMO-MIP and NIP films were well modeled by the LF equation (Fig. 3.6(a)).

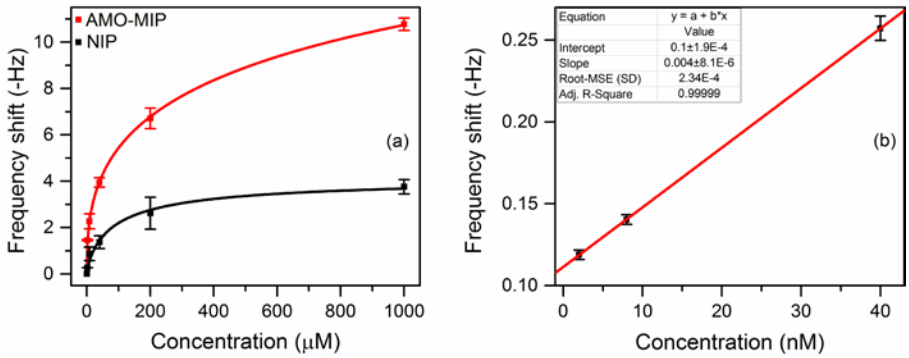

Figure 3.6. (a) Adsorption isotherms of AMO-MIP and NIP films on QCM sensor following the injection of 1.6 to 1000 µM of AMO in PBS buffer (pH 7.4). Bold lines represent fits to the LF isotherm model. (b) Linear regression plot of AMO-induced response on AMO-MIP after low concentration (2 - 40 nM) injection (Paper II).

From the parameters obtained after LF fits of the AMO-MIP and NIP adsorption isotherms, it was observed that the imprinted polymer demonstrates a much higher adsorption for the target than the reference film. This is seen in the value of the calculated relative adsorption capacity where an IF of 7.2 was obtained. Furthermore, the effect of polymer thickness on the binding capacity of AMO-MIP was investigated with 6.3, 15.6 and 25.0 nm thickness of AMO-MIP and NIP films corresponding to −100, −250, and −400 Hz frequency shift of electrodeposition. It was found that an increase in thickness results in an increase in AMO adsorption on AMO-MIP but a decreasing adsorption on the NIP (Fig. 6, Paper II) and thus, a resultant increase in IF. This is possibly due to the increase in the surface area and number of binding sites on AMO-MIP while the active surface area on the NIP decreases (Section 3.3, Paper II). Moreover, the performance analysis (Fig. 3.6(b)) of AMO-MIP in low analyte concentration indicates an LoD of 0.2 nM. This low detection limit is potentially

remarkable since AMO naturally exists in environmental water within the concentration range of 0.2–11 nM [191, 192].

3.4.3 SMZ-MIP(Dex): rebinding study by QCM

To further demonstrate the possibility of improving the specific binding capacity of an electrodeposited MIP on a label-free sensor for detecting antibiotics or other small molecules, an approach aimed at enhancing the amount of the binding sites within the MIP film was experimented. This includes preconcentrating the template molecule on the sensor prior to the electropolymerization. This was illustrated by using SMZ-MIP electrodeposited on QCM. To achieve the template preconcentration, a monolayer assembly of a polycationic anion exchanger, Diethylaminoethyl-dextran (DEAE-Dex) was formed on the QCM sensor before electropolymerization (Fig. 1, Paper III).

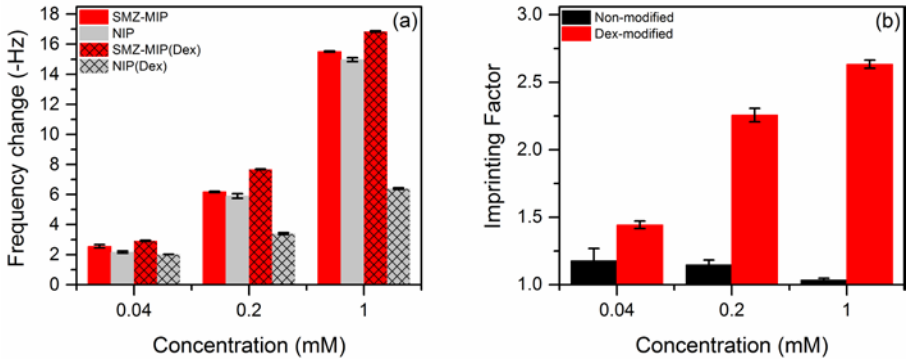

Figure 3.7. (a) Graphical comparison of the equilibrium response signals and (b) the resulting imprinting factors (IF) for the prepared sensors as measured at different concentrations of the analyte (Paper III).

To study the influence of the dextran modification and SMZ-preconcentration on the binding capacity of the SMZ-MIP(Dex), the study of the target rebinding was conducted in a QCM-FIA system using SMZ concentrations of 0.04, 0.2 and 1 mM in PBS (pH 7.4) solution. For adequate comparison, similar analyses were also performed on the QCM modified NIP(Dex), SMZ–MIP, and NIP films. After analyzing the response by fitting to an appropriate kinetic model, the equilibrium signals on each surface were obtained at different analyte concentrations. Evaluation of the binding performance was achieved by the relative recognition capacity computed by the IF (Eq. (2)). By this evaluation approach, it is assumed that with a larger IF, more binding sites are present in the resulting imprinted polymer. As a result, it could be expected that MIP possessing a higher IF should also demonstrate a better selectivity towards the target analyte [99].

As seen in Fig. 3.7(a), the SMZ-MIP(Dex) exhibits relatively higher adsorption capacities at all concentrations as compared to the SMZ-MIP. On the contrary, the NIP(Dex) films showed a lower adsorption relative to the NIP film. Thus, by the DEAE dextran modification, the nonspecific interaction could be greatly reduced while further enhancing the specific interaction of the analyte by the additionally created imprinted sites resulting from the SMZ template preconcentration. This is further revealed by the plot of IF (Fig. 3.7(b)). The IFs obtained for the dextran-modified

surfaces are noticeably higher than those of non-modified films beginning from the first analyte concentration. This difference increases with increasing analyte concentration. Thus, an enhanced relative adsorption, hence, a possibly increased sensitivity is obtainable by the DEAE-Dextran modification enabled SMZ pre-concentration. The result therefore revealed that by immobilizing antibiotic (or other small molecular) templates on the sensor prior to the polymer deposition, more specific recognition sites could be created within the polymer film. This approach therefore demonstrates the possibility to further improve the detection of both SMZ and AMO on label-free sensors.

3.4.4 Hybrid AMO-MIP: rebinding study by SPR

Although a greater number of MIP publications are based on organic polymer matrices, hybrid organic-inorganic MIP can further improve MIP performances by supplying additional properties. Such properties may include high stability, flexibility, long shelf-life, larger surface area and more ordered imprinted cavities. To characterize the rebinding of AMO on the hybrid AMO-MIP, an SPR system was used. The SPR consisted of two channels that support simultaneous monitoring of duplicate measurements. Binding responses recorded after increasing AMO concentration injection were fitted to the pseudo-first order model. However, to account for bulk shift, a common effect in SPR, a bulk shift constant, *BS* was introduced into the fitting equation, as shown in Table 2.

Plotting the adsorption isotherms and fitting the same to the LF model resulted in the achievement of maximum adsorption response of hybrid AMO-MIP for AMO. For comparison, the isotherms were also fitted to both the Langmuir and the Freundlich models but as observed (Fig. 3.8(a)), they do not provide very good fits to the experimental data. This confirms that the hybrid AMO-MIP, similar to most MIPs, possesses some degree of heterogeneity. The relative adsorption capacity, as calculated by the IF, indicates that the imprinted film has about 16 times higher adsorption than the NIP. Thus, it can be said that the hybrid MIP formation helps in generating a very good imprinting effect as compared to the solely organic polymer MIP.

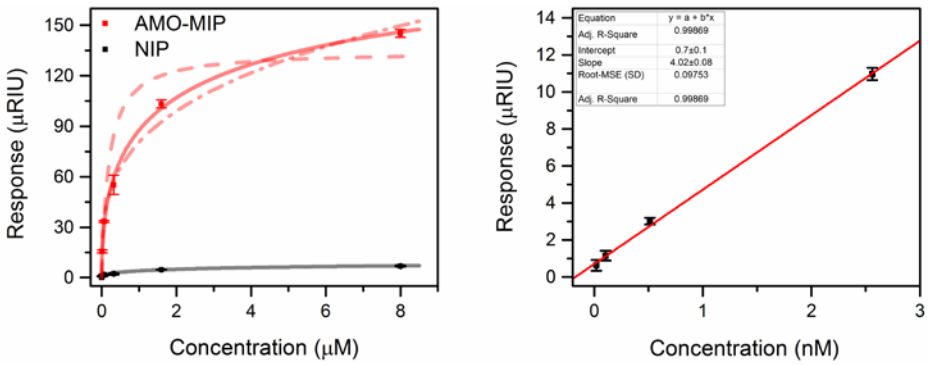

Figure 3.8. (a) Adsorption isotherms of hybrid AMO-MIP and NIP films on SPR sensor following the injection of 12.8 nM - 8 μM of AMO in PBS buffer (pH 7.0). The solid lines are fits to the LF model while the dash and dash-dot lines are fits to the L and F models respectively. (b) Analytical performance of the AMO-MIP modified SPR sensor at low concentration injections of AMO (0.1 to 2.6 nM). The solid line is a linear regression fit.

The low concentration performance of hybrid AMO-MIP was also investigated by injecting low concentrations (0.1 to 2.6 nM) of AMO on its surface. It was revealed that an LoD as low as 73 pM could be reached for the fabricated SPR chemosensor, as calculated from the plot of the linear regression (Fig. 3.8(b)). This result shows an improvement in the trace level detection of AMO when compared to the electrochemically immobilized AMO-MIP on QCM sensor.

3.5 Selectivity of antibiotic-MIPs

In developing sensors for environmental detection of pollutants such as antibiotics, a key aspect is the selectivity of the fabricated chemosensor. By the selectivity, the ability of the sensor to recognize the target molecule(s) while discriminating against others in a complex mixture is presented. Environmental water is a complex matrix of varying substances, some bearing close similarities with the target analytes. Therefore, to ensure a specific determination of the target(s) in the natural environment in which they are found, a sensor must demonstrates good selectivity towards the target molecules.

To study the selectivity of the prepared chemosensors, their responses to the injections of several other antibiotics were studied in both PBS buffer and tap water samples spiked with the same analyte concentration. These responses were analyzed and compared to those of the target at the same experimental conditions. Antibiotic molecules chosen for this purpose consist of very similar analogue of either SMZ or AMO as well as non-closely related antibiotic molecules. They include sulfanilamide, sulfadimethoxine, ampicillin, norfloxacin, and doxycycline (Fig. 3.9). The selectivity investigations carried out on SMZ-MIP, AMO-MIP and hybrid AMO-MIP on either SAW, QCM or SPR sensors revealed that the developed sensors demonstrate notable selectivity towards the target as compared to other analytes. This is evident by the low values of the selectivity coefficients; from 0.1 to 0.5 (Figs. 7 and 8, Table 5, Paper I; Figs. 7 and 8, Table 4, Paper II) thus, indicating up to ten times discriminating recognition for the targets as compared to other interfering molecules.

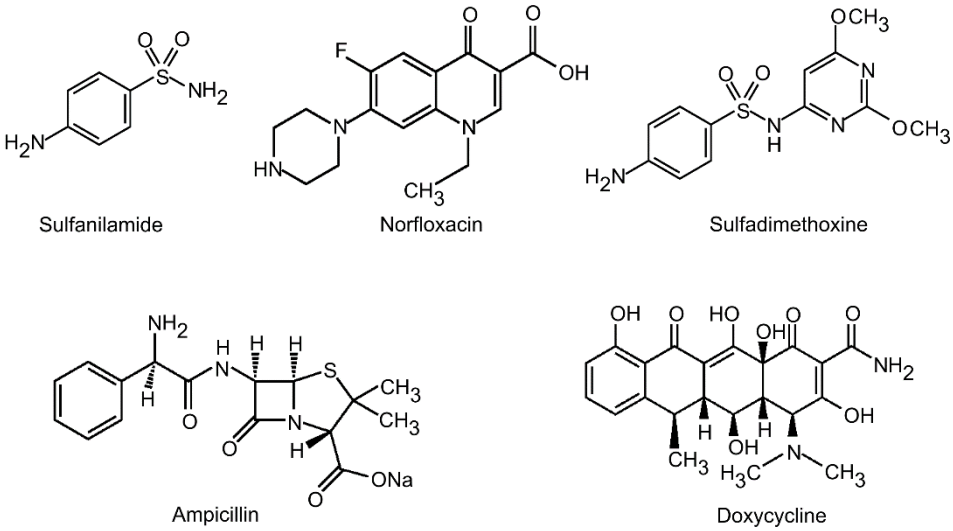

Figure 3.9. Structural formula of antibiotic molecules used in the selectivity study.

4. Conclusions

This thesis presents a novel method for a robust and selective detection of antibiotic water pollutants using the molecular imprinting technology to generate antibiotic recognition cavities in synthetic polymer (MIP) films integrated with label-free sensors, QCM, SPR and SAW. SMZ and AMO were selected as representative antibiotic target pollutants owing to their popular utilization, thus, increased possibility of release into the environment. The following vital conclusions can be drawn from the study:

- Electrosynthesis and sol-gel/spin coating techniques offer a controllable growth of robust and reproducible antibiotic-MIP films (SMZ-MIP, AMO-MIP and hybrid AMO-MIP) on label-free sensor surfaces at thicknesses in the range of 24-65 nm, as confirmed by the spectroscopic ellipsometry measurements.
- Combined use of computational and experimental studies approved the selection of meta-phenylenediamine (mPD) as an excellent electropolymerizable functional monomer to synthesize thin SMZ-MIP and AMO-MIP films on SAW and QCM sensors, respectively.
- Sol-gel coupled with spin coating techniques permits the synthesis of the organic-inorganic hybrid AMO-MIP film and its sturdy integration with the SPR sensor.
- Binding properties of the prepared MIPs were best fitted to Langmuir–Freundlich adsorption isotherm model as compared to either Langmuir or Freundlich models, indicating the heterogeneous nature of the prepared MIP films.
- All prepared films: SMZ-MIP, AMO-MIP and hybrid AMO-MIP demonstrated relative adsorption capacities with imprinting factors (IF) ranging between 7.2 and 16.0. These values represent a much better performance of the fabricated MIPs than those obtained from some recently reported antibiotic-MIPs.
- More specific recognition sites were further created in the electrodeposited films with dextran modification enabled template preconcentration, as demonstrated for SMZ-MIP(Dex) film on QCM.
- All antibiotic-MIPs showed remarkable selectivity to the target antibiotic molecules with up to ten times preferential recognition as compared to other structurally related interfering antibiotics either in PBS or tap water samples.
- Analytically relevant LoD from 1.7 nM down to 73 pM were obtained for the MIP films-modified sensors.
- Repeated usage of the sensors were established for up to three (SMZ-MIP and AMO-MIP) or nine (hybrid AMO-MIP) regeneration-rebinding cycles.
- The presented study demonstrates an easy and reliable manner for developing antibiotic-selective sensors involving the synthesis and robust interfacing of antibiotic-MIP films on SAW, QCM and SPR label-free sensor transducers to afford a direct and selective antibiotic water pollutants detection.

Abstract in English

Molecularly imprinted polymers designed to detect antibiotic pollutants in water

Antibiotics constitute a major class of environmental water pollutants due to their wide and increasing usage in human and veterinary medicines, agriculture, as well as the possibility of passing through sewage water treatment facilities. The potential detrimental effects of antibiotics pollution is seen in their environmental toxicity and the spread of antibiotic resistant strain, causing difficulties in the prevention and cure of microbial infections and diseases. This has an overall effect of jeopardizing the lives of human, animals and other organisms and ecosystem sustainability. Thus, to mitigate this menace, a routine monitoring of environmental water as well as potable tap water is essential.

A critical aspect in this environmental monitoring would involve the detection of the pollutants. Such detection, however, requires the utilization of sensitive and selective analytical methods or devices capable of recognizing trace amount of the target analytes. In this respect, chromatography, mass spectrometry, solid phase extraction, biosensors or ELISA are traditionally used. Nevertheless, the known limitations of such techniques constitute their disadvantages for use in routine monitoring.

Molecularly imprinted polymers (MIPs) are synthetic polymers that are tailored through utilizing natural molecular recognition mechanisms to detect target molecules within a complex matrix with other compounds, with potentially remarkable sensitivities. The beneficial importance of such materials is unquantifiable when channeled towards antibiotic environmental pollutants detection. However, to compete well with and outperform traditional methods of pollutant detection, MIPs should demonstrate functional, selective and reusable properties much better than the existing techniques.

This thesis describes novel protocols to synthesize antibiotic imprinted polymers (antibiotic-MIPs) for detecting antibiotic targets in water. Thin antibiotic-MIP films are expected to be synthesized and interfaced with sensor surface of label-free transducers for a reliable and real-time monitoring of antibiotic recognition events occurring on the transducers. Different transducers including piezoelectric devices, such as surface acoustic wave (SAW) or quartz crystal microbalance (QCM), and an optical device, such as surface plasmon resonance (SPR), were selected to monitor the molecular interactions taken place on the antibiotic-MIP-modified transducer surfaces in a label-free manner.

To interface the films with SAW, QCM or SPR transducers, very simple methodologies including electrochemical and sol-gel techniques that allow the synthesis of thin (24 - 65 nm) polymer films directly on the sensor surfaces were employed. Following the polymer synthesis and integration with sensor transducers, removal of the template molecules from the polymer matrix was achieved by washing in acidic solutions to disrupt noncovalent bonds existing between the template molecules and the polymer functional groups. While electrosynthesis permits the formation of organic polymer derived SMZ-MIP and AMO-MIP on SAW and QCM sensor transducers, the sol-gel technique was specially selected to enable the

synthesis of the organic-inorganic hybrid AMO-MIP film on the SPR sensor. The control of reproducibility of film thicknesses was achieved through either electrochemical quartz crystal microbalance (EQCM) analysis and/or spectroscopic ellipsometry measurements.

The analysis of the recognition characteristics of all prepared antibiotic-MIPs carried out in SAW, QCM and SPR sensor platforms revealed promising properties. These include high relative adsorption capacities, estimated by the imprinting factor (IF) ranging from 7.2 to 16.0, detection limit (LoD) from 1.7 nM down to 73 pM, and a high selectivity for the target antibiotics (SMZ and AMO) as compared to other closely related antibiotic molecules. Moreover, the sensors were found to be reusable for up to three (electrosynthesized MIPs) or nine (sol-gel processed hybrid MIP) regeneration-rebinding cycles and retained their recognition capabilities and selectivities even in representative tap water samples. Also, the possibility to improve the performance of the chemosensors by a dextran-enabled template preconcentration was demonstrated.

The presented approaches of preparing antibiotic-MIP recognition layers and their integration with label-free sensors allowed the real-time monitoring and detection of antibiotic pollutants in water at levels in which they naturally exist, with a potentially acceptable selectivity. Thus, these approaches and their consecutive protocols could lead to a promising breakthrough in the design of a portable analytical tool for sensitive and selective monitoring of antibiotic pollutants in aqueous environment.

Lühikokkuvõte

Molekulaarselt jäljendatud polümeerid antibiootikumide määramiseks vesikeskkonnas

Antibiootikume võib täna lugeda üheks peamiseks keskkonda saastavate ainete rühmaks, kuna nende kasutamine on märkimisväärselt suur nii meditsiinis, veterinaarias kui ka põllumajanduses väetiste ja jääkainete produktidena. Keskkonda sattunud antibiootikumide kahjulik mõju avaldub ennekõike nende toksilisuses ja inimorgamismi vastupanuvõime kahandamises erinevate mikroobsete haiguste suhtes. Pikemas perspektiivis võib see ohustada meie ökosüsteemi jätkusuutlikkust.

Selleks, et seda potentsiaalset ohtu vähendada ja hoida kontrolli all on vajalik ümbritseva keskkonna pidev ja efektiivne monitooring erinevate saasteainete, sealhulgas antibiootikumide jääkide suhtes. Efektiivne monitooring eeldab tundlike ja selektiivsete meetodite kasutamist tuvastamaks ka väikeiseid jääkainete koguseid. Tänapäeval võimalikud analüüsi meetodid nagu kromatograafia, spektromeetria, tahke faasi ekstraktsioon, biosensorid või ELISA on küll täpsed, kuid kallid ja ei võimalda kiiresti ning vahetult sündmuskohal mõõtmisi teostada.

Molekulaarselt jäljendatud polümeerid (MIP) on sünteetilised polümeerid, mis on kujundatud looduslike selektiivsete mehhanismide põhimõtteid järgides erinevate sihtmolekulide äratundmiseks ja sidumiseks spetsiaalselt kujundatud polümeeri maatriksis. Selle põhimõtte kasutamine erinevate keskkonna saasteainete, sealhulgas ravimijääkide ja antibiootikumide määramiseks, on äärmiselt perspektiivne. See eeldab aga, et MIP põhimõttel töötavad sensormaterjalid peavad olema võrreldes senikasutatavate meetoditega vähemalt sama tundlikud, funktsionaalsed ja samal ajal odavamad ning oluliselt lihtsamad kasutamiseks.

Käesoleva doktoritöö eesmärgiks oli välja töötada uus tehnoloogia antibiootikumide suhtes jäljendatud polümeeride valmistamiseks eesmärgiga määrata antibiootikume vees. Õhukesed antibiootikumide suhtes molekulaarselt jäljendatud kiled sünteesiti vahetult sensori pinnale, mis võimaldas märgisevabalt jälgida sihtmolekuli kontsentratsiooni muutust ülekantuna loetava elektrilise signaali kujule. Muutuste jälgimiseks kasutati piezoelektrilise kvatrstkiristalli sageduskarakteristiku muutuse mõõtmist (QCM), pinna akustilise laine muutuse mõõtmist (SAW) või pinnaplasma resonantsi (SPR) muutuse mõõtmist sõltuvalt antibiootikumi kontsentratsioonist.

Antibiootikumide suhtes jäljendatud õhukesed kiled (24 -65 nm) sünteesiti elektorkeemiliselt või „sool-geel“ meetodil vahetult sensori pinnale. Seejärel eemaldati sihtmolekulid sünteesitud polümeeri maatriksist katkestades happelahusega pesemise abil sihtmolekuli ja maatriksit siduvad mittekovalentsed sidemed. Elektrokeemiline süntees võimaldas sünteesida SMZ-MIP ja AMO-MIP vahetult SAW või QCM platvormidele, „sool-geel“ tehnoloogia valiti spetsiaalselt orgaaniliste – anorgaaniliste hübriid AMO – MIP kilede valmistamiseks SPR sensorile. Sünteesil valmistatud kile paksust kontrolliti spektroskoopilise ellipsomeetria abil või elektrokeemilise piezoelektrilise kvartskristalli meetodil (EQCM).

MIP-kilega modifitseeritud SAW, QCM ja SPR sensorplatvormidel mõõdetud signaalid sõltuvalt antibiootikumide kontsentratsioonist olid väga iseloomulikud ja näitasid nimetatud tehnoloogia sobilikkust antibiootikumide määramiseks

vesikeskkonnas. Mõõtmistulemuste analüüsi alusel arvutatud sihtmolekuli sidumise efektiivsus (IF „imprinting factor“) oli vahemikus 7,2–16,0. Väljatöötatud tehnoloogiad võimaldasid saavutada avastamispiiri (LoD) 1,7 nM kuni 73 pM. Samuti oli jäljendatud molekulide SMZ ja AMO sidumise efektiivsus konkureerivate analoogiliste sihtmolekulide suhtes oluliselt kõrgem.

Lisaks eelpooltoodule olid elektrokeemiliselt sünteesitud MIP kiled kasutatavad kuni kolme järjestikuse sidumise – pesemise tsükli järel, samal ajal hübriidsed MIP kiled olid stabiilsete sidumisomadustega kuni üheksa tsükli järel. Samuti säilitasid MIP kiled selektiivsuse kasutades vesikeskkonnana tavalist kraanivett. Töö tulemusena näidati ka, et MIP kile sünteesi protsessi saab muuta efektiivsemaks sihtmolekulide eelkontsentratsioonil dekstraaniga.

Kokkuvõtteks võib väita, et väljatöötatud tehnoloogiad antibiootikumide suhtes jäljendatud polümeeride valmsitamiseks ja sidumiseks märgisevabade sensorplatvormidega võimaldavad reaalajas jälgida antibiootikumide kontsentratsiooni muutusi vesikeskkonnas piisava selektiivsusega reaalselt eksisteerivate kontsentratsioonidel. See loob head eeldused oluliselt odavamate, täpsemate ja kiiremate portatiivsete keskkonnasensorite valmistamiseks molekulaarse jälendamise tehnoloogia alusel.

Acknowledgements

My sincere appreciation goes to my supervisor, Dr Vitali Syritski, for his support, trust and mentorship all through the period of my PhD research and for painstakingly ensuring the quality of my research output. To my co-supervisor, Prof Andres Öpik, for his fatherly advice, encouragement and trust. To Dr Jekaterina Reut, for her guidance and readiness to support and fully participate at every stage of the research. The passion displayed by you all to science has highly and will continue to motivate me towards greatness. Thank you for the understanding you have demonstrated and the platform you provided for achieving my PhD goals.

I also want to appreciate the head of department, Dr Malle Krunks for her support and for providing the very conducive environment to carry out my research.

My appreciation also goes to my colleagues and all the people I have worked with in our department, Dr Roman Boroznjak for his friendliness and readiness to help at all times, Dr Aleksei Tretjakov for encouragement and assistance.

To the leadership and members of RCCG Grace Chapel, Tallinn, thank you for the support and prayers. Your influence will not be easily forgotten.

My profound appreciation goes to my parents, siblings and relatives for believing in my dreams and for their constant words of encouragement and prayers. I could not have asked for a lovelier home.

To my immediate family, my wife and best friend Mrs Joy Oluchi Ayankojo, my great motivator; and my daughter Glory Ifeoluwa Ayankojo, my sunshine. Words will fail me in appreciation of your understanding, persistence and love you always readily displayed during the course of my PhD career. I will forever be indebted to you.

Most importantly, my highest gratitude goes to God, my Lord and savior Jesus Christ who has made everything beautiful in its own time.

This research was carried out at the Chair of Physical Chemistry, Department of Materials and Environmental technology. The work was financially supported by Estonian Science Foundation (PUT150), Estonian Ministry of Education and Research (SF0140033s12), Tallinn University of Technology in the frame of the development project (grant SS425), and European Social Fund's Doctoral Studies and Internationalization Program (DoRa8).

This work has been partially supported by ASTRA "TUT Institutional Development Programme for 2016-2022" Graduate School of Functional Materials and Technologies (2014-2020.4.01.16-0032).

References

[1] F. Hernandez, M. Ibanez, T. Portoles, M.I. Cervera, J.V. Sancho, F.J. Lopez, Advancing towards universal screening for organic pollutants in waters, J Hazard Mater, 282(2015) 86-95.

[2] J. Xu, Y. Xu, H.M. Wang, C.S. Guo, H.Y. Qiu, Y. He, et al., Occurrence of antibiotics and antibiotic resistance genes in a sewage treatment plant and its effluent-receiving river, Chemosphere, 119(2015) 1379-85.

[3] A. Gobel, C.S. McArdell, A. Joss, H. Siegrist, W. Giger, Fate of sulfonamides, macrolides, and trimethoprim in different wastewater treatment technologies, Sci Total Environ, 372(2007) 361-71.

[4] O. Golovko, V. Kumar, G. Fedorova, T. Randak, R. Grabic, Seasonal changes in antibiotics, antidepressants/psychiatric drugs, antihistamines and lipid regulators in a wastewater treatment plant, Chemosphere, 111(2014) 418-26.

[5] B. Kasprzyk-Hordern, R.M. Dinsdale, A.J. Guwy, The removal of pharmaceuticals, personal care products, endocrine disruptors and illicit drugs during wastewater treatment and its impact on the quality of receiving waters, Water Res, 43(2009) 363-80.

[6] R.H. Lindberg, P. Wennberg, M.I. Johansson, M. Tysklind, B.A.V. Andersson, Screening of human antibiotic substances and determination of weekly mass flows in five sewage treatment plants in Sweden, Environ Sci Technol, 39(2005) 3421-9.

[7] N. Nakada, H. Shinohara, A. Murata, K. Kiri, S. Managaki, N. Sato, et al., Removal of selected pharmaceuticals and personal care products (PPCPs) and endocrine-disrupting chemicals (EDCs) during sand filtration and ozonation at a municipal sewage treatment plant, Water Res, 41(2007) 4373-82.

[8] R.J. Fair, Y. Tor, Antibiotics and bacterial resistance in the 21st century, Perspectives in medicinal chemistry, 6(2014) PMC. S14459.

[9] A.G. Ayankojo, A. Tretjakoy, J. Reut, R. Boroznjak, A. Opik, J. Rappich, et al., Molecularly Imprinted Polymer Integrated with a Surface Acoustic Wave Technique for Detection of Sulfamethizole, Anal Chem, 88(2016) 1476-84.

[10] K. Mosbach, Molecular Imprinting, Trends Biochem Sci, 19(1994) 9-14.

[11] K. Haupt, K. Mosbach, Molecularly imprinted polymers and their use in biomimetic sensors, Chem Rev, 100(2000) 2495-504.

[12] L. Ye, K. Mosbach, Molecular imprinting: Synthetic materials as substitutes for biological antibodies and receptors, Chem Mater, 20(2008) 859-68.

[13] D.L. Huang, R.Z. Wang, Y.G. Liu, G.M. Zeng, C. Lai, P. Xu, et al., Application of molecularly imprinted polymers in wastewater treatment: a review, Environ Sci Pollut R, 22(2015) 963-77.

[14] I. Sanchez-Barragan, K. Karim, J.M. Costa-Fernandez, S.A. Piletsky, A. Sanz-Medel, A molecularly imprinted polymer for carbaryl determination in water, Sensor Actuat B-Chem, 123(2007) 798-804.

[15] T.S. Anirudhan, S. Alexander, Design and fabrication of molecularly imprinted polymer-based potentiometric sensor from the surface modified multiwalled carbon nanotube for the determination of lindane (gamma-hexachlorocyclohexane), an organochlorine pesticide, Biosens Bioelectron, 64(2015) 586-93.

[16] S.M. Wang, L. Ge, L. Li, M. Yan, S.G. Ge, J.H. Yu, Molecularly imprinted polymer grafted paper-based multi-disk micro-disk plate for chemiluminescence detection of pesticide, Biosens Bioelectron, 50(2013) 262-8.

[17] K. Das, J. Penelle, V.M. Rotello, Selective picomolar detection of hexachlorobenzene in water using a quartz crystal microbalance coated with a molecularly imprinted polymer thin film, Langmuir, 19(2003) 3921-5.

[18] Q.H. Luo, N. Yu, C.F. Shi, X.P. Wang, J.M. Wu, Surface plasmon resonance sensor for antibiotics detection based on photo-initiated polymerization molecularly imprinted array, Talanta, 161(2016) 797-803.

[19] K.M.M. Kabir, Y.M. Sabri, A.E. Kandjani, S.J. Ippolito, S.K. Bhargava, Development and comparative investigation of Ag-sensitive layer based SAW and QCM sensors for mercury sensing applications, Analyst, 141(2016) 2463-73.

[20] M.J. Whitcombe, N. Kirsch, I.A. Nicholls, Molecular imprinting science and technology: a survey of the literature for the years 2004-2011, J Mol Recognit, 27(2014) 297-401.

[21] A. Walcarius, A. Kuhn, Ordered porous thin films in electrochemical analysis, Trac-Trend Anal Chem, 27(2008) 593-603.

[22] A. Menaker, V. Syritski, J. Reut, A. Opik, V. Horvath, R.E. Gyurcsanyi, Electrosynthesized Surface-Imprinted Conducting Polymer Microrods for Selective Protein Recognition, Adv Mater, 21(2009) 2271-+.

[23] V. Syritski, J. Reut, A. Menaker, R.E. Gyurcsanyi, A. Oepik, Electrosynthesized molecularly imprinted polypyrrole films for enantioselective recognition of L-aspartic acid, Electrochim Acta, 53(2008) 2729-36.

[24] G. Lautner, J. Kaev, J. Reut, A. Opik, J. Rappich, V. Syritski, et al., Selective Artificial Receptors Based on Micropatterned Surface-Imprinted Polymers for Label-Free Detection of Proteins by SPR Imaging, Adv Funct Mater, 21(2011) 591-7.

[25] D.P. Birnie, A Model for Drying Control Cosolvent Selection for Spin-Coating Uniformity: The Thin Film Limit, Langmuir, 29(2013) 9072-8.

[26] V.L.V. Granado, M. Gutierrez-Capitan, C. Fernandez-Sanchez, M.T.S.R. Gomes, A. Rudnitskaya, C. Jimenez-Jorquera, Thin-film electrochemical sensor for diphenylamine detection using molecularly imprinted polymers, Anal Chim Acta, 809(2014) 141-7.

[27] S. Mehrabani, A.J. Maker, A.M. Armani, Hybrid Integrated Label-Free Chemical and Biological Sensors, Sensors-Basel, 14(2014) 5890-928.

[28] P.A. Lieberzeit, F.L. Dickert, Chemosensors in environmental monitoring: challenges in ruggedness and selectivity, Anal Bioanal Chem, 393(2009) 467-72.

[29] B. Alloway, D.C. Ayres, Chemical principles of environmental pollution: CRC press; 1997.

[30] A.S. Mohammed, A. Kapri, R. Goel, Heavy metal pollution: source, impact, and remedies, Biomanagement of metal-contaminated soils, Springer2011, pp. 1-28.

[31] Y.X. Jin, S.S. Wu, Z.Y. Zeng, Z.W. Fu, Effects of environmental pollutants on gut microbiota, Environ Pollut, 222(2017) 1-9.

[32] K.M. Rodgers, J.O. Udesky, R.A. Rudel, J.G. Brody, Environmental chemicals and breast cancer: An updated review of epidemiological literature informed by biological mechanisms, Environ Res, 160(2018) 152-82.

[33] R. Castilla, A. Asuaje, S. Riviere, C.G. Romero, P. Martin, G. Cao, et al., Environmental pollutant hexachlorobenzene induces hypertension in a rat model, Chemosphere, 195(2018) 576-84.

[34] D. Ierodiakonou, A. Zanobetti, B.A. Coull, S. Melly, D.S. Postma, H.M. Boezen, et al., Ambient air pollution, lung function, and airway responsiveness in asthmatic children, J Allergy Clin Immun, 137(2016) 390-9.

[35] E.J. Yanarella, Environmental governance reconsidered: Challenges, choices, and opportunities, Growth Change, 37(2006) 322-5.

[36] V. Geissen, H. Mol, E. Klumpp, G. Umlauf, M. Nadal, M. van der Ploeg, et al., Emerging pollutants in the environment: A challenge for water resource management, Int Soil Water Conse, 3(2015) 57-65.

[37] L.L. Ling, T. Schneider, A.J. Peoples, A.L. Spoering, I. Engels, B.P. Conlon, et al., A new antibiotic kills pathogens without detectable resistance (vol 517, pg 455, 2015), Nature, 520(2015).

[38] M. Mardirossian, R. Grzela, C. Giglione, T. Meinnel, R. Gennaro, P. Mergaert, et al., The Host Antimicrobial Peptide Bac7(1-35) Binds to Bacterial Ribosomal Proteins and Inhibits Protein Synthesis, Chem Biol, 21(2014) 1639-47.

[39] L. Tong, S.B. Huang, Y.X. Wang, H. Liu, M.J. Li, Occurrence of antibiotics in the aquatic environment of Jianghan Plain, central China, Sci Total Environ, 497(2014) 180-7.

[40] R. Gothwal, T. Shashidhar, Antibiotic Pollution in the Environment: A Review, Clean-Soil Air Water, 43(2015) 479-89.

[41] H. Brussow, Growth promotion and gut microbiota: insights from antibiotic use, Environ Microbiol, 17(2015) 2216-27.

[42] T. Garoma, S.K. Umamaheshwar, A. Mumper, Removal of sulfadiazine, sulfamethizole, sulfamethoxazole, and sulfathiazole from aqueous solution by ozonation, Chemosphere, 79(2010) 814-20.

[43] A.K. Sarmah, M.T. Meyer, A.B.A. Boxall, A global perspective on the use, sales, exposure pathways, occurrence, fate and effects of veterinary antibiotics (VAs) in the environment, Chemosphere, 65(2006) 725-59.

[44] P. Sukul, M. Spiteller, Fluoroquinolone antibiotics in the environment, Rev Environ Contam T, 191(2007) 131-62.

[45] C.S. McArdell, E. Molnar, M.J.F. Suter, W. Giger, Occurrence and fate of macrolide antibiotics in wastewater treatment plants and in the Glatt Valley Watershed, Switzerland, Environ Sci Technol, 37(2003) 5479-86.

[46] I. Senta, S. Terzic, M. Ahel, Occurrence and fate of dissolved and particulate antimicrobials in municipal wastewater treatment, Water Res, 47(2013) 705-14.

[47] A. Boxall, L. Fogg, P. Blackwell, P. Kay, E.J. Pemberton, Review of veterinary medicines in the environment: Environment Agency Bristol, UK; 2002.

[48] K. Fent, A.A. Weston, D. Caminada, Ecotoxicology of human pharmaceuticals, Aquat Toxicol, 76(2006) 122-59.

[49] A. Almeida, S. Duarte, R. Nunes, H. Rocha, A. Pena, L. Meisel, Human and veterinary antibiotics used in Portugal—a ranking for ecosurveillance, Toxics, 2(2014) 188-225.

[50] H.Y. Dong, X.J. Yuan, W.D. Wang, Z.M. Qiang, Occurrence and removal of antibiotics in ecological and conventional wastewater treatment processes: A field study, J Environ Manage, 178(2016) 11-9.

[51] Y. Xu, C.S. Guo, Y. Luo, J.P. Lv, Y. Zhang, H.X. Lin, et al., Occurrence and distribution of antibiotics, antibiotic resistance genes in the urban rivers in Beijing, China, Environ Pollut, 213(2016) 833-40.

[52] Y. Valcarcel, S.G. Alonso, J.L. Rodriguez-Gil, A. Gil, M. Catala, Detection of pharmaceutically active compounds in the rivers and tap water of the Madrid Region (Spain) and potential ecotoxicological risk, Chemosphere, 84(2011) 1336-48.

[53] Yiruhan, Q.J. Wang, C.H. Mo, Y.W. Li, P. Gao, Y.P. Tai, et al., Determination of four fluoroquinolone antibiotics in tap water in Guangzhou and Macao, Environ Pollut, 158(2010) 2350-8.

[54] H.X. Wang, N. Wang, B. Wang, Q. Zhao, H. Fang, C.W. Fu, et al., Antibiotics in Drinking Water in Shanghai and Their Contribution to Antibiotic Exposure of School Children, Environ Sci Technol, 50(2016) 2692-9.

[55] A.L. Boreen, W.A. Arnold, K. McNeill, Photochemical fate of sulfa drugs in the aquatic environment: Sulfa drugs containing five-membered heterocyclic groups, Environ Sci Technol, 38(2004) 3933-40.

[56] K. Yaghmaeian, G. Moussavi, A. Alahabadi, Removal of amoxicillin from contaminated water using NH4Cl-activated carbon: Continuous flow fixed-bed adsorption and catalytic ozonation regeneration, Chem Eng J, 236(2014) 538-44.

[57] K. Kummerer, Antibiotics in the aquatic environment - A review - Part I, Chemosphere, 75(2009) 417-34.

[58] L.X. Dong, J. Gao, X.J. Xie, Q.X. Zhou, DNA damage and biochemical toxicity of antibiotics in soil on the earthworm Eisenia fetida, Chemosphere, 89(2012) 44-51.

[59] R.A. Brain, M.L. Hanson, K.R. Solomon, B.W. Brooks, Aquatic plants exposed to pharmaceuticals: Effects and risks, Reviews of Environmental Contamination and Toxicology, Vol 192, 192(2008) 67-115.

[60] D.G. Hillis, J. Fletcher, K.R. Solomon, P.K. Sibley, Effects of Ten Antibiotics on Seed Germination and Root Elongation in Three Plant Species, Arch Environ Con Tox, 60(2011) 220-32.

[61] Z.J. Li, X.Y. Xie, S.Q. Zhang, Y.C. Liang, Wheat Growth and Photosynthesis as Affected by Oxytetracycline as a Soil Contaminant, Pedosphere, 21(2011) 244-50.

[62] F. Liu, G.G. Ying, R. Tao, J.-L. Zhao, J.F. Yang, L.F. Zhao, Effects of six selected antibiotics on plant growth and soil microbial and enzymatic activities, Environ Pollut, 157(2009) 1636-42.

[63] O. Opris, M.L. Soran, V. Coman, F. Copaciu, D. Ristoiu, Determination of some frequently used antibiotics in waste waters using solid phase extraction followed by high performance liquid chromatography with diode array and mass spectrometry detection, Cent Eur J Chem, 11(2013) 1343-51.

[64] J.L. Martinez, Environmental pollution by antibiotics and by antibiotic resistance determinants, Environ Pollut, 157(2009) 2893-902.

[65] M. Woegerbauer, J. Zeinzinger, R.A. Gottsberger, K. Pascher, P. Hufnagl, A. Indra, et al., Antibiotic resistance marker genes as environmental pollutants in GMO-pristine agricultural soils in Austria, Environ Pollut, 206(2015) 342-51.

[66] L.K. Xu, W.Y. Ouyang, Y.Y. Qian, C. Su, J.Q. Su, H. Chen, High-throughput profiling of antibiotic resistance genes in drinking water treatment plants and distribution systems, Environ Pollut, 213(2016) 119-26.

[67] S. Bergeron, R. Boopathy, R. Nathaniel, A. Corbin, G. LaFleur, Presence of antibiotic resistant bacteria and antibiotic resistance genes in raw source water and treated drinking water, Int Biodeter Biodegr, 102(2015) 370-4.

[68] C.I.L. Justino, A.C. Duarte, T.A.P. Rocha-Santos, Recent Progress in Biosensors for Environmental Monitoring: A Review, Sensors-Basel, 17(2017).

[69] K. Kumar, A. Thompson, A.K. Singh, Y. Chander, S.C. Gupta, J. Environ, Enzyme-linked immunosorbent assay for ultratrace determination of antibiotics in aqueous samples (vol 33, pg 250, 2004), J Environ Qual, 33(2004) 797-.

[70] P.H. Wang, T. Yuan, J.Y. Hu, Y.M. Tan, Determination of cephalosporin antibiotics in water samples by optimised solid phase extraction and high performance liquid chromatography with ultraviolet detector, Int J Environ an Ch, 91(2011) 1267-81.

[71] F. Hernandez, J.V. Sancho, M. Ibanez, C. Guerrero, Antibiotic residue determination in environmental waters by LC-MS, Trac-Trend Anal Chem, 26(2007) 466-85.

[72] S. Bayen, X.Z. Yi, E. Segovia, Z. Zhou, B.C. Kelly, Analysis of selected antibiotics in surface freshwater and seawater using direct injection in liquid chromatography electrospray ionization tandem mass spectrometry, J Chromatogr A, 1338(2014) 38-43.

[73] K.R. Rogers, Biosensors for environmental applications, Biosensors and bioelectronics, 10(1995) 533-41.

[74] S. Jarque, M. Bittner, L. Blaha, K. Hilscherova, Yeast Biosensors for Detection of Environmental Pollutants: Current State and Limitations, Trends Biotechnol, 34(2016) 408-19.

[75] D.P. Nikolelis, U.J. Krull, J. Wang, M. Mascini, Biosensors for direct monitoring of environmental pollutants in field: Springer Science & Business Media; 2013.

[76] T. Kunitake, Fundamentals and perspectives of molecular imprinting in sensor applications, Handbook of Molecular Imprinting: Advanced Sensor Applications, (2012) 1.

[77] G. Vasapollo, R. Del Sole, L. Mergola, M.R. Lazzoi, A. Scardino, S. Scorrano, et al., Molecularly Imprinted Polymers: Present and Future Prospective, Int J Mol Sci, 12(2011) 5908-45.

[78] L.X. Chen, X.Y. Wang, W.H. Lu, X.Q. Wu, J.H. Li, Molecular imprinting: perspectives and applications, Chem Soc Rev, 45(2016) 2137-211.

[79] M. Yoshikawa, K. Tharpa, S.O. Dima, Molecularly Imprinted Membranes: Past, Present, and Future, Chem Rev, 116(2016) 11500-28.

[80] A.J. Hall, F. Lanza-Sellergren, P. Manesiotis, B. Sellergren, Non-covalent imprinting of phosphorous esters (vol 538, pg 9, 2005), Anal Chim Acta, 540(2005) 417-.

[81] L. Ye, Molecular imprinting: Principles and applications of micro-and nanostructure polymers: CRC press; 2013.

[82] V. Pichon, F. Chapuis-Hugon, Role of molecularly imprinted polymers for selective determination of environmental pollutants - A review, Anal Chim Acta, 622(2008) 48-61.

[83] G. Vlatakis, L.I. Andersson, R. Muller, K. Mosbach, Drug Assay Using Antibody Mimics Made by Molecular Imprinting, Nature, 361(1993) 645-7.

[84] V. Pichon, K. Haupt, Affinity separations on molecularly imprinted polymers with special emphasis on solid-phase extraction, J Liq Chromatogr R T, 29(2006) 989-1023.

[85] G. Wulff, Enzyme-like catalysis by molecularly imprinted polymers, Chem Rev, 102(2002) 1-27.

[86] B. Sellergren, C.J. Allender, Molecularly imprinted polymers: A bridge to advanced drug delivery, Adv Drug Deliver Rev, 57(2005) 1733-41.

[87] M. Szumski, B. Buszewski, Molecularly imprinted polymers: A new tool for separation of steroid isomers, J Sep Sci, 27(2004) 837-42.

[88] S.-W. Lee, T. Kunitake, Handbook of molecular imprinting: advanced sensor applications: CRC Press; 2012.

[89] J. Nilsson, P. Spegel, S. Nilsson, Molecularly imprinted polymer formats for capillary electrochromatography, J Chromatogr B, 804(2004) 3-12.

[90] A. Cutivet, C. Schembri, J. Kovensky, K. Haupt, Molecularly Imprinted Microgels as Enzyme Inhibitors, J Am Chem Soc, 131(2009) 14699-702.

[91] V.P. M, O. Nazarenko, Nanostructured Polymer Membranes, Volume 1: Processing and Characterization: Wiley; 2016.

[92] R.I. Boysen, L.J. Schwarz, D.V. Nicolau, M.T.W. Hearn, Molecularly imprinted polymer membranes and thin films for the separation and sensing of biomacromolecules, J Sep Sci, 40(2017) 314-35.

[93] D.X. Yin, M. Ulbricht, Antibody-Imprinted Membrane Adsorber via Two-Step Surface Grafting, Biomacromolecules, 14(2013) 4489-96.

[94] T. Zhu, D. Xu, Y.G. Wu, J. Li, M.M. Zhou, T. Tian, et al., Surface molecularly imprinted electrospun affinity membranes with multimodal pore structures for efficient separation of proteins, J Mater Chem B, 1(2013) 6449-58.

[95] X.L. Ma, R.Y. Chen, X. Zheng, H.U. Youn, Z. Chen, Preparation of molecularly imprinted CS membrane for recognizing naringin in aqueous media, Polym Bull, 66(2011) 853-63.

[96] R. Thoelen, R. Vansweevelt, J. Duchateau, F. Horemans, J. D'Haen, L. Lutsen, et al., A MIP-based impedimetric sensor for the detection of low-MW molecules, Biosens Bioelectron, 23(2008) 913-8.

[97] B. Sellergren, Imprinted Polymers with Memory for Small Molecules, Proteins, or Crystals The author is grateful to Dr. Andrew Hall and Dr. Gunter Buchel for linguistic advice, Angew Chem Int Ed Engl, 39(2000) 1031-7.

[98] A.G. Ayankojo, J. Reut, R. Boroznjak, A. Opik, V. Syritski, Molecularly imprinted poly(meta-phenylenediamine) based QCM sensor for detecting Amoxicillin, Sensor Actuat B-Chem, 258(2018) 766-74.

[99] A.G. Ayankojo, J. Reut, A. Öpik, A. Tretjakov, V. Syritski, Enhancing binding properties of imprinted polymers for the detection of small molecules, Proceedings of the Estonian Academy of Sciences, 4017(2018) 2.

[100] A. Tretjakov, V. Syritski, J. Reut, R. Boroznjak, A. Opik, Molecularly imprinted polymer film interfaced with Surface Acoustic Wave technology as a sensing platform for label-free protein detection, Anal Chim Acta, 902(2016) 182-8.

[101] A. Tretjakov, V. Syritski, J. Reut, R. Boroznjak, O. Volobujeva, A. Opik, Surface molecularly imprinted polydopamine films for recognition of immunoglobulin G, Microchim Acta, 180(2013) 1433-42.

[102] P.S. Sharma, M. Dabrowski, F. D'Souza, W. Kutner, Surface development of molecularly imprinted polymer films to enhance sensing signals, Trac-Trend Anal Chem, 51(2013) 146-57.

[103] C.J. Percival, S. Stanley, A. Braithwaite, M.I. Newton, G. McHale, Molecular imprinted polymer coated QCM for the detection of nandrolone, Analyst, 127(2002) 1024-6.

[104] B.S. Ebarvia, C.A. Binag, F. Sevilla, Biomimetic piezoelectric quartz sensor for caffeine based on a molecularly imprinted polymer, Anal Bioanal Chem, 378(2004) 1331-7.

[105] T. Piacham, A. Josell, H. Arwin, V. Prachayasittikul, L. Ye, Molecularly imprinted polymer thin films on quartz crystal microbalance using a surface bound photo-radical initiator (vol 536, pg 191, 2005), Anal Chim Acta, 542(2005) 135-.

[106] S. Cosnier, M. Holzinger, Electrosynthesized polymers for biosensing, Chem Soc Rev, 40(2011) 2146-56.

[107] C. Malitesta, I. Losito, P.G. Zambonin, Molecularly imprinted electrosynthesized polymers: New materials for biomimetic sensors, Anal Chem, 71(1999) 1366-70.

[108] C. Malitesta, E. Mazzotta, R.A. Picca, A. Poma, I. Chianella, S.A. Piletsky, MIP sensors - the electrochemical approach, Anal Bioanal Chem, 402(2012) 1827-46.

[109] B. Schweiger, J. Kim, Y.J. Kim, M. Ulbricht, Electropolymerized Molecularly Imprinted Polypyrrole Film for Sensing of Clofibric Acid, Sensors-Basel, 15(2015) 4870-89.

[110] A.C. Roy, V.S. Nisha, C. Dhand, M.A. Ali, B.D. Malhotra, Molecularly imprinted polyaniline-polyvinyl sulphonic acid composite based sensor for para-nitrophenol detection, Anal Chim Acta, 777(2013) 63-71.

[111] R.B. Pernites, R.R. Ponnapati, R.C. Advincula, Surface Plasmon Resonance (SPR) Detection of Theophylline via Electropolymerized Molecularly Imprinted Polythiophenes, Macromolecules, 43(2010) 9724-35.

[112] K.C. Ho, W.M. Yeh, T.S. Tung, J.Y. Liao, Amperometric detection of morphine based on poly(3,4-ethylenedioxythiophene) immobilized molecularly imprinted polymer particles prepared by precipitation polymerization, Anal Chim Acta, 542(2005) 90-6.

[113] G.J. Owens, R.K. Singh, F. Foroutan, M. Alqaysi, C.M. Han, C. Mahapatra, et al., Sol-gel based materials for biomedical applications, Prog Mater Sci, 77(2016) 1-79.

[114] M.E. Diaz-Garcia, R.B. Laino, Molecular imprinting in sol-gel materials: Recent developments and applications, Microchim Acta, 149(2005) 19-36.

[115] A. Walcarius, M.M. Collinson, Analytical Chemistry with Silica Sol-Gels: Traditional Routes to New Materials for Chemical Analysis, Annu Rev Anal Chem, 2(2009) 121-43.

[116] S. Marx, Z. Liron, Molecular imprinting in thin films of organic-inorganic hybrid sol-gel and acrylic polymers, Chem Mater, 13(2001) 3624-30.

[117] B. Wilson, Kinetics and Molecular Binding of GEPIs on Solid Surfaces: University of Washington; 2010.

[118] V. Hodnik, G. Anderluh, Toxin Detection by Surface Plasmon Resonance, Sensors-Basel, 9(2009) 1339-54.

[119] Y. Liu, Q. Liu, S.M. Chen, F. Cheng, H.Q. Wang, W. Peng, Surface Plasmon Resonance Biosensor Based on Smart Phone Platforms, Sci Rep-Uk, 5(2015).

[120] A. Fernandez-Gonzalez, L. Guardia, R. Badia-Laino, M.E. Diaz-Garcia, Mimicking molecular receptors for antibiotics - analytical implications, Trac-Trend Anal Chem, 25(2006) 949-57.

[121] M. Siemann, L.I. Andersson, K. Mosbach, Separation and detection of macrolide antibiotics by HPLC using macrolide-imprinted synthetic polymers as stationary phases, J Antibiot, 50(1997) 89-91.

[122] R. Levi, S. McNiven, S.A. Piletsky, S.H. Cheong, K. Yano, I. Karube, Optical detection of chloramphenicol using molecularly imprinted polymers, Anal Chem, 69(1997) 2017-21.

[123] J.L. Suarez-Rodriguez, M.E. Diaz-Garcia, Fluorescent competitive flow-through assay for chloramphenicol using molecularly imprinted polymers, Biosens Bioelectron, 16(2001) 955-61.

[124] K. Skudar, O. Bruggemann, A. Wittelsberger, O. Ramstrom, Selective recognition and separation of beta-lactam antibiotics using molecularly imprinted polymers, Anal Commun, 36(1999) 327-31.

[125] J. Cederfur, Y.X. Pei, Z.H. Meng, M. Kempe, Synthesis and screening of a molecularly imprinted polymer library targeted for penicillin G, J Comb Chem, 5(2003) 67-72.

[126] N. Zheng, Q. Fu, Y.Z. Li, W.B. Chang, Z.M. Wang, T.J. Li, Chromatographic characterization of sulfonamide imprinted polymers, Microchem J, 69(2001) 153-8.

[127] N. Zheng, Y.Z. Li, W.B. Chang, Z.M. Wang, T.J. Li, Sulfonamide imprinted polymers using co-functional monomers, Anal Chim Acta, 452(2002) 277-83.

[128] N. Zheng, Y.Z. Li, M.J. Wen, Sulfamethoxazole-imprinted polymer for selective determination of sulfamethoxazole in tablets, J Chromatogr A, 1033(2004) 179-82.

[129] H. Asanuma, T. Akiyama, K. Kajiya, T. Hishiya, M. Komiyama, Molecular imprinting of cyclodextrin in water for the recognition of nanometer-scaled guests, Anal Chim Acta, 435(2001) 25-33.

[130] C. Lubke, M. Lubke, M.J. Whitcombe, E.N. Vulfson, Imprinted polymers prepared with stoichiometric template-monomer complexes: Efficient binding of ampicillin from aqueous solutions, Macromolecules, 33(2000) 5098-105.

[131] B.B. Prasad, S. Banerjee, Preparation, characterization and performance of a silica gel bonded molecularly imprinted polymer for selective recognition and enrichment of beta-lactam antibiotics, React Funct Polym, 55(2003) 159-69.

[132] E.P.C. Lai, S.G. Wu, Molecularly imprinted solid phase extraction for rapid screening of cephalexin in human plasma and serum, Anal Chim Acta, 481(2003) 165-74.

[133] M.C. Moreno-Bondi, E. Benito-Pena, B. San Vicente, F. Navarro-Villoslada, M.E. de Leon, G. Orellana, et al., Molecularly imprinted polymers as selective recognition elements for optical sensors based on fluorescent measurements, Boston Transducers'03: Digest of Technical Papers, Vols 1 and 2, (2003) 975-8.

[134] E. Caro, R.M. Marce, P.A.G. Cormack, D.C. Sherrington, F. Borrull, Synthesis and application of an oxytetracycline imprinted polymer for the solid-phase extraction of tetracycline antibiotics, Anal Chim Acta, 552(2005) 81-6.

[135] Y.W. Tang, Z.F. Huang, T. Yang, X.G. Hu, X.O. Jiang, The characteristic and application of molecularly imprinted polymer: Efficient sample preconcentration of antibiotic cefathiamidine from human plasma and serum by solid phase extraction, Anal Lett, 38(2005) 219-26.

[136] X.J. Liu, C.B. Ouyan, R. Zhao, D.H. Shangguan, Y. Chen, G.Q. Liu, Monolithic molecularly imprinted polymer for sulfamethoxazole and molecular recognition properties in aqueous mobile phase, Anal Chim Acta, 571(2006) 235-41.

[137] M. Frasconi, R. Tel-Vered, M. Riskin, I. Willner, Surface Plasmon Resonance Analysis of Antibiotics Using Imprinted Boronic Acid-Functionalized Au Nanoparticle Composites, Anal Chem, 82(2010) 2512-9.

[138] G. Wulff, Fourty years of molecular imprinting in synthetic polymers: origin, features and perspectives, Microchim Acta, 180(2013) 1359-70.

[139] D.R. Delgado, A. Romdhani, F. Martinez, Solubility of sulfamethizole in some propylene glycol plus water mixtures at several temperatures, Fluid Phase Equilibr, 322(2012) 113-9.

[140] M.J. Garcia-Galan, T. Garrido, J. Fraile, A. Ginebreda, M.S. Diaz-Cruz, D. Barcelo, Simultaneous occurrence of nitrates and sulfonamide antibiotics in two ground water bodies of Catalonia (Spain), J Hydrol, 383(2010) 93-101.

[141] B. Pose-Vilarnovo, I. Perdomo-Lopez, M. Echezarreta-Lopez, P. Schroth-Pardo, E. Estrada, J.J. Torres-Labandeira, Improvement of water solubility of sulfamethizole through its complexation with β-and hydroxypropyl-β-cyclodextrin: Characterization of the interaction in solution and in solid state, European journal of pharmaceutical sciences, 13(2001) 325-31.

[142] C. Ratanajamit, M.V. Skriver, M. Norgaard, P. Jepsen, H.C. Schonheyder, H.T. Sorensen, Adverse pregnancy outcome in users of sulfamethizole during pregnancy: a population-based observational study, J Antimicrob Chemother, 52(2003) 837-41.

[143] H. Dejmkova, M. Mikes, J. Barek, J. Zima, Determination of Sulfamethizole Using Voltammetry and Amperometry on Carbon Paste Electrode, Electroanal, 25(2013) 189-94.

[144] S.M. Ghoreishi, M. Behpour, A. Khoobi, Z. Moghadam, Determination of Trace Amounts of Sulfamethizole Using a Multi-Walled Carbon Nanotube Modified Electrode: Application of Experimental Design in Voltammetric Studies, Anal Lett, 46(2013) 323-39.

[145] M.S. Diaz-Cruz, M.J. Garcia-Galan, D. Barcelo, Highly sensitive simultaneous determination of sulfonamide antibiotics and one metabolite in environmental waters by liquid chromatography-quadrupole linear ion trap-mass spectrometry, J Chromatogr A, 1193(2008) 50-9.

[146] A. Iglesias, C. Nebot, J.M. Miranda, B.I. Vazquez, A. Cepeda, Detection and quantitative analysis of 21 veterinary drugs in river water using high-pressure liquid chromatography coupled to tandem mass spectrometry, Environ Sci Pollut R, 19(2012) 3235-49.

[147] M.J. Garcia-Galan, M.S. Diaz-Cruz, D. Barcelo, Determination of 19 sulfonamides in environmental water samples by automated on-line solid-phase extraction-liquid chromatography-tandem mass spectrometry (SPE-LC-MS/MS), Talanta, 81(2010) 355-66.

[148] R.H. Moseley, Hepatotoxicity of Antimicrobials and Antifungal Agents, Drug-Induced Liver Disease, 3rd Edition, (2013) 463-81.

[149] B.A. de Marco, J.S.H. Natori, S. Fanelli, E.G. Totoli, H.R.N. Salgado, Characteristics, Properties and Analytical Methods of Amoxicillin: A Review with Green Approach, Crit Rev Anal Chem, 47(2017) 267-77.

[150] B.G. Padilla-Robles, A. Alonso, S.A. Martinez-Delgadillo, M. Gonzalez-Brambila, U.J. Jauregui-Haza, J. Ramirez-Munoz, Electrochemical degradation of amoxicillin in aqueous media, Chem Eng Process, 94(2015) 93-8.

[151] F. Sopaj, M.A. Rodrigo, N. Oturan, F.I. Podvorica, J. Pinson, M.A. Oturan, Influence of the anode materials on the electrochemical oxidation efficiency. Application to oxidative degradation of the pharmaceutical amoxicillin, Chem Eng J, 262(2015) 286-94.

[152] A. Lamm, I. Gozlan, A. Rotstein, D. Avisar, Detection of amoxicillin-diketopiperazine-2 ', 5 ' in wastewater samples, J Environ Sci Heal A, 44(2009) 1512-7.

[153] D.A. Spivak, Optimization, evaluation, and characterization of molecularly imprinted polymers, Adv Drug Deliver Rev, 57(2005) 1779-94.

[154] R.J. Ansell, Characterization of the Binding Properties of Molecularly Imprinted Polymers, Adv Biochem Eng Biot, 150(2015) 51-93.

[155] R.J. Umpleby, M. Bode, K.D. Shimizu, Measurement of the continuous distribution of binding sites in molecularly imprinted polymers, Analyst, 125(2000) 1261-5.

[156] R.J. Umpleby, S.C. Baxter, Y.Z. Chen, R.N. Shah, K.D. Shimizu, Characterization of molecularly imprinted polymers with the Langmuir-Freundlich isotherm, Anal Chem, 73(2001) 4584-91.

[157] Y. Liu, L. Shen, From Langmuir kinetics to first- and second-order rate equations for adsorption, Langmuir, 24(2008) 11625-30.

[158] Y.S. Ho, Review of second-order models for adsorption systems, J Hazard Mater, 136(2006) 681-9.

[159] S.J. Li, X. Huang, M.X. Zheng, W.K. Li, K.J. Tong, Molecularly imprinted polymers: Thermodynamic and kinetic considerations on the specific sorption and molecular recognition, Sensors-Basel, 8(2008) 2854-64.

[160] R.J. Umpleby, S.C. Baxter, A.M. Rampey, G.T. Rushton, Y.Z. Chen, K.D. Shimizu, Characterization of the heterogeneous binding site affinity distributions in molecularly imprinted polymers, J Chromatogr B, 804(2004) 141-9.

[161] O.K. Castell, D.A. Barrow, A.R. Kamarudin, C.J. Allender, Current practices for describing the performance of molecularly imprinted polymers can be misleading and may be hampering the development of the field, J Mol Recognit, 24(2011) 1115-22.

[162] C. Baggiani, C. Giovannoli, L. Anfossi, C. Passini, P. Baravalle, G. Giraudi, A Connection between the Binding Properties of Imprinted and Nonimprinted Polymers: A Change of Perspective in Molecular Imprinting, J Am Chem Soc, 134(2012) 1513-8.

[163] C. Hahnefeld, S. Drewianka, F.W. Herberg, Determination of Kinetic Data Using Surface Plasmon Resonance Biosensors, in: J. Decler, U. Reischl (Eds.), Molecular Diagnosis of Infectious Diseases, Humana Press, Totowa, NJ, 2004, pp. 299-320.

[164] D.O. Grigoriev, E. Kolodzlejczyk, M.E. Leser, M. Michel, R. Miller, Effect of fluorescence labelling on the properties of protein adsorption layers at the air/water interface, Food Hydrocolloid, 23(2009) 221-4.

[165] Y. Uludag, S.A. Piletsky, A.P.F. Turner, M.A. Cooper, Piezoelectric sensors based on molecular imprinted polymers for detection of low molecular mass analytes, Febs J, 274(2007) 5471-80.

[166] B. Drafts, Acoustic wave technology sensors, Ieee T Microw Theory, 49(2001) 795-802.

[167] K. Lange, B.E. Rapp, M. Rapp, Surface acoustic wave biosensors: a review, Anal Bioanal Chem, 391(2008) 1509-19.

[168] V. Ferrari, R. Lucklum, Overview of Acoustic-Wave Microsensors, in: A. Arnau Vives (Ed.) Piezoelectric Transducers and Applications, Springer Berlin Heidelberg, Berlin, Heidelberg, 2004, pp. 39-54.

[169] J. Curie, P. Curie, An oscillating quartz crystal mass detector, Rendu, 91(1880) 294-7.

[170] S.J. Martin, G.C. Frye, K.O. Wessendorf, Sensing Liquid Properties with Thickness-Shear Mode Resonators, Sensor Actuat a-Phys, 44(1994) 209-18.

[171] D.X. Wang, P. Mousavi, P.J. Hauser, W. Oxenham, C.S. Grant, Quartz crystal microbalance in elevated temperature viscous liquids: Temperature effect compensation and lubricant degradation monitoring, Colloid Surface A, 268(2005) 30-9.

[172] B. Acharya, M.A. Sidheswaran, R. Yungk, J. Krim, Quartz crystal microbalance apparatus for study of viscous liquids at high temperatures, Rev Sci Instrum, 88(2017).

[173] H.F. Zu, H.Y. Wu, Q.M. Wang, High-Temperature Piezoelectric Crystals for Acoustic Wave Sensor Applications, Ieee T Ultrason Ferr, 63(2016) 486-505.

[174] M.A. Cooper, V.T. Singleton, A survey of the 2001 to 2005 quartz crystal microbalance biosensor literature: applications of acoustic physics to the analysis of biomolecular interactions, J Mol Recognit, 20(2007) 154-84.

[175] T.Y. Lin, C.H. Hu, T.C. Chou, Determination of albumin concentration by MIP-QCM sensor, Biosens Bioelectron, 20(2004) 75-81.

[176] N.M. Maier, W. Lindner, Chiral recognition applications of molecularly imprinted polymers: a critical review, Anal Bioanal Chem, 389(2007) 377-97.

[177] M.I. Rocha-Gaso, C. March-Iborra, A. Montoya-Baides, A. Arnau-Vives, Surface Generated Acoustic Wave Biosensors for the Detection of Pathogens: A Review, Sensors-Basel, 9(2009) 5740-69.

[178] G. Kovacs, M.J. Vellekoop, R. Haueis, G.W. Lubking, A. Venema, A Love Wave Sensor for (Bio)Chemical Sensing in Liquids, Sensor Actuat a-Phys, 43(1994) 38-43.

[179] J. Du, G.L. Harding, J.A. Ogilvy, P.R. Dencher, M. Lake, A study of love-wave acoustic sensors, Sensor Actuat a-Phys, 56(1996) 211-9.

[180] W.A. Groves, E.T. Zellers, Analysis of solvent vapors in breath and ambient air with a surface acoustic wave sensor array, Ann Occup Hyg, 45(2001) 609-23.

[181] A.Z. Sadek, W. Wlodarski, K. Shin, R.B. Kaner, K. Kalantar-zadeh, A layered surface acoustic wave gas sensor based on a polyaniline/In2O3 nanofibre composite, Nanotechnology, 17(2006) 4488-92.

[182] Y. Fuchs, O. Soppera, A.G. Mayes, K. Haupt, Holographic Molecularly Imprinted Polymers for Label-Free Chemical Sensing, Adv Mater, 25(2013) 566-70.

[183] W.M. Mullett, E.P.C. Lai, J.M. Yeung, Surface plasmon resonance-based immunoassays, Methods, 22(2000) 77-91.

[184] R.P.H. Kooyman, R.M. Corn, A. Wark, H.J. Lee, E. Gedig, G. Engbers, et al., Handbook of Surface Plasmon Resonance: Royal Society of Chemistry; 2008.

[185] A.J. Tudos, R.B. Schasfoort, Introduction to surface plasmon resonance, Handbook of surface plasmon resonance, (2008) 1-14.

[186] D.R. Shankaran, K.V.A. Gobi, N. Miura, Recent advancements in surface plasmon resonance immunosensors for detection of small molecules of biomedical, food and environmental interest, Sensor Actuat B-Chem, 121(2007) 158-77.

[187] J. Matsui, K. Akamatsu, N. Hara, D. Miyoshi, H. Nawafune, K. Tamaki, et al., SPR sensor chip for detection of small molecules using molecularly imprinted polymer with embedded gold nanoparticles, Anal Chem, 77(2005) 4282-5.

[188] S.S. Hinman, K.S. McKeating, Q. Cheng, Surface Plasmon Resonance: Material and Interface Design for Universal Accessibility, Anal Chem, 90(2018) 19-39.

[189] H.Y. Yan, K.H. Row, Characteristic and synthetic approach of molecularly imprinted polymer, Int J Mol Sci, 7(2006) 155-78.

[190] L.E. Gomez-Pineda, G.E. Pina-Luis, C.M. Cortes-Romero, M.E. Palomar-Pardave, G.A. Rosquete-Pina, M.E. Diaz-Garcia, et al., Quantum Chemical Calculations on the Interaction between Flavonol and Functional Monomers (Methacrylic Acid and 4-Vinylpyridine) in Molecularly Imprinted Polymers, Molecules, 15(2010) 4017-32.

[191] J. Bengtsson-Palme, D.G.J. Larsson, Concentrations of antibiotics predicted to select for resistant bacteria: Proposed limits for environmental regulation, Environ Int, 86(2016) 140-9.

[192] T.B. Minh, H.W. Leung, I.H. Loi, W.H. Chan, M.K. So, J.Q. Mao, et al., Antibiotics in the Hong Kong metropolitan area: Ubiquitous distribution and fate in Victoria Harbour, Mar Pollut Bull, 58(2009) 1052-62.

Appendix

PAPER I

Akinrinade George Ayankojo, Aleksei Tretjakov, Jekaterina Reut, Roman Borozniak, Andres Öpik, Jörg Rappich, Andreas Furchner, Karsten Hinrichs, and Vitali Syritski. Molecularly imprinted polymer integrated with a surface acoustic wave technique for detection of sulfamethizole, *Analytical chemistry* 88(2) (2016) 1476-1484.

analytical chemistry

Article

pubs.acs.org/ac

Molecularly Imprinted Polymer Integrated with a Surface Acoustic Wave Technique for Detection of Sulfamethizole

Akinrinade George Ayankojo,[†] Aleksei Tretjakov,[†] Jekaterina Reut,[†] Roman Boroznjak,[†] Andres Öpik,[†] Jörg Rappich,[‡] Andreas Furchner,[§] Karsten Hinrichs,[§] and Vitali Syritski*[,†]

[†]Department of Materials Science, Tallinn University of Technology, Ehitajate tee 5, 19086 Tallinn, Estonia

[‡]Helmholtz-Zentrum Berlin für Materialien und Energie GmbH, Institut für Silizium-Photovoltaik, Kekuléstr. 5, 12489 Berlin, Germany

[§]Leibniz-Institut für Analytische Wissenschaften−ISAS−e.V., Schwarzschildstraße 8, 12489 Berlin, Germany

Supporting Information

ABSTRACT: The synergistic effect of combining molecular imprinting and surface acoustic wave (SAW) technologies for the selective and label-free detection of sulfamethizole as a model antibiotic in aqueous environment was demonstrated. A molecularly imprinted polymer (MIP) for sulfamethizole (SMZ) selective recognition was prepared in the form of a homogeneous thin film on the sensing surfaces of SAW chip by oxidative electropolymerization of *m*-phenylenediamine (mPD) in the presence of SMZ, acting as a template. Special attention was paid to the rational selection of the functional monomer using computational and spectroscopic approaches. SMZ template incorporation and its subsequent release from the polymer was supported by IR microscopic measurements. Precise control of the thicknesses of the SMZ-MIP and respective nonimprinted reference films (NIP) was achieved by correlating the electrical charge dosage during electrodeposition with spectroscopic ellipsometry measurements in order to ensure accurate interpretation of label-free responses originating from the MIP modified sensor. The fabricated SMZ-MIP films were characterized in terms of their binding affinity and selectivity toward the target by analyzing the binding kinetics recorded using the SAW system. The SMZ-MIPs had SMZ binding capacity approximately more than eight times higher than the respective NIP and were able to discriminate among structurally similar molecules, i.e., sulfanilamide and sulfadimethoxine. The presented approach for the facile integration of a sulfonamide antibiotic-sensing layer with SAW technology allowed observing the real-time binding events of the target molecule at nanomolar concentration levels and could be potentially suitable for cost-effective fabrication of a multianalyte chemosensor for analysis of hazardous pollutants in an aqueous environment.

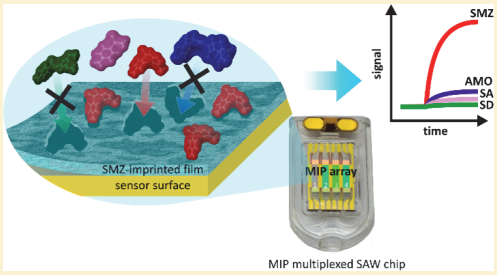

Antibiotics constitute one of the major pharmaceutical pollutants in the aquatic environment because of their extensive use in human and veterinary medicines[1] and contributions from many other sources such as sewage treatment plants.[2] One of the largest and most frequently applied groups of antibiotics is the sulfonamides that possess hypoglycemic, diuretic, anticancer, and antiviral activity.[3,4] Persistence and toxicity of antibiotics in the environment facilitate the expansion or developments of antibiotic-resistant human pathogens.[5,6] As a result, there is an urgent need for an effective and selective method for the detection of these pharmaceuticals from wastewater and drinking water. Many methodologies, including high pressure liquid chromatography and mass spectrometry, liquid chromatography coupled to tandem mass spectrometry, mass spectrometry, and solid phase extraction[7−9] have been used for identifying the occurrence of antibiotics in the aquatic environment. However, the disadvantages of these methods in the demand of complex sample preparation steps and the low analyte concentration typically found in environmental water have called for highly sensitive and selective alternative methods.

Rapid growth of interest is observed in the design and development of synthetic recognition elements, e.g. molecular imprinted polymers (MIPs), aimed at the selective and reliable detection of analytes in multiple applications.[10,11] Molecular imprinting creates cavities of specific recognition within synthetic polymers generated in the presence of a target molecule, acting as a template during polymerization of suitable monomers. Removal of the template after polymerization leaves spatially and functionally complementary sites capable of selectively recognizing (rebinding) the target molecule. Owing to the predefined selectivity of MIPs, they have been employed in a wide range of applications including analytical

Received: December 14, 2015
Accepted: December 25, 2015
Published: December 25, 2015

DOI: 10.1021/acs.analchem.5b04735
Anal. Chem. 2016, 88, 1476−1484

separation,[10] catalysis,[11] and sensor development.[12] There is an increasing number of publications focused on the use of selective MIPs in the detection and analysis of drugs and environmental pollutants, including antibiotics, using solid phase extraction and chromatography techniques.[13−15] Recently, the application of MIP-based selective sorbents in the determination and removal of pollutants from wastewater has been reviewed.[16] For these applications MIPs were mostly prepared as particles, beads, or microspheres that could be easily packed into an HPLC column or solid phase extraction (SPE) cartridge. However, use of MIPs for sensing purposes generally demands a MIP-based material in the form of a uniform thin film and its robust interfacing with a sensor platform capable of responding to relevant sensitivity levels upon interaction between MIP film and a binding analyte. In addition, the use of label-free sensing platforms for integration with MIPs can provide direct information on binding events on MIP surfaces and have increasingly been utilized in many laboratories to study the specific recognition ability and selectivity of MIPs.[17−19] Surface plasmon resonance (SPR) and quartz crystal microbalance (QCM) are the most popular label-free techniques employed for MIP study while the application of a surface acoustic wave (SAW) sensing platform has not been widespread and limited to the detection of gas and vapor.[20,21] Meanwhile, SAW systems utilizing Love-waves sensors that are capable of operating in a liquid environment[22] might provide advances in the study of MIP materials as well as fabrication of MIP-based sensors. SAW systems share a similar principle of operation with other piezogravimetric devices, e.g. QCM, but utilize acoustic waves at surfaces rather than in the bulk of a piezoelectric material, allowing increase of the operating frequencies of the sensors to the range of 100−500 MHz without compromising their mechanical fragility. Generally, owing to the high operating frequencies, SAW technology offers about an order of magnitude higher mass resolution than QCM-based system. This ensures low sensor cost, and it is fully compatible with large-scale fabrication and multiplexing technologies.[23,24] As compared to SPR, SAW technology is not limited to detecting only mass loading onto the surface but also useful in following structural insights of sensing layers through the use of dissipation factor of the acoustic wave propagating along the sensor surface.

Among the various synthetic approaches aiming to integrate a MIP-based recognition element with a sensor transducer, electrosynthesis has been shown to be a convenient method allowing rapid and controlled deposition of polymer films with tunable thickness.[25−30] With electrosynthesized MIPs, polymeric films can be easily grown with strict adherence to conducting electrodes of any shape and size and with a thickness controlled by the amount of circulated charge. This feature gives the possibility of creating a direct communication between the polymer and the surface of the transducer in a simple way. In this respect, electropolymerized films were recently fabricated on the sensor surface of SAW devices.[31,32]

Despite the numerous publications available on MIP-based detection of environmental pollutants, literature on the integration of antibiotic-MIP with sensor platforms, allowing real-time label-free analyte detection, is scarcely presented.[33−36] Very recently, Fourati's group[37] reported on the selective detection of flumequine in aqueous media, combining MIP with SAW sensor transducer. Nevertheless, in the reported studies little attention was paid to the choice of an adequate reference surface (nonimprinted polymer, NIP) that is of great importance for the accurate and reliable interpretation of label-free responses originating from a MIP modified sensor. Indeed, analytical performance of MIP-based sensors can be easily over- or underestimated when they are not properly optimized and characterized. In the concept presented here, the analytical performance of the antibiotic-MIP-based sensors was validated through careful comparison of their label-free responses with the appropriate NIP-modified sensors serving as reference surfaces. Additionally, in this study, a SAW system comprising of a pair of chips with four sensor elements each was used, thus allowing simultaneous running of most experiments in parallel. This further strengthened the data reliability for both MIP and NIP films by eliminating errors arising from deviations in the temperature and concentration of the analyte solutions as well as overcoming variability of the results due to the films and chips reproducibility.

To the best of our knowledge, MIP for detection of any member of sulfonamides employing SAW as a sensor transducer has never been reported. In this study, a facile integration of the sulfamethizole-MIP films with SAW sensing platform, providing their versatile characterization in terms of binding affinity and selectivity toward the target was reported for the first time. A widely used sulfonamide group antibiotic—sulfamethizole (SMZ)—was chosen as a model template molecule and a suitable functional monomer was selected among three electropolymerizable monomers, pyrrole, 3,4-ethylenedioxythiophene (EDOT) and *m*-phenylenediamine (mPD), based on computer modeling and spectroscopic analysis. A special attention was paid to careful control of the thicknesses of SMZ-MIP and corresponding reference films through electrical charge dosage during electrodeposition and its subsequent correlation with ellipsometry measurements. The analytical importance and the benefits inherent in combining high selective properties of MIPs with the sensitivity given by the SAW sensing technique for the detection of small analytes such as SMZ were also highlighted.

EXPERIMENTAL SECTION

Chemicals and Materials. All chemicals, except acetic acid, sulfuric acid, and hydrogen peroxide which were provided by Lachner, were obtained from Sigma-Aldrich. The chemicals were of analytical grade or higher and were used as received without any further purification. Ultrapure water (resistivity 18.2 MΩ·cm, Millipore, USA) was used for preparation of all aqueous solutions. Phosphate buffered saline (PBS) solution (0.01 M, pH 7.4) was used to prepare the synthesis and analyte solutions.

Optimization of the Polymer Matrix. *Computer Modeling.* Three electropolymerizable monomers, pyrrole, 3,4-ethylenedioxythiophene (EDOT), and *m*-phenylenediamine (mPD) were studied as potential functional monomers for SMZ-MIP film formation. GaussView 5.0.9 software was used to generate complexes of SMZ with the selected monomers and their geometries were optimized by semi-empirical PM3 method with Gaussian'09 software to ascertain the presence of hydrogen bonds. The conformational optimizations and binding energies for the complexes were calculated by density functional theory (DFT) method at B3LYP/6-31+G level with Gaussian'09 software.

Nuclear Magnetic Resonance (NMR) Study. ^{13}C NMR spectroscopy was carried out with Bruker SMART X2S benchtop diffractometer model. Samples were prepared in

DOI: 10.1021/acs.analchem.5b04735
Anal. Chem. 2016, 88, 1476−1484

acetonitrile (ACN) solution as a solvent. The molar ratio of template to monomer (SMZ:mPD) used for this study was 1:1.

Electropolymerization. The electrochemical synthesis parameters were varied in order to find optimal conditions for the homogeneous polymer film formation. Applied potential and electric charge density were varied in the range of 0.6−0.8 V and 5−11 mC/cm^2, respectively, while changing monomer concentrations from 2 to 10 mM. The electropolymerization was carried out in both aqueous, including PBS buffer, and organic, acetonitrile (ACN), solutions. The concentration of SMZ was determined by its solubility in the particular solution. The maximum SMZ concentration of 2 mM was achieved when dissolved in water at room temperature. However, in PBS (pH 7.4) increased solubility of up to 3.5 mM was observed while in ACN solution, SMZ solubility of 5 mM concentration was obtained.

SMZ-MIP Preparation and Characterization. *Preparation Procedure.* SMZ-MIP were fabricated directly on the gold (Au) electrodes of SAW chips (NanoTemper Technologies GmbH, München, Germany) comprising four sensor elements each with area 0.09 cm^2. The chips were preliminarily cleaned with a fresh base piranha solution (25% NH_4OH:30% H_2O_2:H_2O, 1:1:5 volume ratio) for 15 min, rinsed abundantly with ultrapure water, and treated in an UV/ozone cleaner followed by rinsing with ethanol and ultrapure water and drying in a nitrogen stream. The chips were placed into the 2 mL electrochemical cell designed to expose only the sensory elements of the chip to the synthesis solution. The electrochemical cell accommodated three electrodes, i.e., the gold surface of the sensor element as a working electrode, a spiral shaped Pt wire as a counter electrode, and Ag/AgCl/KCl_{sat} as a reference electrode, all connected to an electrochemical workstation (Reference 600, Gamry Instruments, Inc., USA). SMZ-MIP films were generated by oxidative electropolymerization of mPD in the presence of SMZ, acting as a template, followed by its extraction from the formed PmPD/SMZ polymer matrix. The potentiostatic electropolymerization process at 0.6 V was controlled by passing an electric charge through the electrode of the sensor. To form the complementary cavities of SMZ in the polymeric matrix, PmPD/SMZ-modified chips were immersed in a mixture of acetic acid/methanol (1:3) with gentle stirring and allowed to stay for a period of 24 h. Then the chips were washed with distilled water and dried under a nitrogen stream. The PmPD films synthesized in the absence of the SMZ in the synthesis solution were used as control surfaces. These nonimprinted polymer (NIP) films were similarly allowed to undergo the treatment in a mixture of acetic acid/methanol to ensure the same chemical influence on the polymer matrix of both MIP and NIP films.

To ensure that SMZ-MIP and NIP films are of equal thickness, their growth was controlled by charge passing through the working electrode according to the calibration plot (see Preparation and Characterization of SMZ-MIP Film). Film thicknesses were determined by spectroscopic ellipsometry (SE 850, Sentech Instruments GmbH, Berlin, Germany), measuring ellipsometric Psi and Delta spectra between 350 and 850 nm at 70° incidence angle in ambient air on three spots of each film. Spectra were evaluated in SpectraRay 3 by performing a simultaneous fit on the film properties (thicknesses and dielectric function) of all samples using the optical layer model air/film/gold. The film dielectric function Epsilon was modeled with a constant part plus a Gaussian oscillator describing the electronic transitions in the benzene ring of the polymer.

IR-Microscopy Analysis. The infrared spectroscopic measurements of the polymer films were performed with a Bruker Hyperion 3000 FTIR microscope (BRUKER, Ettlingen, Germany). A Cassegrain objective (15×) with numerical aperture of 0.4 was used, and the spectra were obtained at an average angle of incidence of about 16.5° with a spectral resolution of 4 cm^{-1} and a lateral resolution of 160 μm × 160 μm. Details of used setup can be found elsewhere.[38] To ensure maximum linearity of the detected signals, the microscope was equipped with a photovoltaic mercury cadmium telluride detector. IR spectroscopy was established in the recent years for the characterization of electrochemically prepared organic films on Au and Si.[39−41]

Rebinding Study. The recognition ability of the fabricated SMZ-MIP films toward SMZ was validated by a SAW sensor system (SamX, NanoTemper Technologies GmbH, München, Germany), capable of handling two SAW chips. The microfluidics of the system provided the option to deliver analyte solutions to the modified sensor elements either individually or in serial fashion. The SAW sensors, modified with SMZ-MIP and NIP films, were loaded into the SAW system and equilibrated with running buffer (PBS, pH 7.4) until a stable baseline was established. Then the consecutive injections of the analyte solutions at a flow rate of 25 μL/min in the order from the lower to higher concentrations were applied and the signal changes were monitored. The analyte solutions with SMZ concentrations of 10.2, 25.6, 64, 160, 400, and 1000 μM were prepared using the running buffer. The recorded sensorgrams were fitted to the single-site Langmuir binding model[42] so as to determine the equilibrium responses for SMZ-MIP and NIP surfaces that were then used to construct the binding isotherms.

Selectivity Study. Selectivity analysis of the SMZ-MIP toward SMZ was carried out by running over the SMZ-MIP and NIP modified sensors different analytes; including structurally similar molecules from the same sulfonamide group of antibiotics, namely sulfanilamide (SA), sulfadimethoxine (SD) and nonstructurally related molecule such as amoxicillin (AMO). After the sensors were equilibrated with the running buffer and a stable baseline was established, the consecutive injections of the concentration series (10.2−1000 μM) of each of the antibiotic solutions were carried out at a flow rate of 25 μL/min and changes on the sensor responses were monitored. The sensor responses obtained were then analyzed and the selective properties of SMZ-MIP were assessed by comparing these responses with that obtained after SMZ injections.

Regeneration Study. To verify the stability of the fabricated SMZ-MIPs, the films were allowed to undergo three rebinding−regeneration cycles. Fixed concentration (1000 μM) of the SMZ solution was injected at every rebinding stage followed by regeneration in acetic acid/methanol (1:3) mixture. The signal responses after every rebinding stage were then monitored and analyzed.

RESULTS AND DISCUSSION

Polymer Matrix Selection and Optimization. The success of molecular imprinting depends to a large extent on the choice of a monomer. Functional monomers are selected to promote the formation of strong noncovalent interactions with a template molecule; hence, a monomer with a functional group complementary to the chemical functionality of the

DOI: 10.1021/acs.analchem.5b04735
Anal. Chem. 2016, 88, 1476−1484

template should be chosen. The noncovalent imprinting approach is more commonly used in molecular imprinting because there is no restriction in the choice of analyte and it allows simpler template extraction process compared to the covalent imprinting.[43] Of the wide variety of electrosynthesized polymers, polypyrrole (PPy),[30,46] polyaniline,[44,45] polythiophene,[46] poly(3,4-ethylenedioxythiophene) (PEDOT),[47] and their derivatives are the most widely used for MIP film formation by electrosynthesis. For our purpose, we have selected pyrrole, EDOT, and mPD (Figure 1) as potential

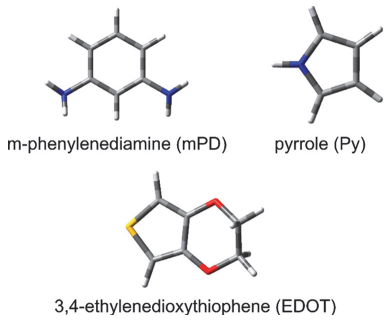

Figure 1. Molecular structures of mPD, pyrrole, and EDOT.

functional monomers for SMZ-MIP film formation. First, the prepolymerization complex formation between SMZ and a monomer was evaluated in terms of binding energies and hydrogen bond lengths via DFT method and the probability of covalent bond formation via ^{13}C NMR spectroscopy. Then, the electropolymerization of the monomers in the presence of SMZ was examined to produce a thin homogeneous polymer film on the sensor electrode. The computational method, DFT, is an increasingly common approach for investigating the interactions between monomer and template in molecularly imprinted polymer research.[48]

Prepolymerization Complex Formation. The optimized geometrical structures and energies of the prepolymerization complexes of SMZ with pyrrole, EDOT, and mPD in vacuum were investigated using a quantum chemical approach. As it can be seen in Table 1, mPD-SMZ complexes of different template/monomer ratio had higher binding energies as compared to the complexes with other monomers. Table 2 shows the corresponding data for the lengths of hydrogen bonds between SMZ and monomers. The simulations clearly indicated that among the three monomers, mPD was able to form stronger hydrogen bond complex with SMZ, where two molecules of mPD and one molecule of SMZ are favorably involved as shown in Figure 2.

Table 1. Binding Energies of SMZ Complex Formed with mPD, Pyrrole, and EDOT as Calculated by Gaussian'09

	binding energy (kcal/mol)	
monomer	complex ratio (1:1)	complex ratio (1:2)
mPD	166.155	181.203
Pyrrole	8.151	80.256
EDOT	30.096	

Table 2. Lengths[a] of Hydrogen Bonds between SMZ and Selected Monomers

SMZ–monomer complex	interacting atoms	length of hydrogen bond, Å
SMZ–mPD	O–H	1.74
SMZ–Py	O–H	2.62
SMZ–EDOT	H–O	2.79

[a]Defined as the distance between electronegative atoms participating in hydrogen bonding. The electronegativity of each atom is estimated by Mulliken charges as shown in Table S-1.

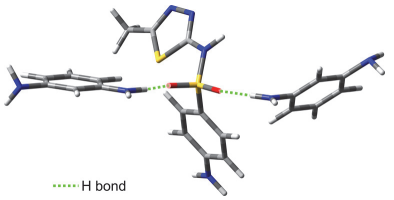

Figure 2. Illustration of hydrogen bonds (H-Bonds) between mPD and SMZ. An example of a possible optimized configuration for two molecules of mPD and one molecule of SMZ as visualized by GaussView 5.0.9.

The ^{13}C NMR spectrum (Figure S-1) of the template/monomer (SMZ/mPD) mixture showed no appearance of new peaks compared to the spectra of individual components, indicating the absence of covalent interactions between mPD and SMZ. Thus, the computational modeling and ^{13}C NMR spectra demonstrated a clear probability of noncovalent complex formation between mPD and SMZ as well as the absence of covalent bonding between these compounds suggesting the suitability of mPD as functional monomer for SMZ-MIP film formation.

Electropolymerization. The electrochemical polymerization of pyrrole, EDOT, and mPD in the presence of SMZ was conducted so as to produce a thin homogeneous polymer film on the sensor electrode. Considering the important role of the solvent, the electropolymerization in both aqueous and organic solutions was examined. The polymer synthesis from the organic solvent, ACN, was believed to be preferable for MIP synthesis because the potential interference with hydrogen bonding between the template molecule and monomer can be reduced and a higher solubility of SMZ (5 mM) was achieved. However, our results demonstrated that polymer films of all studied monomers produced from ACN, in the presence of SMZ were inhomogeneous and consequently, not suitable for further study. Also the electrochemical polymerization of pyrrole and EDOT from the aqueous solution containing polyelectrolyte polystyrenesulfonate as a dopant and SMZ as a template molecule resulted in nonhomogeneous polymer films. This indicates that PPy and PEDOT are not suitable as matrices for imprinting SMZ template molecules under these experimental conditions.

However, when electropolymerization was performed in the aqueous PBS buffer solution (pH 7.4) with mPD as a monomer, a homogeneous film of PmPD was obtained in both the presence and absence of SMZ molecule. The optimal parameters of mPD electropolymerization to produce a polymer matrix for the SMZ-MIP were determined as follows: 5 mM mPD and 3.5 mM SMZ in PBS buffer (pH 7.4) and a constant potential of 0.6 V. The maximum possible

DOI: 10.1021/acs.analchem.5b04735
Anal. Chem. 2016, 88, 1476–1484

concentration of SMZ in the PBS buffer, 3.5 mM, was used with regard to increasing the amount of the prepolymerization complex formed thereby increasing the number of the template imprinted in the polymer matrix.

Preparation and Characterization of SMZ-MIP Film. Using a label-free sensing platform for reliable characterization of MIP materials, in terms of their binding affinity and selectivity toward a target, is elegant but requires accurate avoidance/exclusion of contribution from unwanted nonspecific event to the net sensor response. If nonspecific binding background of an analyte with MIP matrix is difficult to minimize, a very similar polymeric material, but generated in the absence of a template, i.e. nonimprinted polymer (NIP), might serve as a good reference for the accurate analysis of label-free responses originating from a MIP modified sensor. It is important to note that as a polymeric material starts growing, its adsorptive surface area is also usually developed so that more analyte molecules can interact with this extended polymer matrix both specifically and/or nonspecifically per unit area and thus would give a higher analyte response from the modified sensor element, if other parameters remained equal. Thus, to evaluate properly the performance of a molecularly imprinted polymeric material, its physical dimension, i.e., the specific surface area, has to be equal to the respective nonimprinted one to keep any nonspecific contribution on both adsorptive surfaces virtually the same for all investigated film variations.

Figure 3a illustrates potentiostatic electrodeposition processes of PmPD with and without SMZ in the synthesis solution. As it can be easily observed, both processes were transient, however, in the presence of SMZ beyond 6 mC/cm^2, the oxidation process was considerably slower indicating that the conductivity of the growing polymeric material (PmPD/SMZ) was affected. Thus, the growth of PmPD/SMZ at the given conditions appeared as a well-pronounced self-limiting synthesis meaning that electrodeposition of such films thicker than those formed beyond 10 mC/cm^2 would be a rather time-consuming process. Although, after the template washing step, the resulting SMZ-MIP and the corresponding NIP films appeared to be quite equal, an approach ensuring their objectively equal thickness on the sensor elements was still needed. Thus, the spectroscopic ellipsometry of the different SMZ-MIP and NIP films was undertaken to yield a calibration graph of their thicknesses versus the synthesis charge applied (Figure 3b). As it can be seen, the thicknesses of both SMZ-MIP and NIP films varied nearly linearly across the applied charge range, thus making their prediction between ca. 1 and 24 nm quite certain. It should be noted that SMZ-MIP films appeared about 6% thicker than the NIP films on average. This could be related to the differences in the refractive indices n ($n_{SMZ\text{-}MIP}$ = 1.61 ± 0.03 and n_{NIP} = 1.65 ± 0.02), which hints at different densities of SMZ-MIP and NIP films. Since SMZ is a rather small molecular weight compound, greater surface area of a recognition layer would be preferable for its direct detection by label-free methods. Therefore, the thickest SMZ-MIP matrix (ca. 24 nm or 10 mC/cm^2) was formed on SAW sensor element to enhance, as far as possible, a response upon SMZ rebinding at its surface. The respective NIP film was formed by 10.6 mC/cm^2 as predicted by Figure 3a.

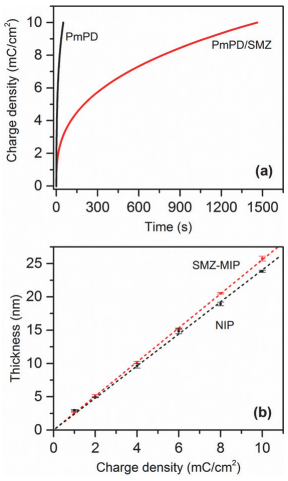

Figure 3. (a) Charge−time dependences recorded during electrodeposition of PmPD and PmPD/SMZ films on Au electrodes of SAW chip at a constant potential of 0.6 V vs Ag/AgCl/3 M NaCl until the charge density reached the value of 10 mC/cm^2. (b) Calibration graph representing the dependence of SMZ-MIP and NIP film thicknesses, as measured by the spectroscopic ellipsometry, on the amount of the charge consumed during the electrodeposition of the corresponding PmPD/SMZ or PmPD films.

To ensure that the SMZ molecules were incorporated and released in/from the polymer matrix after the electropolymerization and the washing-out procedure respectively, the IR microscopic measurements were performed (Figure 4).

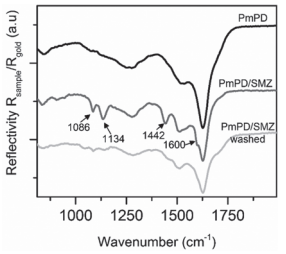

Figure 4. IR spectra of PmPD, PmPD/SMZ, and PmPD/SMZ after the washing out procedure (SMZ-MIP).

In the spectra of PmPD, the characteristic peaks could be clearly distinguished: a strong band at 1627 cm^{-1} as well as a weak band at 1496 cm^{-1} associated with the C═N and C═C stretching vibrations in the aromatic ring. A small peak at 1270 cm^{-1} could be due to C−N stretching vibration in an aromatic ring.[49] Although the spectrum of PmPD/SMZ was similar to the spectrum of PmPD, the appearance of new peaks at 1086, 1134, 1442, and 1600 cm^{-1} can be clearly seen. These peaks could be ascribed to the characteristic vibrations of SMZ molecule such as S═O stretching in sulfonamide group (1134 cm^{-1}), N−H bending in amine group (1086 cm^{-1}), aromatic vibration in thiadiazole ring (1442 cm^{-1}), and N−H bending in secondary amine (1600 cm^{-1}).[50] Moreover, it can be observed that these absorption peaks were significantly decreased in intensity or even disappeared after the washing out procedure. This indicates effective removal of the template from the polymer matrix during the washing out process. The spectral

DOI: 10.1021/acs.analchem.5b04735
Anal. Chem. 2016, 88, 1476−1484

results therefore confirmed the entrapment of SMZ molecules in the PmPD matrix during the electrochemical polymerization as well as their successful removal from the polymer film after the washing out procedure that presumably led to the complementary cavities (specific binding sites) capable of subsequent template molecule recognition.

Rebinding Study. SAW sensor technology was used in this study to quantify the SMZ-MIP in terms of its affinity and selectivity toward the chosen template (SMZ). The SAW system employed had flexibility for multichannel measurements that allowed to scrupulously obtain reliable data simultaneously for both MIP and NIP films, eliminating errors arising from deviations in the temperature, concentration of the analyte solutions, film reproducibility etc.

SMZ-MIP and NIP-modified SAW sensor responses upon injections of increasing concentrations of SMZ analyte solutions were recorded and plotted as binding isotherms

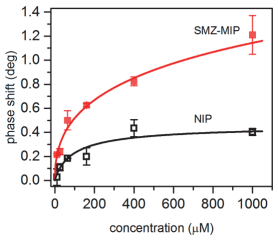

Figure 5. SMZ adsorption isotherms on SMZ-MIP and NIP surfaces. Solid lines represent fits to the Langmuir−Freundlich model.

(Figure 5). The experimental binding isotherms were fitted with the Langmuir−Freundlich (LF) model defined by eq 1:

$$Q = Q_{max}C^m/(K_D + C^m) \quad (1)$$

where C is the concentration of an analyte in a solution, Q and Q_{max} are sensor responses corresponding to the fraction of bound analyte at the concentration C and to its saturation value, respectively. m is the heterogeneity index, which varies from 0 to 1, and K_D is the equilibrium dissociation constant. This model has been shown to describe accurately both saturation and subsaturation regions of adsorption isotherms and was used successfully in modeling the adsorption behavior of many heterogeneous systems, including MIPs.[30,51] The fitting parameters are presented in Table 3.

Table 3. Parameters Obtained from the LF Fitting of the SMZ-MIP and NIP Binding Isotherms

	Q_{max} (deg)	K_D (μM)	m	R^2
SMZ-MIP	3.79 ± 0.09	47.2 ± 1.3	0.44 ± 0.006	0.989
NIP	0.46 ± 0.02	61.0 ± 0.4	0.89 ± 0.002	0.982

The LF isotherm more accurately modeled the binding behavior of SMZ-MIP and NIP films when the heterogeneity index m was below 1. Nevertheless, the imprinted polymer had a noticeably higher degree of heterogeneity (m = 0.44) than its corresponding nonimprinted control (m = 0.89). This can be well explained through the assumption that NIP films might contain nonspecific binding sites of mainly equal adsorption energy, while the imprinting process introduces binding sites with varying degrees of affinity resulting in the heterogeneity of the polymer surface. In addition, the response of SMZ-MIP modified sensor at saturation binding was more than 8 times higher than that of the respective NIP-modified sensor (3.79 vs 0.46 deg) indicating the increase in the total number of the binding sites in MIP relative to the NIP. Moreover, the somewhat lower dissociation constant (K_D) value obtained for SMZ-MIP hints that SMZ-MIP possesses a greater fraction of high-affinity binding sites contributing significantly to the overall affinity of SMZ-MIP as compared to NIP. Since sulfonamides were repeatedly found in the aquatic environment at concentrations ranging from 0.5 to 7 nM,[55,56] an additional experiment to test the performance of SMZ-MIP modified SAW sensor at low analyte concentrations was carried out. It was revealed that the sensor could distinguish the target analyte at least at 8 nM, while the concentration limit of detection (LOD) determined from the regression data of the calibration curve was 1.7 nM (Figure S-2). This suggests a greatly improved performance of the prepared SMZ-MIP sensor compared to other previously reported antibiotic-MIP sensors based on the different detection platforms (Table 4). However, optimization of the MIP sensing layer is needed to sufficiently employ the sensor in the demanded SMZ concentration ranges.

Selectivity Study. The ability of the SMZ-MIP films to selectively bind the target SMZ molecule was explored by exposing them to solutions of various antibiotics. Thus, the responses upon injection of sulfonamide antibiotics such as sulfanilamide (SA) and sulfadimethoxine (SD) as well as a β-lactam antibiotic such as amoxicillin (AMO) (Figure 6) were

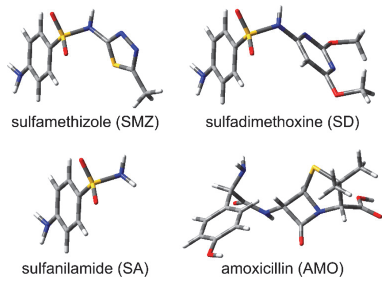

Figure 6. Antibiotics used in the SMZ-MIP selectivity test.

Table 4. Comparison of the Performances (in Terms of LOD Values) of Antibiotic-MIP Sensor Based on Different Detection Platforms

analyte	sensing platform	MIP composition	limit of detection (nM)	ref
levofloxacin	electrochemical	polypyrrole−graphene−gold nanoparticles	5.3×10^2	36
sulfadimethoxine	electrochemical	overoxidized polypyrrole	7×10^4	35
flumequine	SAW	polypyrrole	1×10^3	37
sulfamethizole	SAW	PmPD	ca. 2	this work

DOI: 10.1021/acs.analchem.5b04735
Anal. Chem. 2016, 88, 1476−1484

analyzed and compared with the corresponding response to SMZ at the respective concentration (Figure 7). As expected,

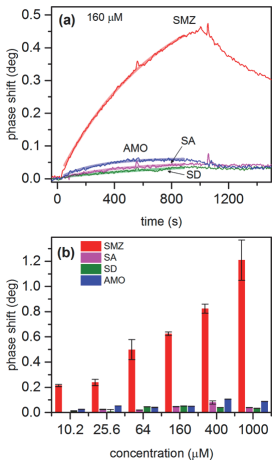

Figure 7. (a) Typical kinetic responses of SMZ-MIP modified SAW sensor upon injections of various antibiotics: SMZ, AMO, SD, and SA at 160 μM concentration in ultrapure water. The bold lines represent the fits to the single-site Langmuir model yielding the equilibrium sensor response at the given analyte concentration, Q_{eq}. (b) Bars representing the equilibrium responses (Q_{eq}) of SMZ-MIP modified SAW sensor to various antibiotics: SMZ, AMO, SD, and SA at different concentrations.

the highest response on SMZ-MIP surface was observed upon binding of the original template molecule, SMZ, while the responses to the other analytes, even though they closely resembled the chemical structure (SD and SA) of the template, were much lower. The response-selectivity coefficient for each analyte was calculated according to eq 2 taking into account the molecular weight of the analyte:

$$k = (Q_i/MW_i)/(Q_t/MW_t) \quad (2)$$

where Q_i and Q_t are responses of SMZ-MIP modified sensor (deg) toward interferent and template molecules having molecular weights of MW_i and MW_t, respectively. The calculated response-selectivity coefficients are summarized in Table 5. The low values of k in the range of 0.009−0.161 demonstrated that no appreciable interferences were caused by AMO, SD, and SA. It is noteworthy that close structural analogues of SMZ such as SD and SA exhibited lower binding to SMZ-MIP even though SA contains only 4-amino-benzenesulfonamide moiety, i.e. has less steric hindrance than SMZ. At the same time there was no clear correlation of k values with the concentration of studied analytes as well as with their chemical structure.

Table 5. Response-Selectivity Coefficients (k) of SMZ-MIP Calculated According to Equation 2 for the Solutions of Different Concentrations of Antibiotics, SD, SA, AMO

concentration, μM	SD	SA	AMO
10.2	0.05	0.01	0.09
25.6	0.03	0.16	0.16
64	0.08	0.06	0.06
160	0.07	0.12	0.06
400	0.04	0.15	0.10
1000	0.02	0.05	0.05

In addition, the performance of SMZ-MIP film to distinguish between the target (SMZ) and its close analogue (SD) in tap water was explored. For this purpose, tap water samples spiked with SD and SMZ (100 μM) were injected into the SAW system, and the sensor responses were recorded (Figure 8). It

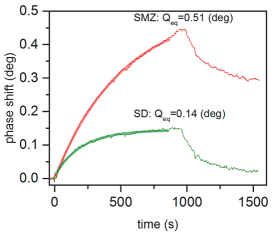

Figure 8. Responses of SMZ-MIP modified SAW sensor upon successive injections of 100 μM of SD and SMZ dissolved in tap water. The bold lines represent the fits to the single-site Langmuir model yielding the equilibrium sensor response at the given analyte concentration, (Q_{eq}).

should be noted that the first injected SD caused a quite reversible response since almost no residual signal remained when the chemical was completely eliminated from the fluidics during the dissociation stage. Successive introduction of SMZ to the system resulted in a substantially higher equilibrium response (Q_{eq} = 0.51 vs Q_{eq} = 0.14 deg), which was in good agreement to that observed for SMZ sample prepared from ultrapure water (Q_{eq} = 0.52 ± 0.1 deg) as approximated from a fit of the adsorption isotherms (see Figure 5) at a concentration of 100 μM. Thus, the fabricated SMZ-MIP possessed a good recovery even after the preceding contact with a chemical analogue of SMZ.

To summarize, the results clearly suggest that the prepared SMZ-MIP films exhibit appreciable selectivity for SMZ due to the presence of specific cavities complementary in size, shape, and arrangement of chemical functionalities to the template molecule.

Regeneration Study. To study the stability of the fabricated SMZ-MIP films, they were allowed to undergo repeated rebinding−regeneration cycles. During regeneration, it is essential to ensure that while the polymer is refurbished efficiently from the previously bound targets, it still retains its capability for subsequent selective rebinding. As it can be seen from Figure 9, the regeneration procedure did not appear to harm the polymer binding sites since after a few rebinding−regeneration cycles, the responses of SMZ-MIP modified sensor were still observed and tended to stabilize showing only about 15% loss in rebinding capacity after the last cycle.

CONCLUSIONS

This study exemplifies the synergistic effect of combining an antibiotic-MIP with SAW sensing platform and excellent applicability of the sensing system to affinity measurement and real-time detection of low molecular weight analyte (antibiotics) in aqueous environment. Selective SMZ-MIP was prepared directly on the surface of SAW sensor in a form of

DOI: 10.1021/acs.analchem.5b04735
Anal. Chem. 2016, 88, 1476−1484

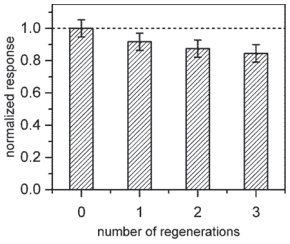

Figure 9. Effect of the regeneration cycles applied on rebinding capability of SMZ-MIP toward SMZ at concentration of 1 mM. The bars represent responses, normalized to that of the freshly synthesized SMZ-MIP surface (cycle 0).

a homogeneous thin film by oxidative electropolymerization of *m*-phenylenediamine (mPD) in the presence of SMZ, acting as a template. The spectroscopic ellipsometry showed that MIP and the control films grew nearly linearly across the applied charge range, thus making their prediction between ca. 1 and 24 nm very certain. Thus, the main advantage of the approach was that antibiotic-MIP layers could be directly fabricated on the metallic sensing surface of an appropriate transducer in an easy and precisely controllable manner. The prepared SMZ-MIP films were characterized by SAW technique in terms of its affinity and selectivity toward SMZ. SMZ-MIP films demonstrated approximately 8.4 times higher binding capacity to SMZ than the respective NIP. Moreover, they were able to discriminate among structurally similar molecules, i.e., sulfanilamide and sulfadimethoxine. SMZ-MIPs could withstand at least three adsorption−regeneration cycles losing only about 15% of the initial adsorption capacity. SMZ-MIP films interfaced with SAW sensor could distinguish the target analyte at 8 nM with LOD of 1.7 nM. The presented approach of a facile integration of the antibiotic-sensing MIP layer with SAW technology allowed observing the real-time binding events of the low molecular weight target at relevant sensitivity levels and could be potentially suitable for cost-effective fabrication of a multianalyte chemosensor for analysis of hazardous pollutants in aquatic environment.

■ ASSOCIATED CONTENT

Supporting Information

The Supporting Information is available free of charge on the ACS Publications website at DOI: 10.1021/acs.analchem.5b04735.

S-1. Computational modeling and spectra analysis. S-2. SMZ-MIP performance analysis at low analyte concentration. Determination of the limit of detection (PDF)

■ AUTHOR INFORMATION

Corresponding Author

*E-mail: vitali.syritski@ttu.ee (V.S.).

Notes

The authors declare no competing financial interest.

■ ACKNOWLEDGMENTS

This work was supported by the Estonian Ministry of Education and Research (grant PUT150) and the European Regional Development Fund under the project 3.2.0801.11-0009. The authors thank Dr. M. Kudryashova for NMR spectroscopic measurements and Mrs. I. Engler and Mr. Ö. Savaş for technical assistance. J.R., A.F., and K.H. acknowledge financial support from the Senatsverwaltung für Wirtschaft, Technologie und Forschung des Landes Berlin, and by the Bundesministerium für Bildung und Forschung.

■ REFERENCES

(1) Diaz-Cruz, M. S.; de Alda, M. J. L.; Barcelo, D. *TrAC, Trends Anal. Chem.* **2003**, *22*, 340−351.
(2) Karthikeyan, K. G.; Meyer, M. T. *Sci. Total Environ.* **2006**, *361*, 196−207.
(3) Moreno-Diaz, H.; Villalobos-Molina, R.; Ortiz-Andrade, R.; Diaz-Coutino, D.; Medina-Franco, J. L.; Webster, S. P.; Binnie, M.; Estrada-Soto, S.; Ibarra-Barajas, M.; Leon-Rivera, I.; Navarrete-Vazquez, G. *Bioorg. Med. Chem. Lett.* **2008**, *18*, 2871−2877.
(4) Scozzafava, A.; Owa, T.; Mastrolorenzo, A.; Supuran, C. T. *Curr. Med. Chem.* **2003**, *10*, 925−953.
(5) Ding, C.; He, J. *Appl. Microbiol. Biotechnol.* **2010**, *87*, 925−941.
(6) Sarmah, A. K.; Meyer, M. T.; Boxall, A. B. a. *Chemosphere* **2006**, *65*, 725−759.
(7) Buchberger, W. W. *Anal. Chim. Acta* **2007**, *593*, 129−139.
(8) Na, G. S.; Gu, J.; Ge, L. K.; Zhang, P.; Wang, Z.; Liu, C. Y.; Zhang, L. *Chin. J. Oceanol. Limnol.* **2011**, *29*, 1093−1102.
(9) Opris, O.; Soran, M. L.; Coman, V.; Copaciu, F.; Ristoiu, D. *Cent. Eur. J. Chem.* **2013**, *11*, 1343−1351.
(10) Pichon, V.; Haupt, K. *J. Liq. Chromatogr. Relat. Technol.* **2006**, *29*, 989−1023.
(11) Wulff, G. *Chem. Rev.* **2002**, *102*, 1−27.
(12) Haupt, K.; Mosbach, K. *Chem. Rev.* **2000**, *100*, 2495−2504.
(13) Jing, T.; Gao, X. D.; Wang, P.; Wang, Y.; Lin, Y. F.; Hu, X. Z.; Hao, Q. L.; Zhou, Y. K.; Mei, S. R. *Anal. Bioanal. Chem.* **2009**, *393*, 2009−2018.
(14) Pichon, V.; Chapuis-Hugon, F. *Anal. Chim. Acta* **2008**, *622*, 48−61.
(15) Qin, S. L.; Deng, S.; Su, L. Q.; Wang, P. *Anal. Methods* **2012**, *4*, 4278−4283.
(16) Huang, D. L.; Wang, R. Z.; Liu, Y. G.; Zeng, G. M.; Lai, C.; Xu, P.; Lu, B. A.; Xu, J. J.; Wang, C.; Huang, C. *Environ. Sci. Pollut. Res.* **2015**, *22*, 963−977.
(17) Liao, H. P.; Zhang, Z. H.; Li, H.; Nie, L. H.; Yao, S. Z. *Electrochim. Acta* **2004**, *49*, 4101−4107.
(18) Sasaki, S.; Ooya, T.; Kitayama, Y.; Takeuchi, T. *J. Biosci. Bioeng.* **2015**, *119*, 200−205.
(19) Uludag, Y.; Piletsky, S. A.; Turner, A. P. F.; Cooper, M. A. *FEBS J.* **2007**, *274*, 5471−5480.
(20) Losev, V. V.; Medved, A. V.; Roshchin, A. V.; Kryshtal, R. G.; Zapadinskii, B. I.; Epinat'ev, I. D.; Kumpanenko, I. V. *Russ. J. Phys. Chem. B* **2009**, *3*, 990−1003.
(21) Wen, W.; He, S. T.; Li, S. Z.; Liu, M. H.; Yong, P. *Sens. Actuators, B* **2007**, *125*, 422−427.
(22) Gizeli, E.; Stevenson, A. C.; Goddard, N. J.; Lowe, C. R. *IEEE Trans. Sonics Ultrason.* **1992**, *39*, 657−659.
(23) Gronewold, T. M. A. *Anal. Chim. Acta* **2007**, *603*, 119−128.
(24) Länge, K.; Rapp, B. E.; Rapp, M. *Anal. Bioanal. Chem.* **2008**, *391*, 1509−1519.
(25) Lautner, G.; Kaev, J.; Reut, J.; Opik, A.; Rappich, J.; Syritski, V.; Gyurcsanyi, R. E. *Adv. Funct. Mater.* **2011**, *21*, 591−597.
(26) Ramanaviciene, A.; Ramanavicius, A. *Biosens. Bioelectron.* **2004**, *20*, 1076−1082.
(27) Sharma, P. S.; Pietrzyk-Le, A.; D'Souza, F.; Kutner, W. *Anal. Bioanal. Chem.* **2012**, *402*, 3177−3204.
(28) Syritski, V.; Reut, J.; Menaker, A.; Gyurcsányi, R. E.; Öpik, A. *Electrochim. Acta* **2008**, *53*, 2729−2736.
(29) Tretjakov, A.; Syritski, V.; Reut, J.; Boroznjak, R.; Öpik, A. *Anal. Chim. Acta* **2016**, *902*, 182−188.
(30) Tretjakov, A.; Syritski, V.; Reut, J.; Boroznjak, R.; Volobujeva, O.; Opik, A. *Microchim. Acta* **2013**, *180*, 1433−1442.

DOI: 10.1021/acs.analchem.5b04735
Anal. Chem. 2016, 88, 1476−1484

(31) Lattach, Y.; Fourati, N.; Zerrouki, C.; Fougnion, J. M.; Garnier, F.; Pernelle, C.; Remita, S. *Electrochim. Acta* **2012**, *73*, 36−44.
(32) Maouche, N.; Ktari, N.; Bakas, I.; Fourati, N.; Zerrouki, C.; Seydou, M.; Maurel, F.; Chehimi, M. M. *J. Mol. Recognit.* **2015**, *28*, 667−678.
(33) Fernandez-Gonzalez, A.; Guardia, L.; Badia-Laino, R.; Diaz-Garcia, M. E. *TrAC, Trends Anal. Chem.* **2006**, *25*, 949−957.
(34) Frasconi, M.; Tel-Vered, R.; Riskin, M.; Willner, I. *Anal. Chem.* **2010**, *82*, 2512−2519.
(35) Turco, A.; Corvaglia, S.; Mazzotta, E. *Biosens. Bioelectron.* **2015**, *63*, 240−247.
(36) Wang, F.; Zhu, L.; Zhang, J. *Sens. Actuators, B* **2014**, *192*, 642−647.
(37) Ktari, N.; Fourati, N.; Zerrouki, C.; Ruan, M.; Seydou, M.; Barbaut, F.; Nal, F.; Yaakoubi, N.; Chehimi, M. M.; Kalfat, R. *RSC Adv.* **2015**, *5*, 88666−88674.
(38) Hinrichs, K.; Furchner, A.; Rappich, J.; Oates, T. W. H. *J. Phys. Chem. C* **2013**, *117*, 13557−13563.
(39) Hinrichs, K.; Eichhorn, K. J. *Ellipsometry of Functional Organic Surfaces and Films*; Springer, 2014; Vol. *52*.
(40) Rappich, J.; Hinrichs, K. *Electrochem. Commun.* **2009**, *11*, 2316−2319.
(41) Roodenko, K.; Mikhaylova, Y.; Ionov, L.; Gensch, M.; Stamm, M.; Minko, S.; Schade, U.; Eichhorn, K. J.; Esser, N.; Hinrichs, K. *Appl. Phys. Lett.* **2008**, *92*, 103102.
(42) Li, X.; Husson, S. M. *Biosens. Bioelectron.* **2006**, *22*, 336−348.
(43) Yan, H.; Row, K. H. *Int. J. Mol. Sci.* **2006**, *7*, 155−178.
(44) Gu, L.; Jiang, X.; Liang, Y.; Zhou, T.; Shi, G. *Analyst* **2013**, *138*, 5461−5469.
(45) Roy, A. C.; Nisha, V. S.; Dhand, C.; Ali, M. A.; Malhotra, B. D. *Anal. Chim. Acta* **2013**, *777*, 63−71.
(46) Vergara, A. V.; Pernites, R. B.; Pascua, S.; Binag, C. A.; Advincula, R. C. *J. Polym. Sci., Part A: Polym. Chem.* **2012**, *50*, 675−685.
(47) Granado, V. L. V.; Gutiérrez-Capitán, M.; Fernández-Sánchez, C.; Gomes, M. T. S. R.; Rudnitskaya, A.; Jimenez-Jorquera, C. *Anal. Chim. Acta* **2014**, *809*, 141−147.
(48) Nicholls, I. A.; Karlsson, B. C. G.; Olsson, G. D.; Rosengren, A. M. *Ind. Eng. Chem. Res.* **2013**, *52*, 13900−13909.
(49) Li, X. G.; Huang, M. R.; Duan, W.; Yang, Y. L. *Chem. Rev.* **2002**, *102*, 2925−3030.
(50) Coates, J. In *Encyclopedia of Analytical Chemistry*; Meyers, R. A., Ed.; John Wiley& Sons Ltd: Chichester, 2000; pp 10815−10837.
(51) Umpleby, R. J.; Baxter, S. C.; Rampey, A. M.; Rushton, G. T.; Chen, Y. Z.; Shimizu, K. D. *J. Chromatogr. B: Anal. Technol. Biomed. Life Sci.* **2004**, *804*, 141−149.
(52) Boreen, A. L.; Arnold, W. A.; McNeill, K. *Environ. Sci. Technol.* **2004**, *38*, 3933−3940.
(53) Kolpin, D.; Furlong, E. T.; Meyer, M. T.; Thurman, E. M.; Zaugg, S. D.; Barber, L. B.; Buxton, H. T. *Environ. Sci. Technol.* **2002**, *36*, 1202−1211.

DOI: 10.1021/acs.analchem.5b04735
Anal. Chem. 2016, 88, 1476−1484

PAPER II

Akinrinade George Ayankojo, Jekaterina Reut, Roman Boroznjak, Andres Öpik, and Vitali Syritski. Molecularly imprinted poly(meta-phenylenediamine) based QCM sensor for detecting Amoxicillin, *Sensors and Actuators B: Chemical 258 (2018) 766-774.*

Sensors and Actuators B 258 (2018) 766–774

Contents lists available at ScienceDirect

Sensors and Actuators B: Chemical

journal homepage: www.elsevier.com/locate/snb

Molecularly imprinted poly(meta-phenylenediamine) based QCM sensor for detecting Amoxicillin

Akinrinade George Ayankojo, Jekaterina Reut, Roman Boroznjak, Andres Öpik, Vitali Syritski *

Department of Material and Environmental Technology, Tallinn University of Technology, Ehitajate tee 5, 19086 Tallinn, Estonia

ARTICLE INFO

Article history:
Received 26 September 2017
Received in revised form
29 November 2017
Accepted 30 November 2017
Available online 1 December 2017

Keywords:
Molecularly imprinted polymers
Antibiotic
Amoxicillin
QCM
Sensor
Electrochemical polymerization

ABSTRACT

A chemical sensor based on molecularly imprinted polymer (MIP) and quartz crystal microbalance (QCM) to detect amoxicillin (AMO) antibiotics in aqueous samples was developed. The thin film of AMO-MIP was generated electrochemically from meta-phenylenediamine (mPD) directly on the QCM transducer. Pre-polymerization complex formation between the template (AMO) and the monomer molecules (mPD) was confirmed by a combination of computational modeling and spectroscopic studies. The electrodeposition process was carefully studied to allow for the selection of the optimal parameters for stable AMO-MIP film deposition. The AMO-MIP QCM sensor showed a significantly better sensitivity and affinity than the reference film displaying more than seven times relative adsorption capacity and a limit of detection down to 0.2 nM. Likewise, the sensor demonstrates good selectivity to the target analyte (AMO) than the other non-templated molecules and remain sensitive to the target even after a prior exposure to other interferents that may be present within the same environment. This remarkable result in the analysis of amoxicillin on QCM sensor without employing any signal amplification methodology demonstrates an important step towards the fabrication of MIP-based environmental sensor.

1. Introduction

The environmental impacts of antibiotics pollution cannot be over-emphasized due to their potential of increasing bacterial resistance [1,2]. Their urgent detection, especially in aqueous environment and food has therefore continued to attract enormous research interests. As a result, analytical devices which combine the selectivity of biological systems with the chemical stability of chemical systems are increasingly becoming a focus of attention in environmental and clinical research [3]. Molecularly imprinted polymers (MIPs) possessing pre-defined cavities for specific recognition of target analytes, are artificial receptors with potential for fabricating state-of-the-art analytical devices. Specific cavities of MIPs are pre-formed by the polymerization of suitable functional monomers in the presence of the target molecules, acting as templates, which after subsequent removal reveal complementary sites capable of selectively recognizing the target molecule by size, shape and functional groups. Antibiotics constitute a larger share of pharmaceuticals contributing to the rising pollution of the aquatic environment [4,5]. Amoxicillin is a broad-spectrum antibiotic that belongs to one of the most widely known antibiotic class, the penicillins. It has low metabolic rate in humans and as a result, up to 90% is being excreted in the raw form [6] and therefore exists in various water bodies in the concentration range of 0.18–4.57 nM [7]. Since amoxicillin possesses a variety of functional groups potentially capable of interacting with functional monomers through the formation of non-covalent bonds, it has the tendency to create recognition cavities that are complementary to those of the template molecules in the resulting imprinted polymer following template extraction.

Thin films of polymers are the most suitable for sensing in label-free configuration [8]. Polymers generated from functional monomers consisting of phenylenediamine parent units are gaining wide popularity among researchers due to their beneficial electroactivity and suitability for a wide variety of applications, including energy storage, electrocatalysis, electrochromism, and sensors [9–12]. Their appropriateness as polymer matrix in molecular imprinting stems from the fact that the growth of their polymer films results in a rigid structure demonstrating important recognition functionalities relevant for molecular recognition, especially by non-covalent interactions [13]. More importantly, the possibility of generating a thin but continuous polymer film that

* Corresponding author.
E-mail address: vitali.syritski@ttu.ee (V. Syritski).

https://doi.org/10.1016/j.snb.2017.11.194
0925-4005/

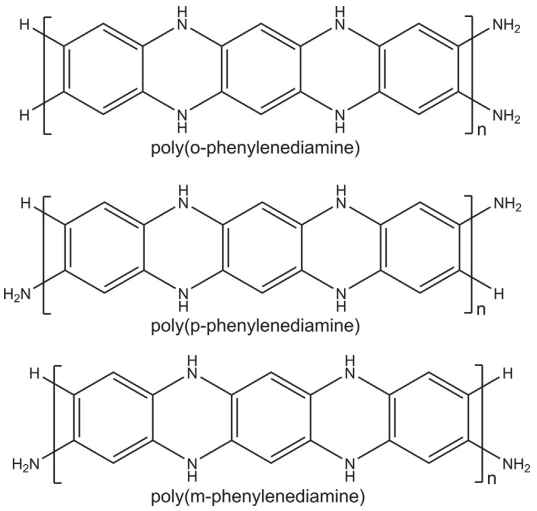

Fig. 1. Ladder-like structures for the polymers of the three isomers of phenylenediamines; oPD, pPD and mPD.

eliminates the long diffusion path through which analytes have to travel to the pre-formed active sites makes them quite preferable for fabricating molecular imprinting chemosensor [14,15]. Consequently, many sensors are being fabricated on piezoelectric and other transducer surfaces via electrochemically synthesized films of poly(phenylenediamine) leading to extended linear concentration range and analytically significant limit of detection (LoD) [16,17]. Of the three isomers of poly(phenylenediamine); Poly(*o*-phenylenediamine), P(oPD), Poly(*m*-phenylenediamine), P(mPD), and Poly(*p*-phenylenediamine), P(pPD) (see Fig. 1), P(oPD)'s structure has been substantially defined while the structure of P(mPD) has not been fully elucidated because the P(mPD) obtained by chemical or electrochemical oxidative polymerization is almost insoluble in most solvents [18]. Nevertheless, FTIR spectroscopic studies [19] demonstrated no significant difference in the chemically and electrochemically synthesized polymers of these isomers in the IR spectra. These polymers have been estimated to yield ladder-like structures [20].

Also, according to the report of Rhemrev-Boom et al. [21], the structural information obtained from electrosynthesized P(mPD) and P(oPD) films by means of ATR-FTIR spectroscopy permitted the conclusion that the formation of P(mPD) films was comparable to that of P(oPD) films. Furthermore, Killoran and O'Neill [22] studied the electrosynthesis and permselective properties of the three poly(phenylenediamine) films and concluded that P(mPD) polymerized faster than P(oPD) and P(pPD) films under identical polymerization conditions and it is the least soluble in methanol and other solvents. These properties of P(mPD) allow its higher suitability for MIP electrosynthesis and its subsequent regeneration by hash solvents such as methanol mixture of acetic acid. Consequently, we have recently reported the detection of small molecule (e.g. sulfamethizole) and large molecule (e.g. IgG) by using an electropolymerized p(mPD) film on a SAW sensor transducer [23,24]. The resulting sensors displayed interesting features including high selectivity and satisfactory stability in aqueous media thus, further establishing the important use of P(mPD) as matrix in molecular imprinting.

Although, MIPs for antibiotic detection have seen quite reasonable publications however, MIP chemosensors exhibiting amoxicillin detection in aqueous media using thin P(mPD) films integrated with QCM sensors and without the use of signal amplifying nanomaterials have not been reported. In this report, an amoxicillin MIP film was developed using electrosynthesized P(mPD) polymer matrix integrated with a quartz crystal microbalance (QCM) sensor having a gold coating as the sensor transducer to facilitate a direct communication of the imprinted polymer film with the transducer during the polymerization and rebinding analysis. To prepare MIPs with a high density of imprinted sites [16], we have investigated different electropolymerization conditions for the synthesis of the MIP films to optimize the binding capacity of the resulting antibiotic-imprinted polymeric material (AMO-MIP) and improve the performance of the fabricated chemosensor. Important parameters of the developed sensor were studied and discussed.

2. Experimental

2.1. Materials and methods

Acetic acid, sulfuric acid and hydrogen peroxide were provided by Lach-ner (Czech Republic). The other chemicals were obtained from Sigma-Aldrich. All chemicals were of analytical grade or higher and were used as received without any further purification. Ultrapure water (resistivity 18.2 MΩ cm, Millipore, USA) was used for preparation of all aqueous solutions. Phosphate buffered saline (PBS) solution (0.01 M, pH 7.4) was used to prepare synthesis and analyte solutions. The gold (Au) electrodes of a 5 MHz QCM (Maxtek, Inc.) was used in this work for antibiotic-MIP and the reference non-imprinted polymer (NIP) film deposition. Ag/AgCl/KCl_{sat} electrode was used as a reference electrode in all electrochemical measurements. Before electrochemical deposition of the films, the QCM sensors were cleaned for 3 minutes in hot piranha solution consisting of 30% H_2O_2 and concentrated H_2SO_4 in 1:3 ratio followed by electrochemical cleaning in 0.1 M H_2SO_4 aqueous solution by cycling the electrode potential in the range of −0.2 to 1.5 V with a scan rate of 50 mV/s, until the cyclic voltammograms were reproducible. This was followed by thorough washing with ultrapure water and drying in nitrogen stream. Electrochemical measurements were made in a custom-made 25 mL Teflon electrochemical cell connected with Reference 600 Potentiostat (Gamry Instruments, USA). A conventional three-electrode system was used with QCM sensor electrode as the working electrode, a rectangular shaped platinum plate ($4 \times 1.5\,cm^2$) as a counter electrode, and Ag/AgCl/KCl_{sat} as a reference electrode.

2.2. Polymer matrix optimization

2.2.1. Computer modeling

The mPD complex formed with the antibiotic template was generated by GaussView 5.0.9 software. Its geometry was also optimized by semi-empirical PM3 method with Gaussian'09 software. The conformational optimizations and binding energies for the complex were calculated by density functional theory (DFT) method at B3LYP/6–31 + G level with Gaussian'09 software.

2.2.2. Spectroscopic analysis

UV–vis absorption spectra of the PBS buffer solutions containing individual components, mPD and AMO as well as their mixture were recorded in a 1 cm quartz cuvette with the Shimadzu 2401 spectrophotometer in the wavelength range from 200 to 320 nm. The changes in absorbance of the solution mixtures are then compared with the spectra of the individual components as references. ^{13}C NMR spectroscopy measurement was conducted using Bruker SMART X2S benchtop diffractometer model. The samples were prepared in D_2O solution as solvent. The molar ratio of template to monomer (AMO: mPD) in the solution mixture was kept at 1:1.

2.3. Amoxicillin-MIP preparation and characterization

2.3.1. Electrosynthesis of antibiotic-MIP films

Thin films of P(mPD) and/or P(mPD)/AMO were electrodeposited on QCM sensors. This was achieved by applying a constant potential (0.6 V vs Ag/AgCl/KCl_{sat}), in PBS buffer solution containing 5 mM mPD and/or mixture of 5 mM mPD and 5 mM AMO, keeping the monomer and template concentration ratio at 1. To obtain similar film thickness, the mPD electrochemical polymerization in the presence of the antibiotics was monitored by the electrochemical quartz crystal microbalance (EQCM). The EQCM measurements were performed using the QCM100 system (Stanford Research Systems, Inc., Sunnyvale, CA, USA) connected to the reference 600TM potentiostat (Gamry Instruments, Inc.) and the PM 6680 B counter (Fluke Corporation) as previously described elsewhere [25]. Film syntheses were continued until the resonant frequency dropped to the designated value (−400 Hz). As a reference, non-imprinted polymer (NIP) was also synthesized at the same conditions but without adding any antibiotics in the synthesis solution. The deposited polymer films were observed to be uniform. The films' thicknesses were then estimated by converting the frequency shift to the corresponding mass by applying the Sauerbrey's equation (Eq. (1)) and dividing the latter by the polymer's density (Eq. (2)). After polymer film electrochemical deposition, the electrode was rinsed with distilled water and dried in a nitrogen stream.

$$\Delta f = -f_0{}^2 \Delta m/N\rho_q = -C_f \Delta m \quad (1)$$

$$t_f = \Delta m/\rho_f \quad (2)$$

where Δf – resonant frequency shift (Hz), f_0–fundamental frequency of the crystal (Hz), Δm – mass change (g/cm^2), N – frequency constant for quartz (167 kHz cm), ρ_q – density of quartz (2.65 g/cm^3), C_f – sensitivity factor (for 5 MHz quartz crystal, 56.6 Hz mg^{-1} cm^2), t_f – thickness of film, ρ_f – density of film.

2.3.2. Characterization of the prepared films

After electrochemical deposition of P(mPD)/AMO film, the removal of the antibiotic molecules from the polymer matrix was carried out to create AMO-MIP film. For this purpose, the polymer modified electrode was immersed in acetic acid/methanol (1:1) solution and held there for 24 h, then the eluted solution was analyzed by UV–vis absorption spectroscopy and amoxicillin concentration was determined at the specific wavelength, λ = 274 nm, of its absorbance. The concentration in the washing solution was also determined by chromatographic measurements using a high-performance liquid chromatography combined with diode array detector and mass-spectrometer, (HPLC-PDA-MS, Shimadzu LC–MS 2020). Phenomenex Gemini-NX 5 u C18 110A 150 × 2.0 mm column, inner diameter 1.7 μm, was used with two eluents; 0.1% acetic acid aqueous solution (eluent A), and acetonitrile (eluent B), with total eluents flow of 0.3 mL min^{-1}. The antibiotic amount in eluted solution was determined and compared with theoretically estimated amount of the antibiotic presented in the polymer film.

2.3.3. Rebinding study

Rebinding of the target AMO molecules on the prepared AMO-MIP film was studied by QCM-FIA technique, which allows real-time monitoring of molecular interactions on the surface of the QCM sensor. The rebinding analysis was carried out in the QCM-FIA system comprising one programmable precision syringe pumps (Cavro XLP 6000® XLP 6000, Tecan Nordic AB, Mölndal, Sweden), a motorized six-way port injection valve (C22-3186EH, VICI® Valco Instruments Company Inc., USA) controlled by a microelectric actuator and a small volume (150 μL) axial flow cell attached to the QCM sensor holder (Stanford Research Systems, Inc.). Sample injection

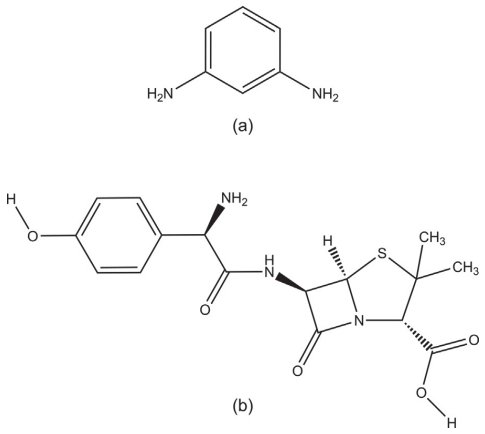

Fig. 2. Structural formulae of the (a) functional monomer, mPD and (b) target molecule, AMO used for the MIP formation.

was carried out by a 5 mL disposable plastic syringe. All elements of the system were connected to a PC and controlled by software written in Labview. A constant flow of degassed PBS buffer solution (pH = 7.4) flowed over the sensor at a flow rate of 25 μL/min until a constant baseline of the QCM sensor resonance frequency was reached. Subsequently, the increasing concentrations of the analyte samples (1.6 μM, 8 μM, 40 μM, 200 μM, 1 mM of the AMO in PBS buffer) were injected into the flow stream via an injection loop (500 μL). Prior to the rebinding study, the P(mPD)/AMO films as well as their P(mPD) references were regenerated by immersing the QCM sensor modified films in acetic acid/methanol (1:1) solution for 24 h. The sensorgrams recorded were then fitted to the appropriate binding model to determine the equilibrium responses for both the MIPs and NIPs surfaces. These equilibrium data were then used for the construction of the binding isotherms.

3. Results and discussion

3.1. Polymer matrix optimization

In a non-covalent or self-assembly molecular imprinting, selectivity of a MIP depends, to a great extent, on the nature and strength of interaction of pre-polymerization complex formed between the target analyte and functional monomers in a porogenic solvent [26]. Therefore, a preliminary study of molecular complexes between a monomer and an analyte (template) molecule is required to design a MIP with optimal performance. This can be realized by a combination of both theoretical (computational modeling) and experimental (spectroscopic analysis) approaches [27].

3.1.1. Computational modeling

Geometrically optimized structure of the pre-polymerization complex formed between the mPD monomer and the AMO antibiotic template molecules (Fig. 2) was estimated by density functional theory (DFT) calculations using Gaussian'09. The strength of interaction was analyzed in terms of the binding energy, length of hydrogen bonds and Mulliken charges. To appreciate the binding energy value, the binding energy of complexes formed between AMO and other electropolymerizable monomers; pyrrole (Py) and 3,4-ethylenedioxythiophene (EDOT) were also estimated by DFT calculations. Table 1 shows the total binding energy as well as the average hydrogen bond length of the monomer-template complexes. The sites of interaction, binding energy for each site, lengths

Table 1
Binding energies of the complexes formed between AMO and three different monomers, mPD, EDOT and Py as calculated by Gaussian'09.

Template-monomer complex	Binding energy at saturation (kJ/mol)	Average hydrogen bond length (Å)
AMO-mPD	273.053	2.54
AMO-EDOT	8.401	4.15
AMO-Py	63.013	1.86

of hydrogen bond(s) calculated for the interactions as well as the Mulliken charges of the different functional groups for each monomer-template interaction are shown in Fig. S1, S2 and S3 and Table S1, S2, S3. As it can be seen from Table 1, the total binding energy between mPD and AMO is significantly higher (273 kJ/mol) as compared to AMO interaction with other monomers, EDOT and Py. Thus, one could expect that the use of P(mPD) as a polymer matrix for AMO imprinting results in AMO-MIP with higher selectivity towards AMO as compared to the use of polypyrrole and PEDOT.

3.1.2. *UV–vis and NMR study of prepolymerization complex formation*

UV–vis spectroscopy was further used to characterize and establish the pre-polymerization complex formed between the monomer and the template molecules prior to the polymerization. For this purpose, the absorption spectra of the monomer, mPD and the template, AMO in the PBS buffer solution (pH = 7.4) were determined and compared to the spectra of their mixture in the concentration ratio 1:1. As shown in Fig. S4, the absorption spectra of mPD and AMO mixture shows a new but broad absorption band at around 284 nm that was different from either that of mPD (289 nm) or AMO (274 nm) as well as the disappearance of bands at 228 nm of AMO and 245 nm of mPD, indicating the presence of binding interactions between the molecules in the mixture. Thus, evidence of possible interaction between mPD and the templates were further established by UV–vis spectroscopic technique. Additionally, ^{13}C NMR spectra of the individual components as well as their mixture clearly indicate that there is no covalent interaction involved in the complex formation as no new peaks were observed in the AMO + mPD spectrum as compared to the individual spectra (Fig. S5). Therefore, it can be concluded that the complex formation is majorly through non-covalent interactions.

3.2. *Electrodeposition of antibiotic-MIP films*

The use of MIPs for sensing purposes generally demands a MIP-based material in the form of a uniform thin film and its robust interfacing with a sensor platform capable of responding to relevant sensitivity levels upon interaction between MIP film and a binding analyte. Electropolymerization has been shown to be especially suitable synthesis method for effectively interfacing MIP with transducer allowing a good control of both film thickness and inner morphology [16,23,24,28].

Therefore, the electrochemical deposition of P(mPD) was studied in detail by EQCM to provide a more accurate control of polymer film growth. To find optimal synthesis parameters for homogeneous polymer film preparation, the electropolymerization of mPD was studied by applying different modes of potential stimulus including, potentiostatic deposition (Fig. 3a), deposition by cyclic potential sweep (Fig. 3b) and potential pulse deposition (Fig. 3c). The P(mPD) films with thickness of 25 nm (as previously obtained from ellipsometry measurement) that correspond to the QCM frequency shift of 400 Hz (as calculated by using Eqs. (1) and (2)) were electrodeposited on the QCM sensor electrode. This relatively high thickness was selected so as to give a greater surface area of recognition for the small molecular weight target analyte. It was observed that in the case of polymer film deposition by potential cycling and potential pulses (Fig. 3b and c), the film growth rate was very low, reaching the 400 Hz frequency shift limit in not less than about 1 h. However, a P(mPD) film of the same thickness can be deposited for approximately 200 s by using the potentiostatic mode (Fig. 3a). This observation, coupled with the identified possible challenges of using potentiodynamic mode inclusive of disordered spatial chains of polymer matrix as well as film defects due to polymer swelling and shrinking, as compared to the well-ordered films produced by potentiostatic condition [16] suggest the preferred use of the latter for the polymer synthesis in this work. Potentiostatic synthesis at 0.6 V vs Ag/AgCl/KCl_{sat} is then chosen to be the optimal parameter for preparing a well adherent and homogeneous P(mPD) films on the electrode sensor.

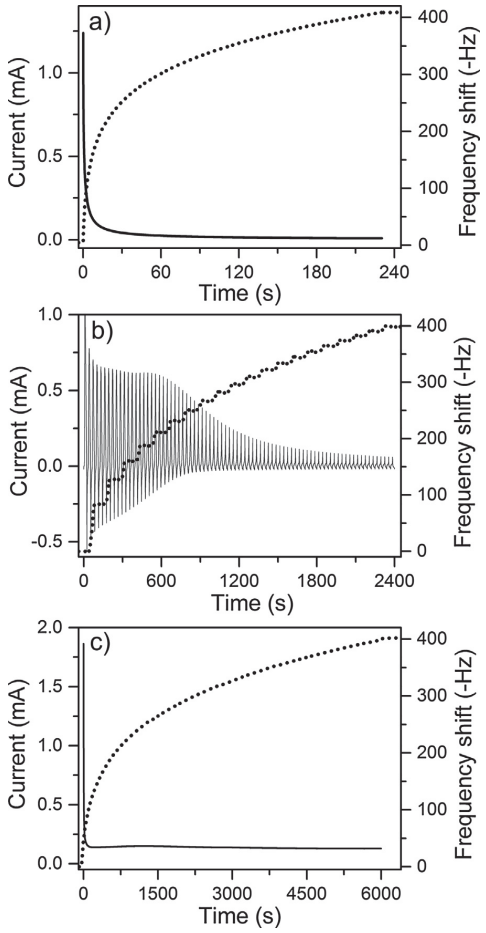

Fig. 3. Current responses during the electrodeposition of P(mPD) from PBS buffer solution, pH 7.4 under: (a) potentiostatic; (b) cyclic voltammetry; (c) potential pulse modes.

Furthermore, to exclude the possibility of the oxidation of the antibiotic template during the polymerization, an initial study of the electrochemical behavior of AMO in PBS buffer was carried out with the purpose of elucidating its electrochemical stability within the potential window used for the polymerization. For this purpose, cyclic voltammetry (CV) scan was applied to determine the

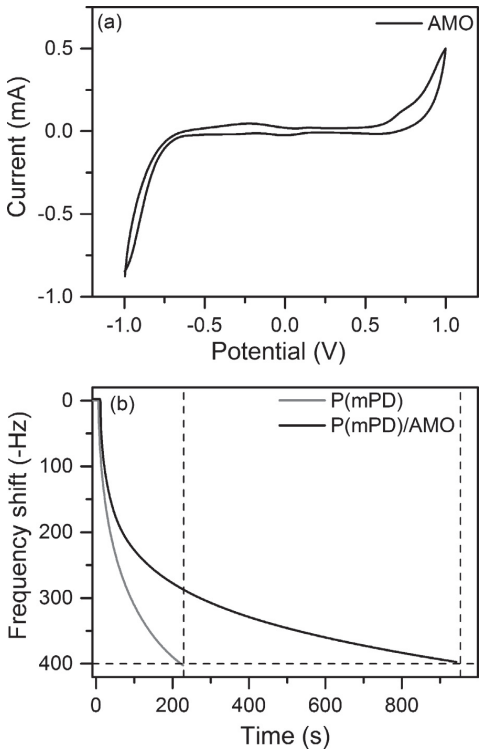

Fig. 4. (a) Cyclic voltammogram of a gold electrode in PBS buffers (pH 7.4) containing 5 mM AMO. Scan rate: 50 mV/s. (b) Resonant frequency responses during the potentiostatic electrodeposition of P(mPD) and P(mPD)/AMO films on gold electrode of QCM sensor.

electrochemical activity of the antibiotic within a specific potential window as shown in Fig. 4(a). The cyclic voltammogram indicate that the AMO molecules do not demonstrate any electroactivity at the potential (0.6 V) used for monomer polymerization hence, its stability during the polymer synthesis.

Fig. 4b shows typical resonance frequency responses of the EQCM during P(mPD) potentiostatic electrodeposition. As easily observed, the P(mPD) films grew non-linearly demonstrating a faster growth in the beginning of the process, followed by its gradual slowing-down until the constant resonant frequency value was reached, thus indicating a self-limiting polymerization. It should be noted that the film growth rate of the P(mPD) in the presence of the antibiotic was much slower than the rate for the pure P(mPD) film at the very same polymerization conditions. It is assumed that the dominant species of the targeted AMO antibiotic in PBS buffer solution (pH = 7.4) are negatively charged ions considering its acid-base properties [29]. Therefore, during the oxidative polymerization of mPD, negatively charged antibiotic species are expected to be inserted into the positively charged P(mPD) backbone due to electrostatic interactions, thus resulting in the formation of P(mPD) film containing the template molecules (P(mPD)/AMO).

3.3. Rebinding and selectivity study

For a rebinding of the target analyte on the P(mPD)/AMO film, the template molecules must be eluted from the polymer matrix to reveal complementary cavities in the film. This was achieved by treatment in solution mixture of acetic acid and methanol,

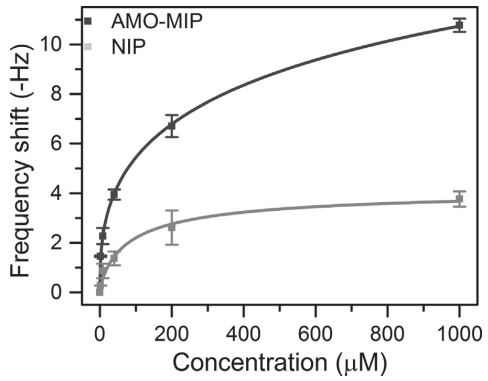

Fig. 5. Adsorption isotherms of the injection of increasing AMO concentration on AMO-MIP and NIP surfaces. Solid lines represent fits to the Langmuir–Freundlich model.

as discussed in the experimental (Section 2.3.2). However, the chromatographic analysis of the eluted solution indicates a low removal of the template molecules from the polymer matrix with an elution efficiency of about 20% thus indicating that some of the template molecules may still be trapped within the polymer. The analysis of the antibiotic rebinding capability of the prepared AMO-MIP film was achieved by employing the QCM-FIA technique. For a proper analysis of the rebinding interaction and to ascertain that the interaction between the target and the MIP film was specific, a control experiment was performed with the non-imprinted polymer (NIP) modified electrode sensor. The NIP was prepared like the MIP but excluding the template addition in the pre-polymerization mixture. To minimize signal fluctuation due to temperature change, the rebinding experiments were carried out in a closed custom-designed insulating chamber at room temperature. After equilibrating the film surfaces with the running buffer to obtain a stable baseline, the signal following injection of each concentration of analyte was monitored, recorded and analyzed by fitting to a pseudo first order kinetic equation to obtain the equilibrium responses shown in Fig. 5. These equilibrium signals data were fitted to the Freundlich-Langmuir (FL) model (Eq. (3)) using a nonlinear regression to obtain the kinetic data of the interaction. According to Shimidzu and co-workers [30], FL model is more universally applicable in characterizing MIPs because it can provide heterogeneity information and is able to model adsorption behavior over the entire range of concentration including both sub-saturated and saturated region and therefore the FL model is most commonly used for characterizing MIPs [31].

As evident from Fig. 5 the MIP film clearly demonstrates the increased antibiotic adsorption compared to the NIP for all injections. Moreover, a very noticeable difference in the adsorption between the MIP and NIP was observed already after the injection of the antibiotic sample with the lowest concentration (1.6 μM), while the NIP film showed a low non-significant response. As the concentration increased, the adsorption became more pronounced for the MIP while the NIP film approaches saturation as the injected concentration becomes larger. The parameters obtained from the fitting of the binding isotherm to Eq. (3) are as shown in Table 2.

$$B = B_{\max} C^m / (K_D + C^m) \quad (3)$$

where C is the concentration of AMO in solution, B and $B_{\max}$ are the fractions of bound AMO and its saturation value, respectively, m is the heterogeneity index, which varies from 0 to 1, with increasing heterogeneity as m values decreases. K_D is the equilibrium dissoci-

Table 2
Parameters obtained from the LF fitting of the MIPs and NIPs binding isotherms.

	B_{max} (Hz)	K_D (μM)	m (Heterogeneity index)	IF (imprinting factor) B_{maxMIP}/B_{maxNIP}	R^2
AMO-MIP	−30.2 ± 2.4	28.8 ± 3.2	0.4 ± 0.02	7.2	0.998
NIP	−4.2 ± 0.4	36.5 ± 9.6	0.8 ± 0.06	–	0.969

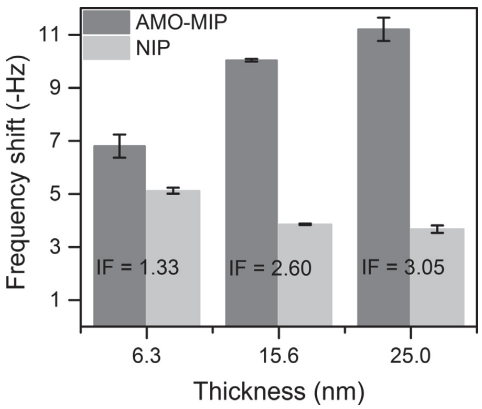

Fig. 6. Effect of film thickness on the analytical performance of AMO-MIP and NIP sensors at the injection of 1 mM AMO. Number labels on bars indicate the relative adsorption or imprinting factor (IF) values obtained at each thickness.

ation constant used to assess the affinity of the prepared MIP films to the template antibiotic.

From Table 2, one can observe that the AMO-MIP has a much higher adsorption capability as compared to the reference NIP film (-30.23 Hz vs −4.21 Hz) thus yielding an imprinting factor of 7.2. This indicate the relative capability of adsorption of the MIP compared to NIP. Likewise, the lower value of K_D for AMO-MIP relative to NIP indicates that the imprinted polymer has higher affinity for the target analyte as compared to the NIP, which mostly show non-specific interaction. This is because a lower K_D indicates a slower tendency of the target molecule to dissociate from the predefined active sites after rebinding and hence a strong binding affinity. This correlates well with the computational and spectroscopic studies that show a high binding energy, low hydrogen bond length and the presence of new UV–vis absorbance peaks in the solution mixture between AMO and mPD. Furthermore, since the removal of template molecules from the polymer matrix introduces within the MIP film binding sites with differing affinities towards the target, MIPs are generally expected to be more heterogeneous than their corresponding reference NIP films. Therefore, the lower m value observed for the AMO-MIP when compared to that of the NIP is quite familiar in MIP research. To characterize the effect of polymer matrix thickness on the analytical performance of the sensor, the AMO-MIP and NIP films with thicknesses of 6.3, 15.6 and 25.0 nm were interfaced with the sensor surface. This was realized by varying the time of electrodeposition process occurring directly on the sensor surface till the resonant frequency shift of the sensor reach −100, −250, and −400 Hz, respectively. Following the washing out process, the rebinding experiments were carried out with the injection of 1 mM concentration of AMO, as previously achieved (Fig. 6). As observed from the figure, an increasing thickness is accompanied by a corresponding increase in AMO-MIP adsorption and decrease in NIP adsorption. This is most likely due to the increase in specific surface area with increasing thickness and a corresponding increase in the number of binding sites in the AMO-MIP films. Consequently, an increasing adsorption is observed. In the case of NIP however, the decreasing but stabilizing adsorption observed could be assumed to be associated with the generation of denser film layers with decreasing active surface area. This assumption stems from the nucleation and growth mechanism of polymerization similar to that of polyaniline, in which the density, uniformity and/or morphology of the final film depend on the interaction of nucleates with the underlying substrate. However, in the case of PmPD growth, the hydrophilic nucleates which adsorb on the hydrophobic polycrystalline gold substrate likely lead to the formation of rough profiles, island-like layer with pinholes that may permit access of template molecules to the electrode surface at low film thickness. But as polymer film grows, these pinholes are obstructed thus, decreasing the nonspecific adsorption signal hence, an increasing value of imprinting factor (IF) from 1.33 to 3.05 [32,33]. Furthermore, to test the selectivity of the prepared AMO-MIP, two non-targets but widely used antibacterials belonging to different antibiotics classes were selected and their binding responses on both AMO-MIP and NIP upon separate injections of increasing concentration were analyzed and compared to that of AMO. Fig. 7a indicates the ratio of the equilibrium binding response of each analyte on the AMO-MIP to that on the NIP. As expected, the imprinted surface had a greater relative adsorption for amoxicillin target molecules. In contrast, the adsorption of the non-template antibiotics, SMZ and DOXY, was revealed to be considerably lower. Considering the little higher molecular weight of DOXY (444.4 g/mol) as compared to AMO (365.4 g/mol), one may expect DOXY's response signal on AMO-MIP to be quite comparable with that of AMO, especially at low concentration but a quick look at Fig. 7a indicates the opposite. This thus prompts the closer attention into the signals received from the NIP film following injection of the different concentrations of all samples. As shown in Fig. 7b, a greater non-specific adsorption is displayed by the NIP surface towards the non-targeted molecules as compared to AMO. This observation leads to the reasonable conclusion that the major part of the adsorption response displayed on the AMO-MIP by SMZ and DOXY are non-specific in nature and different from the specific recognition of the target AMO. Furthermore, the signal obtained from the injection of 1.6 μM AMO following a prior injection of 1.6 μM SMZ and DOXY (Fig. 8) indicates that the prior injection of other antibiotics does not influence, to any noticeable extent, the selective recognition of AMO on AMO-MIP.

Table 3
Parameters obtained from the fit of signals shown in Fig. 8.

Analyte	B_{max} (-Hz)	R^2
AMO	1.48 ± 0.03	0.999
DOXY	0.48 ± 0.03	0.999
SMZ	0.32 ± 0.01	0.997

Thus, the AMO adsorption equilibrium response as shown in Table 3, reflects at least 3 times higher signal with respect to both SMZ and DOXY at this concentration. More importantly, the selectivity coefficients (α) of the MIP film, defined by the index of the polymer selectivity towards other analytes, was calculated (Table 4) according to Eq. (4) for increasing concentration of each analyte taking cognizance of their molecular weight.

$$\alpha = (B_{max(a)}/M_{(a)})/B_{max(t)}/M_{(t)}) \quad (4)$$

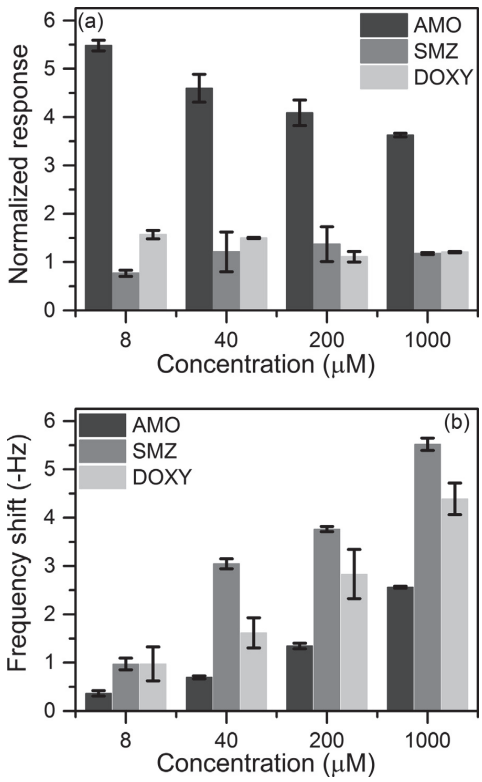

Fig. 7. (a) Normalized equilibrium resonant frequency responses of AMO-MIP modified QCM sensors upon injection of different antibiotics. (These data were obtained by dividing the response of the AMO-MIP by that of the NIP for each analyte injection) (b) Equilibrium resonance frequency responses of NIP film after injection of increasing concentration of the three different antibiotics.

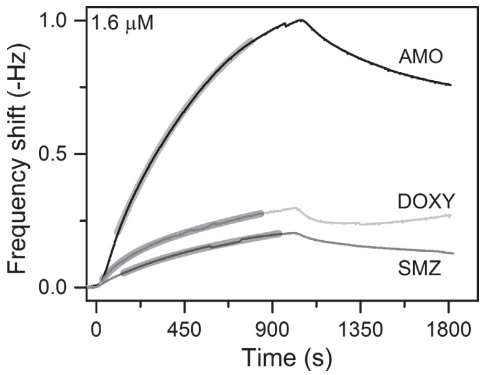

Fig. 8. Typical response signals of the injection of 1.6 μM concentration of each of the sample solution on AMO-MIP film sensor. Thick lines represent fits to the pseudo first-order equation.

where $B_{max(a)}$ and $B_{max(t)}$ represent responses of AMO-MIP (in Hz) toward non-imprinted analyte and template molecules possessing molecular weights of $M_{(a)}$ and $M_{(t)}$, respectively.

The low values of the selectivity coefficients as shown in Table 4 indicates that the polymer selectively recognizes the template

Table 4
Response-Selectivity Coefficients (α) of AMO-MIP Calculated Using Eq. (4) for Sample Solutions Containing Different Concentrations of Antibiotics, SMZ and DOXY.

Concentration (μM)	SMZ	DOXY
1.6	0.12	0.34
8.0	0.39	0.49
40.0	0.48	0.42
200.0	0.54	0.32
1000.0	0.56	0.35

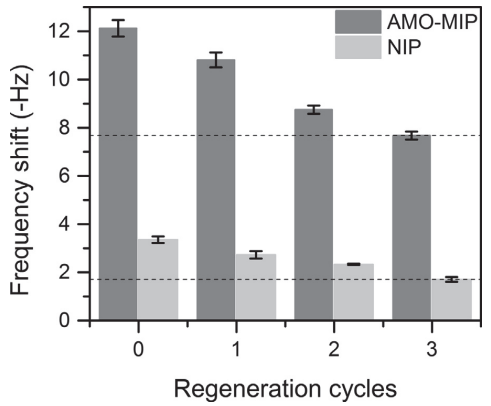

Fig. 9. Effects of regeneration-rebinding cycles on the adsorption capacity of both AMO-MIP and NIP films at the injection of 1 mM AMO.

molecules but non-specifically, and with very low affinity (similar to the non-imprinted polymers) binds non-templated interfering molecules. We also went further to analyze the lowest detectable concentration of the analyte by the prepared QCM sensor. For this purpose, the limit of detection (LoD) value was calculated from the standard deviation and slope of the regression line for the linear portions of the response signals at low concentrations (2–40 nM) injections (Fig. S6). A value of 0.2 nM was obtained, indicating that the sensor can detect the target analyte down to this low concentration. Since AMO exists in the aqueous environment within a concentration range of 0.18–4.57 nM as earlier reported, the developed chemosensor shows very promising suitability for detecting the target molecule within the low concentration range that they exist naturally. Thus, the prepared AMO-MIP sensor demonstrates an immense potential for selectively recognizing AMO antibiotic in aqueous media. Furthermore, to characterize the sensor for reusability and stability, we perform several cycles of regeneration-rebinding experiments on both AMO-MIP and NIP sensors (Fig. 9). It was observed that after the third cycle, AMO-MIP and NIP films have lost 37% and 49% adsorption capacities respectively. This result may likely reveal that with subsequent regeneration process, less bound analytes are eluted from the polymer film thus reducing the chances of analyte binding in the following rebinding step. The results therefore demonstrate that the AMO-MIP is quite stable and reusable for at least three cycles while still retaining almost 70% of its adsorption capacity.

4. Conclusions

This study draws special attention to the development of a selective MIP for amoxicillin detection by synthesizing homogeneous thin polymer film on QCM sensor using electrochemically polymerizable m-phenylenediamine (mPD) as a functional monomer. A careful study of the electrodeposition of the polymer in the

presence or absence of the template molecules was carried out to ascertain the optimal parameters for the fast synthesis of a homogeneous and stable polymer films that affords the template stability during the polymer electrodeposition. The prepared AMO-MIP film as well as its reference counterpart were characterized by QCM technique for their affinity and selectivity towards the target analyte. The AMO-MIP film showed at least seven times higher binding capacity and better affinity than the reference film. The prepared AMO-MIP modified QCM sensor could detect AMO with LoD of 0.2 nM and discriminate between the antibiotics of different classes; i.e. tetracycline (doxycycline) and sulfonamide (sulfamethizole). Further research is being undertaken to optimize the performance of the sensor and to enhance its capacity in detecting amoxicillin in real aqueous environment.

Acknowledgements

This work was supported by Estonian Ministry of Education and Research (grant PUT150), the European Regional Development Fund (project 3.2.0801.11-0009). The authors like to thank Dr. M. Kudryashova for NMR analysis and Dr. Deniss Klauson for assistance in HPLC measurements.

Appendix A. Supplementary data

Supplementary data associated with this article can be found, in the online version, at https://doi.org/10.1016/j.snb.2017.11.194.

References

[1] C. Ding, J.Z. He, Effect of antibiotics in the environment on microbial populations, Appl. Microbiol. Biot. 87 (2010) 925–941.
[2] L. Chow, L. Waldron, M.R. Gillings, Potential impacts of aquatic pollutants: sub-clinical antibiotic concentrations induce genome changes and promote antibiotic resistance, Front. Microbiol. 6 (2015).
[3] R. Thoelen, R. Vansweevelt, J. Duchateau, F. Horemans, J. D'Haen, L. Lutsen, et al., A MIP-based impedimetric sensor for the detection of low-MW molecules, Biosens. Bioelectron. 23 (2008) 913–918.
[4] J. Corcoran, M.J. Winter, C.R. Tyler, Pharmaceuticals in the aquatic environment: a critical review of the evidence for health effects in fish, Crit. Rev. Toxicol. 40 (2010) 287–304.
[5] T. Zhang, B. Li, Occurrence, Transformation, and Fate of Antibiotics in Municipal Wastewater Treatment Plants, Crit. Rev. Env. Sci. Tec. 41 (2011) 951–998.
[6] D. Dixit, A. Verma, S. Gupta, P. Bansal, Assessment of solar photocatalytic degradation and mineralization of amoxicillin trihydrate (AMT) using slurry and fixed-bed batch reactor: efficacy of parabolic trough collector, RSC Adv. 6 (2016) 36109–36117.
[7] T.B. Minh, H.W. Leung, I.H. Loi, W.H. Chan, M.K. So, J.Q. Mao, et al., Antibiotics in the Hong Kong metropolitan area: ubiquitous distribution and fate in Victoria Harbour, Mar. Pollut. Bull. 58 (2009) 1052–1062.
[8] N. Iqbal, P.A. Lieberzeit, Artificial Receptors for Mass-Sensitive Sensors: Targeting Analytes from Surfaces, Nanoparticles, and Bioanalytes by Molecular Imprinting, Molecularly Imprinted Sensors, Elsevier, Amsterdam, 2012, pp. 195–235.
[9] H. Peng, G.F. Ma, K.J. Sun, J.J. Mu, Z. Zhang, Z.Q. Lei, Facile synthesis of poly(p-phenylenediamine)-derived three-dimensional porous nitrogen-doped carbon networks for high performance supercapacitors, J. Phys. Chem. C 118 (2014) 29507–29516.
[10] P. Gajendran, R. Saraswathi, Electrocatalytic performance of poly(o-phenylenediamine)-Pt-Ru nanocomposite for methanol oxidation, J. Solid State Electr. 17 (2013) 2741–2747.
[11] H. Gulce, A. Yetkin, E. Akgul, A. Gulce, A ferrocene functionalized polymer: poly [N-(ferrocenylmethyl)-o-phenylenediamine]. Electrochemical production and spectroelectroelectrochemical investigation in acetonitrile medium, Thin Solid Films 545 (2013) 81–88.
[12] X.G. Li, W. Duan, M.R. Huang, Y.L. Yang, D.Y. Zhao, Q.Z. Dong, A soluble ladder copolymer from m-phenylenediamine and ethoxyaniline, Polymer 44 (2003) 5579–5595.
[13] G.J. Guan, B.H. Liu, Z.Y. Wang, Z.P. Zhang, Imprinting of molecular recognition sites on nanostructures and its applications in chemosensors, Sensors-Basel 8 (2008) 8291–8320.
[14] K. Haupt, Molecular imprinting preface, Top. Curr. Chem. 325 (2012) Ix–Xii.
[15] J. Gauczinski, Z.H. Liu, X. Zhang, M. Schonhoff, Surface molecular imprinting in layer-by-layer films on silica particles, Langmuir 28 (2012) 4267–4273.
[16] P.S. Sharma, A. Pietrzyk-Le, F. D'Souza, W. Kutner, Electrochemically synthesized polymers in molecular imprinting for chemical sensing, Anal. Bioanal. Chem. 402 (2012) 3177–3204.
[17] S. Han, B.Q. Li, Z. Song, S.H. Pan, Z.C. Zhang, H. Yao, et al., A kanamycin sensor based on an electrosynthesized molecularly imprinted poly-o-phenylenediamine film on a single-walled carbon nanohorn modified glassy carbon electrode, Analyst 142 (2017) 218–223.
[18] I. Amer, D.A. Young, H.C.M. Vosloo, Chemical oxidative polymerization of m-phenylenediamine and its derivatives using aluminium triflate as a co-catalyst, Eur. Polym. J. 49 (2013) 3251–3260.
[19] X.G. Li, M.R. Huang, W. Duan, Y.L. Yang, Novel multifunctional polymers from aromatic diamines by oxidative polymerizations, Chem. Rev. 102 (2002) 2925–3030.
[20] J. Stejskal, Polymers of phenylenediamines, Prog. Polym. Sci. 41 (2015) 1–31.
[21] M.M. Rhemrev-Boom, M.A. Jonker, K. Venema, G. Jobst, R. Tiessen, J. Korf, On-line continuous monitoring of glucose or lactate by ultraslow microdialysis combined with a flow-through nanoliter biosensor based on poly(m-phenylenediamine) ultra-thin polymer membrane as enzyme electrode, Analyst 126 (2001) 1073–1079.
[22] S.J. Killoran, R.D. O'Neill, Characterization of permselective coatings electrosynthesized on Pt-Ir from the three phenylenediamine isomers for biosensor applications, Electrochim. Acta 53 (2008) 7303–7312.
[23] A.G. Ayankojo, A. Tretjakoy, J. Reut, R. Boroznjak, A. Öpik, J. Rappich, et al., Molecularly imprinted polymer integrated with a surface acoustic wave technique for detection of sulfamethizole, Anal. Chem. 88 (2016) 1476–1484.
[24] A. Tretjakov, V. Syritski, J. Reut, R. Boroznjak, A. Öpik, Molecularly imprinted polymer film interfaced with Surface Acoustic Wave technology as a sensing platform for label-free protein detection, Anal. Chim. Acta 902 (2016) 182–188.
[25] V. Syritski, J. Reut, A. Menaker, R.E. Gyurcsanyi, A. Öpik, Electrosynthesized molecularly imprinted polypyrrole films for enantioselective recognition of L-aspartic acid, Electrochim. Acta 53 (2008) 2729–2736.
[26] J.O. Mahony, K. Nolan, M.R. Smyth, B. Mizaikoff, Molecularly imprinted polymers-potential and challenges in analytical chemistry, Anal. Chim. Acta 534 (2005) 31–39.
[27] L.E. Gomez-Pineda, G.E. Pina-Luis, C.M. Cortes-Romero, M.E. Palomar-Pardave, G.A. Rosquete-Pina, M.E. Diaz-Garcia, et al., Quantum chemical calculations on the interaction between flavonol and functional monomers (Methacrylic acid and 4-vinylpyridine) in molecularly imprinted polymers, Molecules 15 (2010) 4017–4032.
[28] G. Lautner, J. Kaev, J. Reut, A. Öpik, J. Rappich, V. Syritski, et al., Selective artificial receptors based on micropatterned surface-imprinted polymers for label-free detection of proteins by SPR imaging, Adv. Funct. Mater. 21 (2011) 591–597.
[29] S. Babic, A.J.M. Horvat, D.M. Pavlovic, M. Kastelan-Macan, Determination of pK(a) values of active pharmaceutical ingredients, Trac-Trend Anal Chem 26 (2007) 1043–1061.
[30] R.J. Umpleby, S.C. Baxter, A.M. Rampey, G.T. Rushton, Y.Z. Chen, K.D. Shimizu, Characterization of the heterogeneous binding site affinity distributions in molecularly imprinted polymers, J. Chromatogr. B 804 (2004) 141–149.
[31] G. Vasapollo, R. Del Sole, L. Mergola, M.R. Lazzoi, A. Scardino, S. Scorrano, et al., Molecularly imprinted polymers: present and future prospective, Int. J. Mol. Sci. 12 (2011) 5908–5945.
[32] I. Sapurina, J. Stejskal, The mechanism of the oxidative polymerization of aniline and the formation of supramolecular polyaniline structures, Polym. Int. 57 (2008) 1295–1325.
[33] I.Y. Sapurina, M.A. Shishov, Oxidative polymerization of aniline: molecular synthesis of polyaniline and the formation of supramolecular structures, New Polymers for Special Applications (2012) 251–312.

Biographies

Akinrinade George Ayankojo received his M.Sc. (2014) from the Department of Material and Environmental Technology, Tallinn University of Technology, Estonia. Since 2014 he has been studying for a Ph.D. in the same department. His research interests are major in developing label-free chemical sensors for detecting antibiotics pollutants in water using molecular imprinting technology.

Jekaterina Reut is currently a research scientist at the Department of Material and Environmental Technology in Tallinn University of Technology. She received her PhD (2004) in the field of electrically conducting polymers from Tallinn University of Technology. Her research interest is in the area of the design and synthesis of molecularly imprinted polymers for biosensing applications.

Roman Boroznjak received his MSc (2007) in organic chemistry and PhD (2017) in natural and exact sciences from Tallinn University of Technology. His research interests include computational modeling and rational design of molecularly imprinted polymers.

Andres Öpik received his PhD in chemistry from the University of Tartu in 1980. He is currently Professor of physical chemistry at the Department of Material and Environmental Technology in Tallinn University of Technology. His main research field is material science and technology: investigation of the physical and chemical properties and possibilities of practical applications of different electronic materials such as electrically conductive polymers and inorganic semiconductive compounds. Cur-

rently his research interests include the development of novel functional materials based on molecularly imprinted polymers for biomedical diagnostics.

Vitali Syritski is a head of the Laboratory of Biofunctional Materials at the Department of Material and Environmental Technology of Tallinn University of Technology. He received his PhD (2004) in the field of inherently conducting polymers. Presently, his major research interest lies in the area molecular imprinting. In particular, he has focused on development of chemical and biosensors for accurate and fast detection of disease biomarkers and environmental contaminants.

PAPER III

Akinrinade George Ayankojo, Jekaterina Reut, Andres Öpik, Aleksei Tretjakov and Vitali Syritski. Enhancing Binding Properties of Imprinted Polymers for Small Molecules Detection, *Proceedings of the Estonian Academy of Sciences*, 67 (2) (2018).

Proceedings of the Estonian Academy of Sciences,
2018, **67**, 2, 138–146
https://doi.org/10.3176/proc.2018.2.04
Available online at www.eap.ee/proceedings

MATERIALS SCIENCE

Enhancing binding properties of imprinted polymers for the detection of small molecules

Akinrinade George Ayankojo*, Jekaterina Reut, Andres Öpik, Aleksei Tretjakov, and Vitali Syritski

Department of Materials and Environmental Technology, Tallinn University of Technology, Ehitajate tee 5, 19086 Tallinn, Estonia

Received 19 October 2017, revised 15 January 2018, accepted 18 January 2018, available online 27 March 2018

Abstract. This study demonstrates the promising steps towards improving the detection of small analytes in an aqueous solution by the quartz crystal microbalance (QCM) modified with a molecularly imprinted polymer (MIP) based sensitive layer. A homogeneous thin polymer film of poly(*m*-phenylenediamine) (PmPD) was electrochemically deposited on the surface of a QCM sensor in the presence of sulphamethizole (SMZ) acting as a template molecule. The binding capacity of the resulting SMZ–MIP films was enhanced by modifying the sensing surface with a diethylaminoethyl-dextran (DEAE-Dex) layer, forming a SMZ–MIP(Dex) film. The dextran layer allows further preconcentration of template molecules on the sensor electrode before polymer electrodeposition. The relative adsorption of the SMZ–MIP(Dex) films, as designated by the imprinting factors, was found to be in all cases significantly higher than that of the other films. At least about three times enhanced relative binding capacity of the modified imprinted polymer on the QCM sensor was established. A probe of the analysed sensor signals revealed that the modification steps significantly reduced the contribution from nonspecific interaction of the polymer matrix, thus suggesting beneficial effects of the dextran modification and template preconcentration. The presented approach promises a positive route towards an improved specific detection of small molecules by molecular imprinting on QCM sensor transducers.

Key words: molecularly imprinted polymer, small molecule detection, sulphamethizole, quartz crystal microbalance, DEAE-dextran.

1. INTRODUCTION

The detection of small molecular weight analytes (drugs, toxins, chemicals, pollutants, etc.) is vital for environmental and biological interests (food safety, public security, environmental monitoring as well as pharmaceutical and biomedical analyses). Numerous analytical techniques (enzyme-linked immunosorbent assay, liquid chromatography, gas chromatography, mass spectrometry, and their coupling techniques) exist for the detection of various small analytes [1–4]. However, most of these techniques lack high specificity and their continued utilization is limited by the expensive detection instruments and complex procedures involved. Molecular imprinting is a technique that creates synthetic recognition materials, the so-called molecularly imprinted polymer (MIP), for detecting any molecule of interest, thus mimicking biological receptors. It polymerizes functional monomers in the presence of the target molecule that acts as a template. During polymerization, the template induces binding sites in the reticulated polymer that are capable of selectively recognizing the target molecules or similar structures following the removal of the templates from the polymer. The challenges of the traditional methods of detection are thus greatly overcome since MIP has been shown to

* Corresponding author, akinrinade.ayankojo@ttu.ee

possess several advantages as an alternative recognition material. These include low cost, ease of preparation, storage stability, durability to heat and pressure, as well as applicability in harsh chemical media [5,6].

For the accurate analysis and interpretation of the performance of a MIP, its robust interface with a sensor transducer that converts the molecular recognition into a readable electrical signal, is very crucial. Consequently, numerous MIPs have been fabricated on different sensor transducers: electrochemical, calorimetric, optical, and piezoelectric, with mass-sensitive (piezoelectric) devices making up a somewhat substantial proportion [7–17]. Mass-sensitive devices such as the quartz crystal microbalance (QCM), also known as the bulk acoustic wave sensor, respond to mass changes on their surface by a resonant frequency shift that is directly proportional to the mass of the analyte adsorbed. This allows them to play a pivotal role in molecular detection and analysis since mass is a fundamental property of all compounds [18]. As a result, the QCM has been employed in the fabrication of MIP-based sensors for small analyte detection with literature reviews published on the subject matter [19–22].

In sensor fabrication, sensitivity is one of the critical factors. However, the sensitivity of the QCM, like of other affinity sensors, is comparable to the molecular mass of the analyte among other factors. Furthermore, the universal sensitivity of the QCM sensor encourages unsolicited contributions to the sensor signal, especially when operated in a liquid [23]. Also, QCM transducers integrated with a MIP recognition layer, although offering an elegant label-free detection platform, suffer from an intrinsic limitation of the contribution to the sensor signals from nonspecific binding of other matrix elements [24,25]. As the degree of nonspecific interaction affects the sensitivity of a sensor, reducing nonspecific adsorption is of importance in MIP sensor fabrication.

While an increased sensitivity for piezoelectric transducers can be achieved by increasing the device frequency, increasing the amount of the binding sites in the recognition element (e.g. MIP) will also lead to a lower contribution from nonspecific interaction to the sensor signal, thereby facilitating the specific adsorption of the target molecules [18,26]. For small molecule detection by mass-sensitive devices, increasing the number of the recognition sites is therefore key to achieving a higher sensitivity. This leads to a shift in frequency only when a sensible amount of the template has been adsorbed unto the recognition sites. This can be accomplished by the bulk molecular imprinting approach in which the template molecule provides the sterical and chemical qualities as well as the diffusion path for the subsequent recognition of the analytes [27]. Furthermore, to reduce the nonspecific interaction, a quantitative association of the functional monomer with the template molecules is essential for increasing the imprinted sites while reducing the chances of nonspecific interaction. This is achieved by ensuring that an appreciable amount of the template is available within the forming polymer during the preparative stage, thus resulting in the MIP having a considerable rebinding of the template as compared with the reference non-imprinted polymer (NIP) [28].

Diethylaminoethyl-dextran (DEAE-Dex) is a polycationic stabilizing molecule having an average molecular weight of up to 500 kDa. It is commonly used in nucleic acid transfection, sustained protein delivery, and in biosensors for cell immobilization. It is quite similar to the carboxymethyl dextran (CM-Dex) analogue that has been employed in developing certain sensor chips for the surface plasmon resonance (SPR) sensing platform but differs in the absence of a carboxyl functional group. The dextran immobilized sensor layer has a tendency to minimize the nonspecific binding of the analyte on the sensor due to the barrier formation between the analyte and the underlying electrode substrate of the sensor [29,30]. Most interesting is the flexible nature of the layer that encourages binding site accessibility on a recognition layer, thus enhancing sensitivity especially for small molecular weight analytes.

This work attempts to improve the specific binding capacity of a MIP on a QCM sensor as a mass-sensitive, label-free transducer for small molecule detection. For this purpose, a promising approach to enhance the amount of the binding sites within the MIP matrix was adopted. This involves the preconcentration of the small molecular weight template molecules on the sensor surface prior to the electropolymerization. To achieve the template preconcentration, a monolayer assembly of an anion exchanger, DEAE-Dex, was formed on the sensor electrode prior to the electropolymerization. The different stages of the modification were probed by the electrochemical impedance spectroscopic (EIS) technique. Although DEAE-Dex has been widely used in cell and/or enzyme immobilization biosensor technology [31], this is, to the best of our knowledge, its first use for the preconcentration of a small target molecule in MIP research. Sulphamethizole (SMZ) was selected as a model small molecule and *m*-phenylenediamine (mPD) as an electropolymerizable functional monomer for polymer matrix formation based on the previously established strong, non-covalent interaction existing between their complementary functional groups [32]. Efforts were made to optimize the performance of the prepared MIP on the chosen QCM sensor transducer. This involves ensuring a homogeneous film

deposition and accurate control of the polymer film growth. The beneficial influence of such dextran modification and the following preconcentration on the binding capacity of the prepared MIP are presented as an important step towards an improved detection of small analytes by MIPs on mass sensitive transducers.

2. EXPERIMENTAL SECTION

2.1. Chemicals and materials

All chemicals, except acetic acid, sulphuric acid, and hydrogen peroxide that were provided by Lachner, were purchased from Sigma-Aldrich. All chemicals were of analytical grade and were used as received without any further purification. Ultrapure water (resistivity 18.2 MΩ·cm, Millipore, USA) was used to prepare all aqueous solutions, and phosphate buffered saline (PBS) solution (0.01 M, pH 7.4) was used in preparing the synthesis and analyte solutions.

2.2. Sensor modification and characterization

The gold (Au) electrodes of a 5 MHz QCM (Maxtek, Inc.) were used in this work for SMZ–MIP and the reference NIP film deposition. An $Ag/AgCl/KCl_{sat}$ electrode was used as the reference electrode in all electrochemical measurements. Before electrochemical deposition of the films, the QCM sensors were cleaned for 3 min in the hot piranha solution consisting of 30% H_2O_2 and concentrated H_2SO_4 in 1 : 3 ratio followed by electrochemical cleaning in 0.1 M H_2SO_4 aqueous solution by cycling the electrode potential in the range from –0.2 to +1.5 V with a scan rate of 50 mV/s until the cyclic voltammograms were reproducible. Finally, the electrodes were washed thoroughly with ultrapure water and dried again in nitrogen stream. A pre-cleaned Au surface of the sensor was modified with DEAE-Dex ($M_r \approx 500\,000$ g/mol), purchased from Sigma-Aldrich, by directly applying DEAE-Dex solution (0.1 mg/mL) for 30 min after which the surface was rinsed with water and dried under nitrogen stream. Then SMZ was pre-adsorbed on the Au/DEAE-Dex surface by a direct covering of the surface with the PBS buffer solution containing 3.5 mM SMZ and allowed to stand for 30 min followed by careful rinsing with water and drying under nitrogen. Each stage of the modification processes was monitored by EIS by measuring, fitting in ZView software, and comparing the EIS data collected from bare Au, Au/DEAE-Dex, and Au/DEAE-Dex with adsorbed SMZ (Au/DEAE-Dex/SMZ) surfaces.

2.3. Preparation of SMZ–MIP films

After SMZ preconcentration on a sensor electrode, electropolymerization of mPD was conducted on the modified electrode at a constant potential of 0.6 V in PBS buffer solution containing 5 mM mPD and 3.5 mM SMZ resulting in a PmPD/SMZ film on the sensor electrode. Following electrodeposition, the template molecules (SMZ) were removed from the polymeric matrix of the electrodeposited PmPD/SMZ film to create SMZ–MIP(Dex) with complementary cavities suitable for the specific recognition of SMZ molecules. This was achieved by immersing the PmPD/SMZ-modified sensors in a mixture of acetic acid/methanol (1 : 3) and allowed to stay for a period of 24 h with continuous stirring. Then the sensors were washed with distilled water and dried under nitrogen stream.

For the control studies, the following films were fabricated omitting one or several of the above steps: (a) the DEAE-Dex modified non-imprinted PmPD film (NIP(Dex)) was prepared without the SMZ template preadsorption step as well as excluding SMZ molecules from the pre-polymerization solution, (b) the imprinted PmPD (SMZ–MIP) is the same as SMZ–MIP(Dex) but without the DEAE-Dex surface modification and pre-adsorption steps, (c) the non-imprinted PmPD (NIP) is the same as NIP(Dex) but without the DEAE-Dex modification and preadsorption steps. It should be noted that all films were subjected to the template washing step, independent of whether a SMZ template was introduced in their matrices or not, in order to ensure similar treatments for all films.

2.4. Rebinding studies

The capability of the fabricated SMZ–MIP films to recognize SMZ was studied by QCM combined with a flow injection analysis (FIA) to set up a QCM–FIA system allowing on-line analysis of SMZ rebinding on the SMZ–MIP surface. The system consists of a programmable precision pump (M6, VICI® Valco Instruments Company Inc., USA), a motorized six-way port injection valve controlled by a microelectric actuator (C22-3186EH, VICI® Valco Instruments Company Inc., USA), and a small volume (150 μL) axial flow cell attached to the QCM sensor holder (Stanford Research Systems, Inc.). Sensors modified with SMZ–MIP, SMZ–MIP(Dex), NIP(Dex), and NIP films were loaded into the QCM–FIA system and equilibrated by running a PBS buffer through the system till a stable baseline was established. Then analyte solutions were consecutively injected into the QCM–FIA system at a flow rate of

40 µL/min in the order from the lower to the higher concentrations, and the signal changes of the sensors were monitored. The analyte solutions with SMZ concentrations in the range of 0.040–1.0 mM were prepared in a filtered and degassed PBS buffer (pH 7.4). The prepared analyte solutions were also degassed before their injection into the sensor system. The sensorgrams recorded were fitted to a pseudo-first-order kinetic binding model in order to determine the equilibrium responses for all prepared films. At least three replicas of all experiments were conducted. The scheme representing the entire molecular imprinting approach from dextran modification to the rebinding study is shown in Fig. 1.

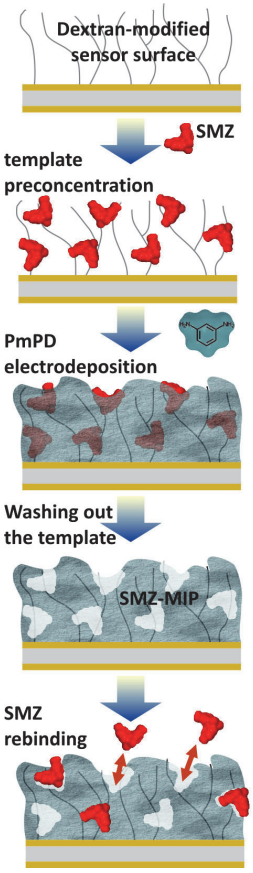

Fig. 1. Schematic representation of the molecular imprinting approach for the preparation of sulphamethizole–molecularly imprinted polymer–dextran (SMZ–MIP(Dex)) films on a gold electrode of a sensor.

3. RESULTS AND DISCUSSION

3.1. Sensor surface modification and characterization

The surface modification with a dextran layer was applied to preconcentrate the small molecular weight template molecules at the sensor surface before polymer matrix formation. This aims to enhance the imprinting capacity of the resulting MIP-based sensor. The EIS technique was used to evaluate the changes in the electrochemical behaviour of the Au electrode. This technique has already been shown as an effective method for probing the hindrances towards electron transfer reactions across a surface-modified electrode/electrolyte interface using the $K_3[Fe(CN)_6]/K_4[Fe(CN)_6]$ redox couple as a probe solution [33,34].

The EIS data and fitted spectra of the different modification steps were as shown in Fig. 2. An equivalent circuit consisting of a solution resistance (R_s), a charge transfer resistance (R_{ct}), a constant phase element (CPE1), and a Warburg impedance (Wd), shown in the inset figure, was used to model the EIS pattern. As shown in Table 1, the solution resistances for all surfaces have a similar value of approximately 5 Ω; however, as evident in the EIS spectra in Fig. 2 and the fitting parameters in Table 1, the modification of the Au electrode by a DEAE-Dex layer results in an increase in the semicircle diameter corresponding to the charge

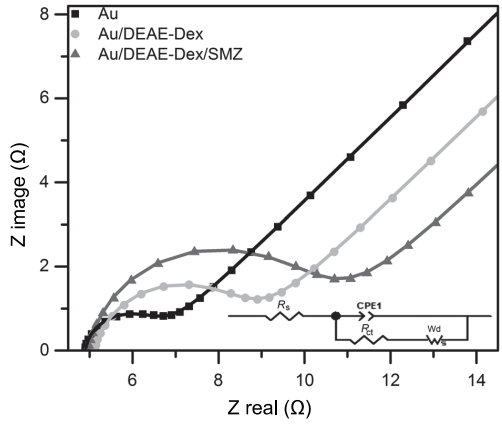

Fig. 2. Electrochemical impedance spectroscopic images of a bare gold electrode (Au), Au–diethylaminoethyl–dextran (Au/DEAE-Dex), and Au/DEAE-Dex–sulphamethizole (Au/DEAE-Dex/SMZ) modified surfaces in 0.1 M KCl containing 4 mM $Fe(CN)_6^{3-}/Fe(CN)_6^{4-}$ at a scan rate of 50 mV/s. R_s – solution resistance, R_{ct} – charge transfer resistance, Wd – Waburg impedance.

Table 1. Summary of the results of electrochemical impedance spectroscopic fitting

	Au	Au/DEAE-Dex	Au/DEAE-Dex/SMZ
Solution resistance, Ω	4.90 ± 0.02	5.13 ± 0.02	4.97
Charge transfer resistance, Ω	1.67 ± 0.04	3.47 ± 0.07	5.37

DEAE-Dex – diethylaminoethyl-dextran, SMZ – sulphamethizole.

transfer resistance (R_{ct}) at the electrode interface. The R_{ct} value of 3.5 Ω for DEAE-Dex modified gold is more than two times the R_{ct} value of bare gold (1.7 Ω).

The slight inhibition of the electron transfer despite the significant molecular weight of DEAE-Dex, can be possibly explained by the nature of the electrostatic interactions between the polycationic dextran and anions of the redox probe. Namely, the polycationic sites of DEAE can attract the negatively charged $Fe(CN)_6^{3-}/Fe(CN)_6^{4-}$, thus facilitating the electron transfer between the solution and the electrode surface. After the incubation in the SMZ solution, R_{ct} has a further increased value revealing an enhanced inhibition of the electron transfer at the interface due to the SMZ adsorption on the DEAE-Dex-modified surface. The electrochemical measurements therefore confirmed the sensor surface modification with the DEAE-Dex layer and the subsequent SMZ preconcentration on the surface. It is worth mentioning that the ion permeability of the DEAE-Dex layer, which allows the charge transfer at the modified electrode interface, is essential for the subsequent electrodeposition of the PmPD matrix.

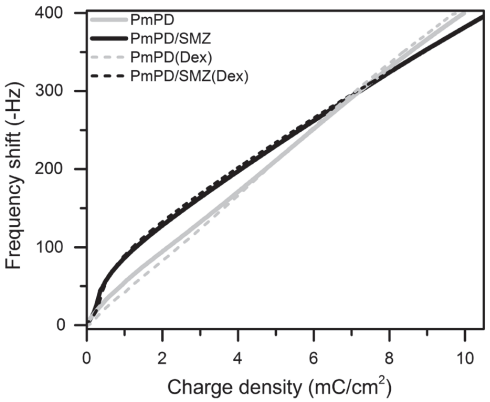

Fig. 3. In situ responses of a quartz crystal microbalance (QCM) sensor as a function of the electrical charge passed during the potentiostatic (0.6 V vs Ag/AgCl) electrodeposition of *m*-phenylenediamine (PmPD) and PmPD–sulphamethizole (PmPD/SMZ) on diethylaminoethyl–dextran modified and unmodified sensor electrodes from the phosphate buffered saline solution (pH = 7.4).

3.2. Preparation of SMZ–MIP films

The electrochemical syntheses of PmPD/SMZ and PmPD films were performed directly on the unmodified (PmPD and PmPD/SMZ) as well as on the dextran-modified (PmPD(Dex) and PmPD/SMZ(Dex)) QCM sensor surfaces. In the case of the PmPD(Dex), the preadsorption of SMZ on the dextran-modified sensor was skipped. The potentiostatic electrodeposition process was controlled by passing an amount of charge through the electrode of the sensor with respect to QCM responses that were being recorded at the same time (Fig. 3). This is to ensure that the resulting imprinted SMZ–MIP and SMZ–MIP(Dex) films forming on the sensor surfaces had equal thickness with their corresponding non-imprinted control films, NIP and NIP(Dex), respectively. Thus, PmPD and PmPD/SMZ films with the possible thicknesses corresponding to a QCM sensor frequency decay of –400 Hz, under the given experimental conditions, were prepared. As seen in Fig. 3, the electrodeposition of mPD in the presence of SMZ required less charge to produce polymer films of identical response compared with the mPD electrodeposition in the absence of SMZ. It also reveals that the difference in the generated polymer amount became less pronounced after 6 mC/cm^2. More importantly, it should be noted that the dextran modification did not affect to any significant extent the electrodeposition of the PmPD and PmPD/SMZ polymer films as predicted earlier (see Section 3.1).

3.3. Rebinding study

The rebinding of the target antibiotic molecule (SMZ) on the imprinted film was studied by the QCM-FIA technique, which allows real-time monitoring of molecular interactions in a film on the surface of the sensor. To estimate the relative binding capacity of the fabricated MIP towards the SMZ template molecules, a control experiment was performed with the corresponding NIP film. This was followed by the analysis

of the sensor signals and evaluation of the relative recognition capacity of the MIP by the imprinting factor (IF), a parameter that indicates the relative binding ability of the interaction of the imprinted polymer towards the analyte as compared with its non-imprinted counterpart. With larger IF values, more binding sites are available in the resulting imprinted polymer as compared with the reference polymer suggesting thus that a MIP with a higher IF should give a correspondingly higher selectivity as observed in many reported works [32,35–37].

The following equation was used to calculate IF:

$$\mathrm{IF} = Q_{\mathrm{eq(MIP)}}/Q_{\mathrm{eq(NIP)}}, \qquad (1)$$

where $Q_{\mathrm{eq(MIP)}}$ and $Q_{\mathrm{eq(NIP)}}$ are equilibrium binding capacities of MIP and NIP, respectively. To calculate the value of Q_{eq}, the adsorption kinetics data from the corresponding sensor responses (Fig. 4) were firstly modelled as the sum of two integrated rate equations for the association phase:

$$Q_{\mathrm{eq}} = Q_{\mathrm{eq1}}[1-e^{-kobs1*t}] + Q_{\mathrm{eq2}}[1-e^{-kobs2*t}], \qquad (2)$$

where *kobs*1, *kobs*2, and Q_{eq1}, Q_{eq2} are pseudo-first-order kinetic constants and equilibrium adsorption capacities for binding sites of types 1 and 2, respectively. Such approach postulates the presence of two types of binding sites offering different binding interactions and provides improved goodness of fit for heterogeneous imprinted polymers [38]. The value of Q_{eq} was calculated as the sum of the respective Q_{eq1} and Q_{eq2} obtained from fitting the kinetics data to Eq. (2). The calculated values of the IF for the sensor response at 1 mM SMZ injection are presented in Table 2.

Table 2. Binding capacities, correlation coefficients, and imprinting factors derived from the fitting of the kinetic data of 1 mM injection signals of Fig. 4 to Eq. (2)

Polymer matrix	Q_{eq} (Hz)	R^2	IF
SMZ–MIP	–15.52 ± 0.04	0.999	
NIP	–14.97 ± 0.13	0.996	1.0
SMZ–MIP(Dex)	–16.85 ± 0.04	0.999	
NIP(Dex)	–6.40 ± 0.06	0.992	2.6

Figure 4a shows the frequency responses of the QCM sensors coated with the SMZ–MIP and NIP films upon consecutive injections of the solution with increasing concentrations of SMZ in the PBS buffer. It can be seen that the SMZ injections of 0.04 mM caused the response of the SMZ–MIP coated sensor to be only slightly higher than that from the corresponding NIP. The difference in the responses of the SMZ–MIP and NIP films was more evident only after the SMZ injection of 1 mM. The calculated IF for this MIP–NIP pair is 1.0 (Table 2), indicating a weak adsorption capacity of the given SMZ–NIP film over its corresponding NIP along with the high nonspecific adsorption of SMZ.

However, analysis of the signal responses of the SMZ–MIP(Dex) and NIP(Dex) modified QCM sensors reveals a rather different behaviour (Fig. 4b). Namely, the MIP sensor has noticeably higher frequency shifts than those of the NIP sensor starting from 0.04 mM analyte injection. Moreover, the signal difference became more pronounced with the injection of increasingly higher SMZ concentrations, yielding in the end an IF value of approximately 3 at 1 mM SMZ injection

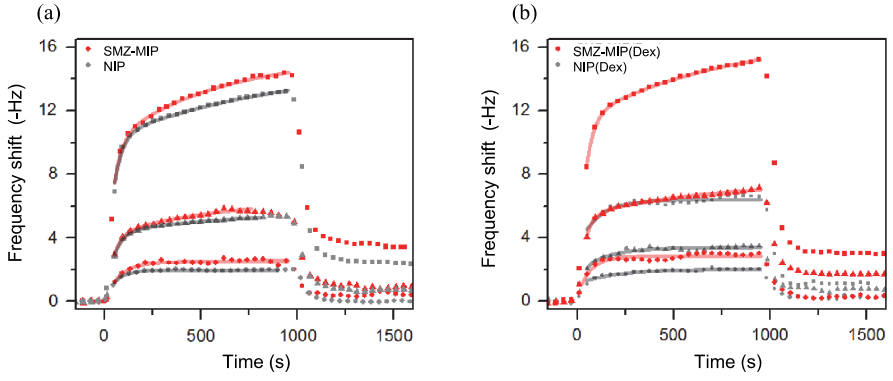

Fig. 4. Frequency responses of the quartz crystal microbalance (QCM) sensor modified with (a) sulphamethizole–molecularly imprinted polymer (SMZ-MIP; red) and non-imprinted polymer (NIP; grey) and (b) SMZ-MIP(Dex) (red) and NIP(Dex) (grey) upon injections of 0.04 (circle), 0.2 (triangle), and 1 mM (square) SMZ concentrations in phosphate buffered saline solution. The solid lines represent the fits to Eq. (2).

(Table 2), which is significantly better than the corresponding IF for the non-dextran modified films (IF = 1.0).

A careful observation of the response signals in Fig. 4 and the equilibrium parameters obtained from the kinetic fit of the signals (Table 2) reveals two important phenomena, including the fact that the dextran modification substantially decreases SMZ adsorption on the NIP film (–14.97 Hz vs –6.40 Hz). This means that unsolicited interactions of the analyte with the polymer matrix are greatly reduced on the reference film and by extension, on the imprinted polymer. Secondly, the dextran-enabled SMZ immobilization improves the binding capacity of the SMZ–MIP film (–16.85 Hz vs –15.52 Hz) by providing, probably, more binding sites in the reticulated polymer matrix. Although little difference can be observed between the equilibrium signals for dextran-modified and non-modified imprinted films, it can be explained by the fact that the reduction of the contribution from nonspecific signals leads to a corresponding reduction in the overall signals. Furthermore, Fig. 5a shows that the dextran-modified imprinted (SMZ–MIP(Dex)) and non-imprinted (NIP(Dex)) films show higher and lower change in frequency responses, respectively, as compared to their non-modified counterparts. The corresponding IF values (Fig. 5b) clearly indicate the significantly higher relative binding capacities of the dextran-modified surfaces as compared with the non-modified ones, starting from the very first concentration, with observable increasing difference as the injected concentration increases. These results thus demonstrate, within the space of the available experimental details, the beneficial effects of the SMZ-preconcentrated dextran modification step in the SMZ–MIP synthesis procedure allowing an enhanced sensitivity of the SMZ–MIP(Dex) films towards SMZ.

4. CONCLUSIONS

Quartz crystal microbalance (QCM) has been largely utilized as a low-cost mass-sensitive label-free sensor platform for monitoring and analysing molecular interaction. However, owing to the diminishing sensitivity of the QCM with the decreasing size of the observed target molecules, its reliability for an accurate direct detection and analysis of a small analyte by molecular imprinted polymer (MIP) is limited. This study proposes preliminary steps towards improving the detection of a small analyte by the QCM modified with a MIP-based sensitive layer. By immobilizing sulphamethizole (SMZ) molecules using a preadsorbed dextran layer on the sensor electrode before the electropolymerization of the template–monomer solution complex, more specific recognition sites were created within the SMZ–MIP(Dex) matrix after the SMZ washing out process as compared with the SMZ–MIP having no such dextran modification. This exemplifies the advantage of the sensor surface modification by DEAE–Dex that allows the template preconcentration before the polymer film synthesis, thus yielding an additional entrapment of SMZ molecules within the polymer matrix and thereby leading to an increased imprinting sites within the polymer and consequently an enhanced recognition capacity of the SMZ–MIP(Dex) film. Although further studies are being carried out to analyse the selectivity of detection as well as optimizing and/or improving the binding capacity to cater for analytically relevant sensitivity levels, the presented protocol, within the space of the available experimental details, could be a promising route towards an improved detection of small molecules by molecular imprinting on mass-sensitive sensor transducers such as the QCM.

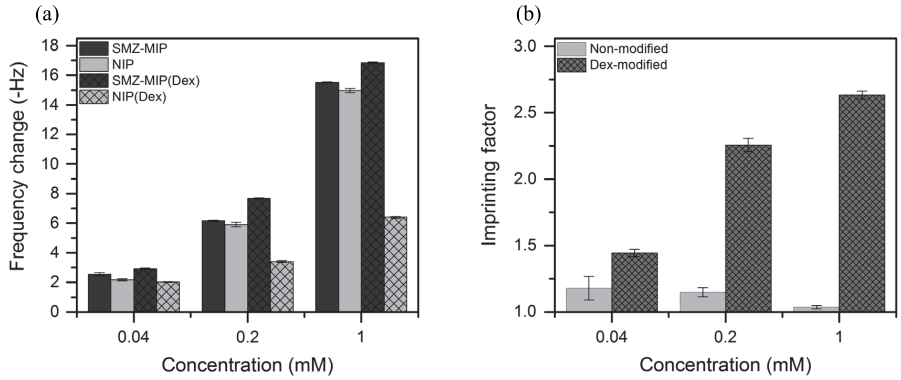

Fig. 5. Graphical comparison of the response signals (a) and the resulting imprinting factors (b) for the prepared sensors as measured at different concentrations of the analyte.

ACKNOWLEDGEMENTS

This work was supported by the European Regional Development Fund under project 3.2.0801.11-0009 and the Estonian Ministry of Education and Research (grant PUT150). The publication costs of this article were covered by the Estonian Academy of Sciences.

REFERENCES

1. Wang, Y. Z., Wei, D. P., Yang, H., Yang, Y., Xing, W. W., Li, Y., and Deng, A. P. Development of a highly sensitive and specific monoclonal antibody-based enzyme-linked immunosorbent assay (ELISA) for detection of Sudan I in food samples. *Talanta*, 2009, **77**(5), 1783–1789.
2. Bicker, J., Fortuna, A., Alves, G., and Falcão, A. Liquid chromatographic methods for the quantification of catecholamines and their metabolites in several biological samples – a review. *Anal. Chim. Acta*, 2013, **768**, 12–34.
3. Lee, C. H., Shin, Y., Nam, M. W., Jeong, K. M., and Lee, J. A new analytical method to determine non-steroidal anti-inflammatory drugs in surface water using *in situ* derivatization combined with ultrasound-assisted emulsification microextraction followed by gas chromatography–mass spectrometry. *Talanta*, 2014, **129**, 552–559.
4. Paya, P., Anastassiades, M., Mack, D., Sigalova, I., Tasdelen, B., Oliva, J., and Barba, A. Analysis of pesticide residues using the Quick Easy Cheap Effective Rugged and Safe (QuEChERS) pesticide multiresidue method in combination with gas and liquid chromatography and tandem mass spectrometric detection. *Anal. Bioanal. Chem.*, 2007, **389**(6), 1697–1714.
5. Svenson, J. and Nicholls, I. A. On the thermal and chemical stability of molecularly imprinted polymers. *Anal. Chim. Acta*, 2001, **435**(1), 19–24.
6. Hillberg, A. L., Brain, K. R., and Allender, C. J. Molecular imprinted polymer sensors: implications for therapeutics. *Adv. Drug Deliv. Rev.*, 2005, **57**(12), 1875–1889.
7. Tretjakov, A., Syritski, V., Reut, J., Boroznjak, R., Volobujeva, O., and Öpik, A. Surface molecularly imprinted polydopamine films for recognition of immunoglobulin G. *Microchim. Acta*, 2013, **180**(15–16), 1433–1442.
8. Malitesta, C., Mazzotta, E., Picca, R. A., Poma, A., Chianella, I., and Piletsky, S. A. MIP sensors – the electrochemical approach. *Anal. Bioanal. Chem.*, 2012, **402**(5), 1827–1846.
9. Cennamo, N., D'Agostino, G., Pesavento, M., and Zeni, L. High selectivity and sensitivity sensor based on MIP and SPR in tapered plastic optical fibers for the detection of L-nicotine. *Sensor. Actuat. B-Chem.*, 2014, **191**, 529–536.
10. Verma, R. and Gupta, B. D. Optical fiber sensor for the detection of tetracycline using surface plasmon resonance and molecular imprinting. *Analyst*, 2013, **138**(23), 7254–7263.
11. El-Sharif, H. F., Aizawa, H., and Reddy, S. M. Spectroscopic and quartz crystal microbalance (QCM) characterisation of protein-based MIPs. *Sensor. Actuat. B-Chem.*, 2015, **206**, 239–245.
12. Kotova, K., Hussain, M., Mustafa, G., and Lieberzeit, P. A. MIP sensors on the way to biotech applications: targeting selectivity. *Sensor. Actuat. B-Chem.*, 2013, **189**, 199–202.
13. Wang, Y., Tang, J., Luo, X. Y., Hu, X. Y., Yang, C., and Xu, Q. Development of a sensitive and selective kojic acid sensor based on molecularly imprinted polymer modified electrode in the lab-on-valve system. *Talanta*, 2011, **85**(5), 2522–2527.
14. Hong, C. C., Chang, P. H., Lin, C. C., and Hong, C. L. A disposable microfluidic biochip with on-chip molecularly imprinted biosensors for optical detection of anesthetic propofol. *Biosens. Bioelectron.*, 2010, **25**(9), 2058–2064.
15. Liu, Y. X., Wang, Y., Liu, L., He, Y. H., He, Q. H., and Ji, Y. H. The detection method for small molecules coupled with a molecularly imprinted polymer/quantum dot chip using a home-built optical system. *Anal. Bioanal. Chem.*, 2016, **408**(19), 5261–5268.
16. Syritski, V., Reut, J., Menaker, A., Gyurcsanyi, R. E., and Öpik, A. Electrosynthesized molecularly imprinted polypyrrole films for enantioselective recognition of L-aspartic acid. *Electrochim. Acta*, 2008, **53**(6), 2729–2736.
17. Lakshmi, D., Akbulut, M., Ivanova-Mitseva, P. K., Whitcombe, M. J., Piletska, E. V., Karim, K., et al. Computational design and preparation of MIPs for atrazine recognition on a conjugated polymer-coated microtiter plate. *Ind. Eng. Chem. Res.*, 2013, **52**(39), 13910–13916.
18. Li, S., Ge, Y., Piletsky, S. A., and Lunec, J. *Molecularly Imprinted Sensors: Overview and Applications.* Elsevier, 2012.
19. Ayankojo, A. G., Reut, J., Boroznjak, R., Öpik, A., and Syritski, V. Molecularly imprinted poly(meta-phenylenediamine) based QCM sensor for detecting amoxicillin. *Sensor. Actuat. B-Chem.*, 2018, **258**, 766–774.
20. Dai, J., Zhang, Y., Pan, M. F., Kong, L. J., and Wang, S. Development and application of quartz crystal microbalance sensor based on novel molecularly imprinted sol-gel polymer for rapid detection of histamine in foods. *J. Agr. Food Chem.*, 2014, **62**(23), 5269–5274.
21. Ebarvia, B. S., Ubando, I. E., and Sevilla, F. B. Biomimetic piezoelectric quartz crystal sensor with chloramphenicol-imprinted polymer sensing layer. *Talanta*, 2015, **144**, 1260–1265.
22. Uludağ, Y., Piletsky, S. A., Turner, A. P. F., and Cooper, M. A. Piezoelectric sensors based on molecular imprinted polymers for detection of low molecular mass analytes. *Febs. J.*, 2007, **274**(21), 5471–5480.
23. Mecea, V. M. Is quartz crystal microbalance really a mass sensor? *Sensor. Actuat. A-Phys.*, 2006, **128**(2), 270–277.
24. Cooper, M. A. Label-free screening of bio-molecular interactions. *Anal. Bioanal. Chem.*, 2003, **377**(5), 834–842.

25. Ertekin, Ö., Öztürk, S., and Öztürk, Z. Z. Label free QCM immunobiosensor for AFB1 detection using monoclonal IgA antibody as recognition element. *Sensors (Basel)*, 2016, **16**(8), 1274.
26. Schneider, H. J., Tianjun, L., and Lomadze, N. Sensitivity increase in molecular recognition by decrease of the sensing particle size and by increase of the receptor binding site – a case with chemomechanical polymers. *Chem. Commun.*, 2004, **0**(21), 2436–2437.
27. Avila, M., Zougagh, M., Escarpa, A., and Rios, A. Molecularly imprinted polymers for selective piezoelectric sensing of small molecules. *TrAC Trends Anal. Chem.*, 2008, **27**(1), 54–65.
28. Sellergren, B. Imprinted polymers with memory for small molecules, proteins, or crystals. *Angew. Chem. Int. Ed. Engl.*, 2000, **39**(6), 1031–1037.
29. Jung, S. H., Jung, J. W., Suh, I. B., Yuk, J. S., Kim, W. J., Choi, E. Y., et al. Analysis of C-reactive protein on amide-linked N-hydroxysuccinimide-dextran arrays with a spectral surface plasmon resonance biosensor for serodiagnosis. *Anal. Chem.*, 2007, **79**(15), 5703–5710.
30. Wijaya, E., Lenaerts, C., Maricot, S., Hastanin, J., Habraken, S., Vilcot, J. P., et al. Surface plasmon resonance-based biosensors: from the development of different SPR structures to novel surface functionalization strategies. *Curr. Opin. Solid St. M.*, 2011, **15**(5), 208–224.
31. Tkáč, J., Navrátil, M., Šturdík, E., and Gemeiner, P. Monitoring of dihydroxyacetone production during oxidation of glycerol by immobilized *Gluconobacter oxydans* cells with an enzyme biosensor. *Enzyme Microb. Tech.*, 2001, **28**(4), 383–388.
32. Ayankojo, A. G., Tretjakov, A., Reut, J., Boroznjak, R., Öpik, A., Rappich, J., et al. Molecularly imprinted polymer integrated with a surface acoustic wave technique for detection of sulfamethizole. *Anal. Chem.*, 2016, **88**(2), 1476–1484.
33. Sezgintürk, M. K. and Uygun, Z. O. An impedimetric vascular endothelial growth factor biosensor-based PAMAM/cysteamine-modified gold electrode for monitoring of tumor growth. *Anal. Biochem.*, 2012, **423**(2), 277–285.
34. Chang, B. Y. and Park, S. M. Electrochemical impedance spectroscopy. *Annu. Rev. Anal. Chem.*, 2010, **3**, 207–229.
35. Zhang, L. and Chen, L. Fluorescence probe based on hybrid mesoporous silica/quantum dot/molecularly imprinted polymer for detection of tetracycline. *ACS Appl. Mater. Inter.*, 2016, **8**(25), 16248–16256.
36. Yang, C. C., Yan, X. M., Guo, H., and Fu, G. Q. Synthesis of surface protein-imprinted nanoparticles endowed with reversible physical cross-links. *Biosens. Bioelectron.*, 2016, **75**, 129–135.
37. Kadhirvel, P., Azenha, M., Shinde, S., Schillinger, E., Gomes, P., Sellergren, B., and Silva, A. F. Imidazolium-based functional monomers for the imprinting of the anti-inflammatory drug naproxen: comparison of acrylic and sol-gel approaches. *J. Chromatogr. A*, 2013, **1314**, 115–123.
38. Li, X. and Husson, S. M. Adsorption of dansylated amino acids on molecularly imprinted surfaces: a surface plasmon resonance study. *Biosens. Bioelectron.*, 2006, **22**(3), 336–348.

Parendatud omadustega molekulaarselt jäljendatud polümeerid väikeste molekulide määramiseks

Akinrinade George Ayankojo, Jekaterina Reut, Andres Öpik, Aleksei Tretjakov ja Vitali Syritski

Molekulaarse jäljendamise meetodi kasutamine erinevate ravimijääkide, nagu sulfametisool (SMZ), määramiseks vesikeskkonnas on keskkonnaseireks täpne, lihtne ja odav tehnoloogia. Antud artiklis on esitatud tehnoloogilised täiendused väikese sihtmolekuli sulfametisooli suhtes molekulaarselt jäljendatud polümeeri (SMZ–MIP) valmistamiseks. Molekulaarse jäljendamise tehnoloogia on kombineeritud piezoelektrilise kvartskristallanduriga, mis võimaldab sihtmolekuli sidumisel tekkiva signaali kiire ja täpse edastamise. Molekulaarselt jäljendatud polümeerkile valmistati elektrokeemilisel polümerisatsioonil piezoelektrilise kvartskristalli kuldelektroodile, kasutades monomeerina *m*-fenüleendiamiini sihtmolekuli SMZ-i juuresolekul. Sihtmolekuli parema sidumise tagamiseks käsitleti jäljendatud polümeeri SMZ–MIP-ga piezoelektrilise kvartskristalli kuldelektroodi eelnevalt dietüülaminoetüül-dekstraani (Dex) lahusega nii, et elektrokeemilise polümerisatsiooni tulemusena tekkis sulfometisooli suhtes jäljendatud SMZ–MIP(Dex)-kile. Eelkäsitlus dekstraaniga võimaldas elektrokeemilisel polümerisatsioonil sihtmolekuli SMZ paremini elektroodi pinnale kontsentreerida ja seeläbi oluliselt suurendada sihtmolekuli suhtes jäljendatud pesade arvu SMZ–MIP(Dex)-kiles. Nagu näitasid sidumise efektiivsuse analüüsi tulemused, oli dekstraaniga käsitletud SMZ–MIP(Dex)-kiledel ilma eelkäsitluseta SMZ–MIP-ga võrreldes sihtmolekuli spetsiifilise sidumise efektiivsus kolm korda suurem. Eelkäsitlus dekstraaniga vähendas ka mittespetsiifilist sihtmolekuli adsorptsiooni, mis omakorda suurendas SMZ–MIP(Dex) efektiivsust sihtmolekuli SMZ sidumisel. Uuringutest võib järeldada, et aluspinna dekstraaniga eelkäsitlus parandab oluliselt SMZ–MIP(Dex)-kilede SMZ-i spetsiifilise sidumise efektiivsust ja on rakendatav ka teiste analoogiliste väikeste molekulide molekulaarsel jäljendamisel ning määramisel piezoelektrilist kvartskristalli kui sensorit kasutades.

Curriculum vitae

1. Personal data

Name	Akinrinade George Ayankojo
Date and place of birth	31.10.1983, Nigeria
Citizenship	Nigeria
E-mail address	georgekojo2003@gmail.com

2. Education

Educational institution	Graduation year	Education (field of study/degree)
Tallinn University of Technology	2014 - 2018	Chemical and Materials Technology/PhD
Tallinn University of Technology	2012 - 2014	Materials and Processes of Sustainable Energetic / MSc
Federal University of Agriculture, Abeokuta	2005 - 2010	Biochemistry / BSc
School of Science, Ogbomoso	1999 - 2002	Secondary education

3. Language competence/skills

Language	Level
Yoruba	Native
English	Fluent
Estonian	Basic
Hausa	Basic

4. Special courses/Conference

Period	Educational or other organization
2014-2018	Graduate school "Functional materials and technologies FMTDK", Tallinn University of Technology, Estonia
June, 2018	10th International Conference on Molecular Imprinting, Jerusalem, Israel
September, 2017	Baltic Polymer Symposium, Tallinn, Estonia
March, 2017	5th International Conference on Multifunctional, Hybrid and Nanomaterials, Lisbon, Portugal
June, 2016	9th International Conference on Molecular Imprinting, Lund, Sweden
September, 2014	Baltic Polymer Symposium, Laulasmaa, Estonia

5. Professional employment

Period	Organization	Position
2012 - 2018	Tallinn University of Technology, Department of Materials Science	Scientific projects participant
2014-2014	Dana Dairy group Ltd, Switzerland	Sales agent

6. Research activity, including honors

Projects

01.01.2013	31.12.2016	Investigation and development of new generation biosensing selective recognition elements based on Molecularly Imprinted Polymers	PUT150
01.01.2012	31.12.2015	p-type ZnO and ZnS	ETF9243
01.01.2010	31.12.2013	Design for new ultrahard while tough (nano)composites	ETF8211

Honors

2015, Award for the best publication in the field of natural and exact sciences in 2015 at Tallinn University of Technology: **Akinrinade George Ayankojo**, Aleksei Tretjakov, Jekaterina Reut, Roman Boroznjak, Andres Öpik, Jörg Rappich, Andreas Furchner, Karsten Hinrichs, Vitali Sõritski (2015). ”Molecularly Imprinted Polymer Integrated with a Surface Acoustic Wave Technique for Detection of Sulfamethizole“. Analytical Chemistry Article ASAP, DOI: 10.1021/acs.analchem.5b04735.

Elulookirjeldus

1. Isikuandmed

Ees- ja perekonnanimi	Akinrinade George Ayankojo
Sünniaeg ja -koht	31.10.1983, Nigeria
Kodakondsus	Nigeria
E-posti aadress	georgekojo2003@gmail.com

2. Hariduskäik

Õppeasutus (nimetus lõpetamise ajal)	Lõpetamise aeg	Haridus (eriala/kraad)
Tallinna Tehnikaülikool	2014 - 2018	Keemia- ja materjalitehnoloogia / doktoriõpe
Tallinna Tehnikaülikool	2012 - 2014	Materjalid ja protsessid jätkusuutlikus energeetikas/ Magistrikraad
Põllumajandusülikool, Abeokuta, Nigeria	2005 - 2010	Biokeemia / Bakalaureusekraad
Loodusteaduste keskkool, Ogbomoso, Nigeria	1999 - 2002	Keskharidus

3. Keelteoskus

Keel	Tase
Yoruba	Emakeel
Inglise	Kõrgtase
Eesti	Algtase
Hausa	Algtase

4. Täiendusõpe/Konverentsid

Õppimise aeg	Täiendusõppe korraldaja nimetus
2014-2018	TÜ ja TTÜ doktorikool “Funktsionaalsed materjalid ja tehnoloogiad” (FMTDK), Eesti
September, 2017	Rahvusvaheline konverents “Baltic Polymer Symposium, BPS2017” Tallinn, Eesti, suuline ettekanne
Märts, 2017	Rahvusvaheline konverents “5th International Conference on Multifunctional, Hybrid and Nanomaterials”, Lissabon, Portugal, stendiettekanne.
Juuni, 2016	Rahvusvaheline konverents “9th International Conference on Molecular Imprinting, MIP 2016”, Lund, Rootsi, stendiettekanne
September, 2014	Rahvusvaheline konverents “Baltic Polymer Symposium, BPS2014” Laulasmaa, Eesti, suuline ettekanne

5. Teenistuskäik

Töötamise aeg	Tööandja nimetus	Ametikoht
2012 - 2018	Tallinna Tehnikaülikool, Materjaliteaduse (al 2017. a. Materjali- ja keskkonnatehnoloogia) instituut	Uurimisprojekti täitja
2014-2014	Dana Dairy group Ltd, Šveits	Müügiesindaja

6. Teadustegevus, sh tunnustused ja juhendatud lõputööd

Projektid

01.01.2013 - 31.12.2016	Uue põlvkonna biotundlike süsteemide uurimine ja väljatöötamine molekulaarselt jäljendatud polümeeride baasil	PUT150
01.01.2012 - 31.12.2015	p-tüüpi ZnO ja ZnS	ETF9243
01.01.2010 - 31.12.2013	Suurendatud sitkusega ülikõva keramiliste komposiitmaterjalide disain	ETF8211

Tunnustused

TTÜ 2015 aasta parim teadusartikkel loodus-, täppis- ja terviseteaduste valdkonnas: **Akinrinade George Ayankojo**, Aleksei Tretjakov, Jekaterina Reut, Roman Borozнjak, Andres Öpik, Jörg Rappich, Andreas Furchner, Karsten Hinrichs, and Vitali Syritski, Molecularly Imprinted Polymer Integrated with a Surface Acoustic Wave Technique for Detection of Sulfamethizole, Analytical Chemistry, 88(2) (2016) 1476–1484.